Politecnico di Milano
Corso di Laurea Magistrale in Ingegneria Energetica
Scuola di Ingegneria Industriale e dell'Informazione

Hydropower Modelling in Mid-Term Adequacy Forecasts

the peculiar case of Austria

in collaboration with
Austrian Power Grid AG

Thesis Supervisor: Prof. Massimo Tavoni
Co-Supervisor: Marlene Petz

Author:
Gregorio Iotti, Matr. 875424

Anno Accademico 2019-2020

Acknowledgments

I am grateful to Austrian Power Grid, in particular to Johannes, Marlene, Klaus, Kurt and Stefan, who warmly welcomed and supported me in making this thesis possible. A special thanks to prof. Massimo Tavoni, who helped me with his guidance while developing this work.

For a long time I have been thinking about this moment: writing the acknowledgments of my Master Thesis as the "end" of this terrific journey called Laurea Magistrale in Ingegneria Energetica. "Terrific". I believe that the twofold meaning of this adjective, marvelous and frightening, perfectly fits the bittersweet mix of feelings that pervades me now that this moment has finally come. I started this journey in Milano and moved to four different cities in three different countries in the past three years. I am thankful for all the new and different experiences made, either happy or sad, that shaped me into who I am now, both personally and professionally. I thank the Politecnico di Milano, the Technical University of Delft, and UNITECH for opening these and many other opportunities to me, and for helping me decide which ones to choose, among all the different possibilities.

I am grateful for all the new amazing people I met alongside this path, and for the ones who were close to me before, and still are, despite the distance. My fellow Unitechers and Bouwpub-Crawlers, who were a source of mutual inspiration and personal growth, as well as the best party companions. Chiara, who is the friend I needed in a new and stranger city. Andrea, Andrea, Davide e Diego, who always make me feel at home every time we meet.

Thanks to Andrea, Alessio, Francesco, Marcello, Mario, and all my uni-mates with whom I shared countless hours of studying and laughing, lunch and coffee breaks for five years and more. A special thanks to Giulia for supporting me with her bright personality and genuine kindness anytime I needed.

Grazie alla mia famiglia, che mi ha sempre sostenuto con stima e affetto, lasciandomi libero di fare le mie scelte e di perseguire le mie ambizioni in totale libertà.

Gregorio

Disclaimer

The sentences, remarks and conclusions presented in this report are the expression of my personal reflections and opinions as the author of this thesis; thus, they shall not be deemed as statements from Austrian Power Grid AG or any other institution or firm mentioned.

The results reported are the outcome of simulations performed under artificially stressed system conditions, as part of an academic exercise with pure theoretical and speculative interest. Hence, they do not provide a realistic estimate of the future expected adequacy status of the bidding zones represented in the models. It follows that these results are valid and meaningful only in the context and framework presented in this thesis and any out of scope misinterpretation must be avoided.

Abstract

In the fast-changing electricity sector in Europe, new challenges and complexities have been arising over the past decades, due to the growing penetration of Renewable Energy Sources (RES) and the progressive phaseout of nuclear and fossil fuel-fired power plants. In this context, several generation adequacy assessments have been established to estimate the capability of the electric power system to always fulfill the demand for electricity and grant its secure supply in future scenarios. Under the umbrella of the European Network of Transmission System Operators for Electricity (ENTSO-E), the Mid-Term Adequacy Forecast (MAF) is the reference study and methodology for both national and multilateral mid to long-term generation adequacy forecasting. In the MAF 2019 framework, a new database for hydropower data was added to the Pan-European Climate Database (PECD), whose main novelties were the collection of 35 inferred historical time series for the hydro energy inflows (from 1982 till 2016), as well as new criteria for the categorization and aggregation of hydropower plants. I investigated the impact of the new PECD Hydro database on (i) the hydropower modelling methodology, (ii) the expected adequacy metrics, and (iii) the hourly solution of the Unit Commitment and Economic Dispatch (UCED) optimization. I used ANTARES v6.1 power system simulator as the modelling tool. The geographical perimeter was set on three interconnected bidding zones, namely Austria (AT), Switzerland (CH) and Italy North (ITN), with a special focus on the peculiar hydro-dominated electricity mix of Austria. The results for Austria showed highly deteriorated adequacy metrics, mainly attributable to the new run-of-river & pondage modelling methodology. It caused a shift of hydro storage energy to non-dispatchable river generation, thus underestimating pondage flexibility. Instead, the old methodology was overestimating its potential, being merged in ANTARES into the aggregated reservoir generation. I developed an R-coded visualization tool to scrutinize the hourly UCED results, which allowed me to critically evaluate the impact of the reduced maximum power from hydro storage and to monitor Pumped Storage Plant (PSP) generation. Several of the changes identified were imposed by the limitations of the modelling tool, rather than solely by the new structure of the PECD Hydro database. Thus, the remarks above shall be deemed as tool-specific. The findings were reported and discussed in the ENTSO-E MAF modelling team. As part of the future work fostered in my thesis, an improved methodology for pondage modelling is being developed within the MAF 2020 assessment.

Keywords: Adequacy; Hydropower Modelling; MAF; UCED; ANTARES.

Sommario

Nuove e crescenti complessità hanno caratterizzato il settore elettrico negli ultimi decenni, principalmente a causa dell'ingente diffusione di fonti di energia rinnovabile e della progressiva dismissione degli impianti termoelettrici a combustibile fossile o nucleare. In questo contesto si possono osservare numerosi studi atti a monitorare e valutare l'adeguatezza del sistema elettrico, ossia la sua capacità di garantire la fornitura di energia elettrica, specialmente per scenari futuri. Sotto la supervisione dell'Associazione Europea dei Gestori di Rete dei Sistemi di Trasmissione per l'Elettricità (ENTSO-E), le Previsioni di Adeguatezza a Medio Termine (MAF) costituiscono in Europa il report e la metodologia di riferimento sia a livello nazionale che multilaterale. Per lo svolgimento del MAF 2019, un nuovo database per la generazione idroelettrica fu introdotto all'interno del Database Climatico Pan-Europeo (PECD). Le principali novità furono l'arricchimento dei dati per gli afflussi idroelettrici, resi disponibili per 35 anni climatici passati (dal 1982 al 2016), e la definizione di nuovi criteri per la categorizzazione degli impianti idroelettrici. Ho studiato l'impatto del nuovo "PECD Hydro" database (i) sulla metodologia per la modellazione idroelettrica, (ii) sugli indici di adeguatezza, (iii) sui risultati dell'ottimizzazione ora per ora del cosiddetto "Unit Commitment and Economic Dispatch" (UCED). Ho utilizzato il software ANTARES v6.1 per modellare il sistema elettrico, includendo nel modello tre zone di mercato interconnesse, ossia Austria (AT), Svizzera (CH) e Nord Italia (ITN). Inoltre, ho analizzato con particolare attenzione il caso dell'Austria, data la particolare varietà e complessità della sua flotta idroelettrica. I risultati in Austria hanno mostrato un notevole deterioramento dei parametri di adeguatezza, principalmente attribuibili alla nuova metodologia di modellazione per la categoria "run-of-river & pondage". Ciò ha causato uno spostamento di flussi idroelettrici verso una tipologia di generazione ad acqua fluente, quindi "non-programmabile". Al contrario, la metodologia precedente sovrastimava la flessibilità di tali portate, in quanto erano conteggiate come afflussi ai bacini idroelettrici. Inoltre, ho sviluppato uno strumento di visualizzazione (programmato in R) che mi ha permesso di analizzare nel dettaglio il dispaccio idroelettrico e gli Impianti di Accumulo mediante Pompaggio (PSP). Molti tra gli effetti individuati sono riconducibili a limitazioni e peculiarità del software ANTARES v6.1, perciò non direttamente isolabili o attribuibili alle differenze introdotte dal nuovo PECD Hydro database. Le osservazioni e le riflessioni maturate durante lo svolgimento della mia tesi sono state apertamente presentate e discusse con i colleghi del team di ENTSO-E responsabile per il MAF. Una nuova metodologia per la modellazione degli impianti idroelettrici ad acqua fluente con capacità di accumulo è in fase di sviluppo nella nuova edizione del MAF 2020.

Executive Summary

General Framework

Over the past decades, increasing complexities and challenges have been arising in the electric power sector in Europe. The massive deployment of intermittent Renewable Energy Sources (RES) [1], the growing market integration and cross-border participation, together with the progressive decarbonization of the power generation fleet [2] and nuclear phaseout policies in several Member States [3], are impacting the daily operational procedures of Transmission System Operators (TSOs). High uncertainties on the generation side may not only increase the need for ancillary services and balancing reserves, but also jeopardize the security of supply due to insufficient firm generation or transmission capacity. Security of supply concerns, including energy dependence on foreign resources [4], are gaining strong political and economic importance, as shown in Europe by the emerging needs and employment of Strategic Reserves (SR) or other types of Capacity Remuneration Mechanisms (CRMs). In this context, it is crucial to monitor the adequacy of the system in future scenarios, i.e. its capability to meet the demand for electricity every hour of the year. Several generation adequacy studies have been established under the umbrella of the ENTSO-E, in compliance with the European Electricity Regulations.

State of the Art

The concept of adequacy relies upon the need for a continuous balance between available generation and demand for electricity via the network infrastructure. When it comes to adequacy forecasting, both the supply and demand-side estimates can be assessed either through a purely deterministic methodology or through the combination of a deterministic forecast, together with stochastic uncertainties. Such uncertainties arise from climatic variables and their influence on RES infeed, load profiles, as well as unpredictable forced outages affecting transmission assets and generating units. The ENTSO-E's MAF [5, 6, 7] is a yearly process assessing and reporting generation adequacy for the pan-European network up to 10 years ahead. Soon to be integrated and expanded within the new European Resource Adequacy Assessment (ERAA) methodology [8], as required by the Clean Energy for all Europeans Package (CEP) [9], the MAF is nowadays the reference framework for state-of-the-art mid-term generation adequacy assessments in Europe, either at a multilateral or national level. In the MAF, system adequacy is evaluated through expected adequacy metrics, namely Loss of Load Expectation (LOLE), Expected Energy not Served (EENS) and Loss of

Load Probability (LOLP), which are computed leveraging large-scale Monte Carlo simulations. The input data are collected and maintained by ENTSO-E in two main databases gathering climate data as well as the best estimates for generation capacity and demand evolution provided by the TSOs. The Pan-European Market Modelling Database (PEMMDB) collects detailed data and technical parameters concerning the fleet of generating units, while the Pan-European Climate Database (PECD) collects historical climate data used to model the variability of RES. At the time of the MAF 2019 assessment, PECD data were collected per each bidding zone and reported as time series for 35 historical Climate Years (CYs) from 1982 until 2016.

A substantial change in the hydropower data and modelling methodology was introduced in the MAF 2019 edition [10], for which a new PECD Hydro database was employed [11]. The major novelties, compared to the hydro database formerly used in the MAF 2018, included a new methodology to infer historical data for hydro natural inflows The data were for the first time provided for the 35 CYs consistently with the other PECD data. The old template only considered three possible hydrologic climate conditions, namely "dry", "normal" and "wet". New criteria for the categorization and aggregation of hydropower plants were also defined. In the Hydro 2018 data, they were consolidated into five main categories: (i) Run-of-River (ROR), (ii) swell ROR & Daily storage, (iii) Daily PSP reservoir, (iv) Weekly PSP reservoir, and (v) Annual PSP reservoir. As the names suggest, the criteria to aggregate PSP and large-dam reservoirs were based on the time ratio [h] between the reservoir size [MWh] and the installed pump (or turbine if not a PSP plant) capacity [MW]. Instead, the new categories introduced with the PECD Hydro were: (i) run-of-river & pondage, (ii) traditional reservoirs, i.e. reservoirs without pumping capabilities, (iii) open-loop PSP reservoirs, i.e. PSP plants with natural inflows, and (iv) closed-loop PSP reservoirs, i.e. PSP plants without natural inflows.

The establishment of this new hydro database was the main driver of my research. As an employee of the Austrian Power Grid AG (APG) and a member of the ENTSO-E MAF modelling team, I aimed to deepen the understanding of how the underlying assumptions and format of this new hydro database, thus of the new hydropower modelling methodology developed, affected the results of mid-term generation adequacy forecasts within the MAF 2019 framework. My analysis focused on the data and modelling for the future target year 2025. The spotlight was naturally set on the peculiar case of Austria, the control region where APG operates the grid as TSO and acts as the Control Area (CA) manager. The Austrian fleet of ROR and storage hydropower plants counts more than 10 GW of installed capacity (equal to around 50% of the total net generation capacity in 2019) and supplies around two-thirds of the total electric energy generated in the country every year.

Methodology

My thesis inherits the same methodology and definitions adopted in the MAF 2019 process. To perform the simulations, I used ANTARES v6.1 [12], a large-scale multi-area Monte Carlo simulator developed by le Réseau de Transport de l'Èlectricité (RTE), which is available open-source. I restricted the geographical boundaries to Austria (AT) and two neighboring bidding zones with high hydropower capacity, namely Switzerland (CH) and Italy North (ITN). Such a tri-lateral model was set up and calibrated for the target year 2025 using the same input data of the MAF 2019 and used as a "test bench" for the analysis. I performed two Monte Carlo simulations based on two versions of the same tri-lateral model, which were identical except for the hydropower modelling methodology. One was labelled as "Hydro 2018 model" and used the approach of the MAF 2018, while the other one was labelled as "Hydro 2019 model" and leveraged the new method developed for the MAF 2019. For this purpose, I reaggregated the same hydro data collected in the new PECD Hydro database to fit the old MAF 2018 hydro data template and to comply with the old power plant type classification. The data granularity and historical time series for the hydro natural inflows were also adapted to the old methodology, thanks to a clustering process based on the total yearly energy inflows to the hydro storages. This allowed to exclude any difference in the results potentially driven by new estimates of installed capacity and hydro inflows, with respect to 2018 expectations.

The results of the Monte Carlo simulations were analyzed and compared with multiple approaches ranging from averaged yearly results down to the hourly UCED solution. The comparison of the results was supported by a visualization tool that I developed in the R environment [13]. Conclusive statements were made thanks to the insights provided by the analysis of the results and the detailed benchmark of the hydropower modelling methodologies.

Structure

The structure of the report is the following. Chapter 1 introduces the landscape of adequacy forecasting, its definition and the key generation adequacy processes in Europe. I present the motivation for my work and the research question and methodology in Chapter 2. Then, I summarize the key elements of the ENTSO-E MAF 2019 framework, including the definition of the adequacy metrics typically reported in mid-term adequacy studies (Chapter 3). I proceed to report the main features of ANTARES v6.1 (Chapter 4), together with a synthetic mathematical formulation of the UCED optimization problem. In Chapter 5 I describe the structure and the key data available in the hydro database used for the MAF 2018 and MAF 2019 editions. The criteria used to categorize and aggregate the hydropower units are also reported. Moving to Chapter 6, I extensively describe the hydropower modelling methodologies developed for ANTARES v6.1 to handle the input data previously reported. Finally, I elaborate on the results obtained from the tri-lateral models and their comparison in Chapter 7. I close my thesis in Chapter 8, pondering on the insights gathered thanks to the anal-

ysis of the results, as well as the lessons learnt on hydropower modelling in ANTARES v6.1. Statements on envisaged future work and developments are also placed.

Comparison of the Results

The Monte Carlo simulations counted 30 forced outage patterns repeated per each of the 35 climate years, hence reaching a total sample size of 1050 simulated years. Convergence was monitored through a coefficient of variation α, defined on the adequacy metric EENS for the total system. Only the appreciable differences between the results from the two models were relevant for the comparative analysis. Setting up the models with the arbitrary tri-lateral configuration allowed on the one hand to reduce the complexity and better isolate the effects of hydropower modelling. On the other hand, such an islanded configuration determined a highly stressed and not secure status of the grid, making the results far from being representative of the system behavior under real conditions within the interconnected pan-European network. The above statements shall be intended as a disclaimer to avoid any potential misinterpretation of the results, which do not give any realistic estimate of the future adequacy status of the system, that being clearly out of the scope of my work.

Yearly averaged results: Table 1 contains the expected adequacy indices and the averaged yearly generation per fuel type, reporting the absolute and percentage deltas (taking as a basis the results from the Hydro 2018 model).

	Delta [GWh]			Delta [%]		
Averaged results	AT	CH	ITN	AT	CH	ITN
Run-of-river	**6812.7**	**67.5**	**143.0**	**27.60%**	**0.40%**	**0.88%**
Tot PSP Turbine	568.0	81.2	13.6	77.66%	33.19%	0.80%
Tot PSP Pump	757.3	108.3	18.1	77.66%	33.19%	0.80%
Tot hydro gen.	**455.5**	**24.3**	**-32.2**	**1.14%**	**0.07%**	**-0.09%**
Hydro stor. exc. PSP	-6925.2	-124.5	-188.7	-47.99%	-0.63%	-1.07%
Tot hydro storage	**-6357.2**	**-43.2**	**-175.2**	**-41.93%**	**-0.22%**	**-0.91%**
Net country balance	-172.2	-253.9	426.0	-2.08%	-7.43%	3.65%
EENS	**280.9**	**-160.7**	**152.0**	**43.14%**	**-12.58%**	**3.15%**
LOLE [hour]	**166.1**	**-52.5**	**24.1**	**34.86%**	**-4.98%**	**2.16%**

Table 1: Absolute and relative differences (w.r.t. Hydro 2018) in the yearly averaged results.

Austria showed the main differences, with an increase of ROR generation of around 27% at the expense of the total hydro storage generation, which decreased by 49% (excluding PSP). This did not come as a surprise, since in the Hydro 2019 methodology the inflows to the swell ROR & Daily storage were merged into the new run-of-river & pondage category. This reduction of hydro storage availability was one of the drivers of the increased employment of PSP generation, + 78%, as an attempt

of the system to partially compensate for such deficiency. It is interesting to point out that despite the total hydro energy generated in Austria increased by around 500 GWh, the adequacy status of the system strongly deteriorated. This clearly confirms that generation adequacy is a matter of contingent availability of resources and their maximal dispatch during peak hours, rather than their average availability.

UCED results: the scrutiny of the optimal UCED solution for the climate year 2016, the one chosen as "normal" reference hydrologic conditions, provided further insight on the hourly hydropower dispatch of the system during hours of scarcity, as shown in Figure 1 on a dimensionless comparative scale.

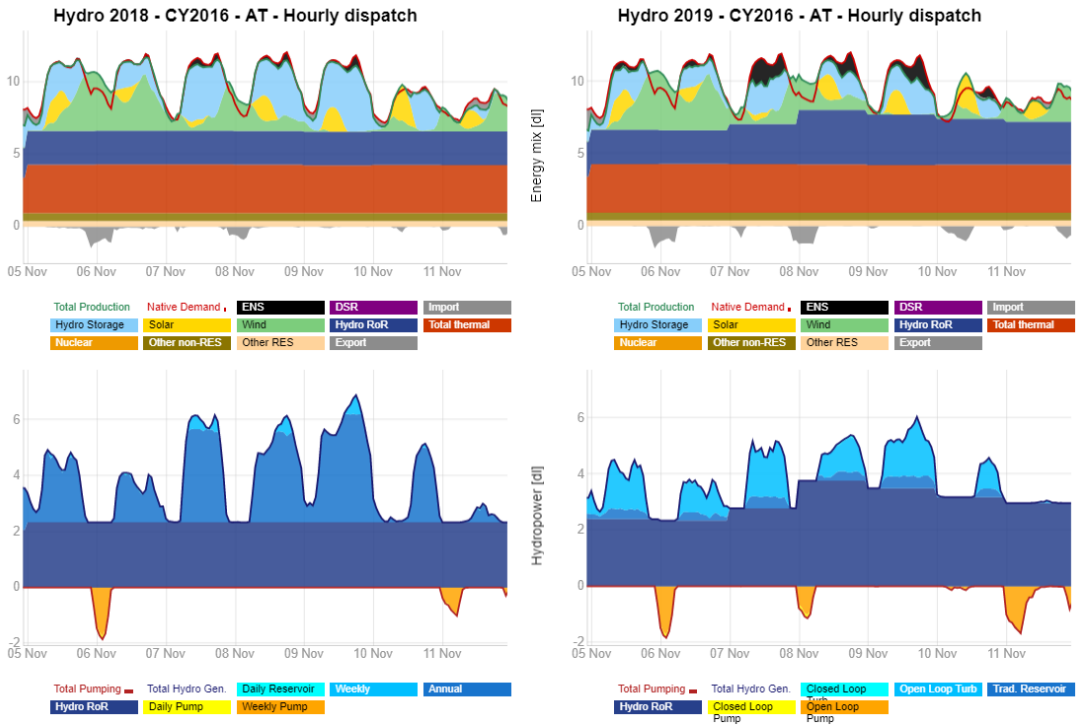

Figure 1: Hourly UCED results for Austria, climate year 2016, CW45.

The ROR generation (dark blue band) for the Hydro 2019 model (lower right side) was inflated by the inflows from the swell ROR & Daily storage, which however needed to be continuously dispatched at a constant rate by ANTARES v6.1. Instead, those and all the other storage natural inflows were treated as available to the Annual reservoir category in the Hydro 2018 model (lower left side), for which the total hydro storage generation is sensibly higher. Moreover, there was a substantial difference in the peak hydropower generation, which rose multiple times above 6 in the Hydro 2018 dispatch, while it was always conspicuously below the threshold of 6 in the Hydro 2019 results. As a consequence, the duration and intensity of ENS (the black band) were far more critical for the Hydro 2019 results.

LOLP hourly distribution: the analysis of the hourly LOLP distribution showed

that the EENS of the Hydro 2019 results was more homogeneously distributed during the winter months, with lower absolute values but protracting longer in spring and autumn. The main reason for these differences was identified in the different distribution of hydro energy natural inflows. In fact, the Hydro 2019 model included all the 35 historical time series of hydro energy inflows, whose intrinsic variability was reflected also in the occurrence of EENS. Instead, the Hydro 2018 model inherited the simplified "dry, "normal" and "wet" clustering, with only three different profiles for hydro energy availability recurring in all Monte Carlo years.

Lessons Learnt and Future Work

The tri-lateral system framework proved to be a flexible test bench for my simulations, thanks to the lower computational and time complexity. The two additional market nodes provided a simplified cross-border configuration, as well as an insightful benchmark for the results. On the other hand, the arbitrarily stressed and inadequate setting of such a configuration implicitly affected the optimization, which would deliver different results, likely more mitigated, in the full pan-European network configuration. The impact of hydropower modelling on the adequacy metrics was clearly amplified by the peculiar energy mix of Austria, which counted for a numerous and diverse fleet of hydropower units, including high river pondage capacity. Accordingly, the new methodology did not affect so severely the neighboring zones. Moreover, the comparison of the hydropower modelling methodologies highlighted that several modelling choices and assumptions were imposed by the specific design, requirements and limitations of the ANTARES v6.1 modelling tool, rather than by the actual availability and structure of the hydro databases. It follows that the findings here reported should be considered as tool-specific and may differ if the same research methodology would be applied to a different simulator. A second modelling tool among the ones used for the ENTSO-E MAF simulations, not available at APG at the time of my assessment, could provide an interesting counterpart to the results obtained with ANTARES v6.1. The key lessons learnt on hydropower modelling in ANTARES v6.1 addressed three critical aspects: (i) the generation from natural inflows to hydro storages in the Hydro 2018 methodology, (ii) run-of-river & pondage generation in the Hydro 2019 methodology, and (iii) PSP modelling.

(i) **Aggregating all natural hydro energy inflows to the various storage categories into one main reservoir**, as done for the Hydro 2018 methodology, **likely overestimated the flexibility of hydro storage generation**. In fact, the preallocation of hydro energy performed by the tool allowed to dispatch the inflows to Daily PSP reservoirs or even to swell ROR & Daily storages over a longer timeframe compared to the real-life techno-economical operation of these types of power plants.

(ii) Conversely, the modelling in ANTARES of **the new run-of-river & pondage category**, as defined in the Hydro 2019 methodology, **likely underestimated the dispatch flexibility granted by pondage capacity**. In fact, the hydro

energy inflows to this category were treated as "pure" run-of-river generation, thus non-dispatchable but continuously processed according to their hourly availability time series. However, since the input data provided lacked of consistent minimum and maximum generation profiles to properly modulate its dispatch, this rigid approach was deemed to be more conservative and suitable to generation adequacy assessments.

(iii) **PSP modelling** in ANTARES v6.1 was achieved employing two virtual nodes. The optimization occurred within independent daily or weekly cycles, during which the energy pumped was constrained to be equal to the one generated (accounting for the efficiency losses). **Due to the lack of internal memory of the reservoir level** at the beginning and the end of consecutive cycles, this approach **may lead to violations of the reservoir level constraints**. Pumped storage plants characterized by a low pump (or turbine) capacity/size ratio are more susceptible.

Improvements are expected thanks to the ANTARES v7.x releases. A detailed investigation and testing of the new functionalities and how they may affect the hydropower modelling methodology and the adequacy results is envisaged and planned.

Acknowledged the crucial role of pondage modelling in Austria, APG provided new consistent data for the minimum and maximum daily power profiles for the run-of-river & pondage category and exhorted other TSOs to do the same as an update to the PECD Hydro data. I openly presented and discussed the findings and the lessons learnt from my thesis within the ENTSO-E MAF modelling team. The same challenge was also recognized and endorsed by the Ten-Year Network Development Plan (TYNDP) working group for their transmission adequacy assessments. A common agreement was finally reached to enhance the modelling methodology for ROR & pondage generation. I started the development of such a methodology in ANTARES v7.1 for the MAF 2020.

Future works promoting further developments of the methodology in the field of hydropower modelling for adequacy studies, as well as benchmarks between different modelling tools, are warmly encouraged, especially alongside the pathway towards the new ERAA.

Contents

Acknowledgments **I**

Disclaimer **III**

Abstract **V**

Sommario **VII**

Executive Summary **IX**

Acronyms **XXI**

1 Introduction **1**
1.1 The concept of Adequacy Forecasting 2
1.2 Key Adequacy Processes in Europe 2

2 Motivation and Framework **5**
2.1 Hydropower Modelling in Adequacy Assessments 5
2.2 Research Question 6
2.3 Research Methodology 7
2.4 Thesis Structure 8

3 The MAF 2019 Framework **11**
3.1 MAF 2019 Input Data 11
3.1.1 PEMMDB Data 11
3.1.2 PECD Data 12
3.1.3 Electricity Demand and Additional Inputs 13
3.2 Delivering Results 13
3.2.1 Underlying Assumptions 13
3.2.2 The Optimization Problem 14
3.2.3 Monte Carlo Samples 15
3.2.4 Key Adequacy Metrics 16
3.2.5 Result Consolidation 17

4 ANTARES Simulator **19**
4.1 ANTARES Simulation Session 20
4.2 Monte Carlo Scenario Builder 21
4.3 Hydro Energy Manager 21
4.3.1 Breakdown Parameters 22
4.3.2 Monthly Hydro Energy Preallocation 22
4.3.3 Daily Hydro Energy Preallocation 23
4.4 Power Schedule & Unit Commitment Optimizer 25
4.4.1 Economy Mode 25
4.5 Synthetic Formulation of the Elementary Problem 26

5 The PECD Hydro Data **29**
5.1 The Hydro Data for the MAF 2018 29
5.2 The Hydro Data for the MAF 2019 31
5.3 Hydro Data Preparation 32
5.3.1 Aggregation of Hydropower Plants 33
5.3.2 Clustering of Historical Inflows 34

6 Hydropower Modelling **39**
6.1 The Hydro 2018 Modelling Methodology 40
6.1.1 Run-of-River 40
6.1.2 Reservoir Generation from Natural Inflows 41
6.1.3 Reservoir PSP Generation 42
6.1.4 Swell ROR & Daily Storage 43
6.2 The Hydro 2019 Modelling Methodology 44
6.2.1 Run-of-River & Pondage 44
6.2.2 Traditional Reservoir 45
6.2.3 Reservoir Exceptions for Maximum and Minimum Power 46
6.2.4 Closed-Loop PSP Reservoir 47
6.2.5 Open-Loop PSP Reservoir 48
6.2.6 Open-Loop Exceptions for Maximum and Minimum Power . . . 49
6.3 Hydro Energy Reservoir Management 50
6.4 Preliminary Findings 51

7 Simulation and Results **53**
7.1 Convergence 55
7.2 Yearly Averaged Results 56
7.3 Hourly UCED Results 58
7.4 Loss of Load Probability Distribution 62

8 Conclusions and Future Work **65**
8.1 Reflections on Hydropower Modelling 66
8.2 Future Work 68

Acronyms

ANTARES A New Tool for Adequacy Reporting of Electric Systems

APG Austrian Power Grid AG

AT Austria

CA Control Area

CEP Clean Energy for all Europeans Package

CH Switzerland

CRMs Capacity Remuneration Mechanisms

CYs Climate Years

DSR Demand Side Response

EENS Expected Energy not Served

ENS Energy not Served

ENTSO-E European Network of Transmission System Operators for Electricity

ERAA European Resource Adequacy Assessment

GUI Graphical User Interface

ITN Italy North

LLD Loss of Load Duration

LOLE Loss of Load Expectation

LOLP Loss of Load Probability

LP Linear Programming

MAF Mid-Term Adequacy Forecast

MCYs Monte-Carlo Years

MILP Mixed-Integer Linear Programming

NGC Net Generation Capacity

NRAA National Resource Adequacy Assessment

NRAs National Regulatory Authorities

NTCs Net Transfer Capacities

PECD Pan-European Climate Database

PEMMDB Pan-European Market Modelling Database

PLEF Pentalateral Energy Forum

PSP Pumped Storage Plant

RES Renewable Energy Sources

ROR Run-of-River

RS Reliability Standard

RTE Réseau de Transport de l'Èlectricité

SMCS Sequential Monte-Carlo Simulator

SOR Summer Outlook Report

SR Strategic Reserves

STA Short-Term Adequacy Assessment

TSOs Transmission System Operators

TYNDP Ten-Year Network Development Plan

UCED Unit Commitment and Economic Dispatch

VoLL Value of Lost Load

WOR Winter Outlook Report

Chapter 1

Introduction

Increasing complexities and challenges have been arising in the electricity sector due to the growing penetration of non-dispatchable RES. The integration of wind, solar and other distributed generation technologies comes along with their intrinsic variability and high uncertainties on contingent and forecasted availability on the grid [1]. Moreover, complex climate and geopolitical matters can be identified in the landscape. Examples are, among others:

(i) climate change and global warming, leading to more frequent and unpredictable extreme climate events [14], like summer heatwaves or occasional cold winter extremes, which can have a sudden boosting effect on the demand (e.g. the winter cold spell experienced in several EU countries including France, Belgium and Italy in January 2017 [15]);

(ii) nuclear phase-out programs in Germany, Belgium and other countries, driven by the aging of the nuclear fleet, as well as by security concerns and political streams after the Fukushima incident in 2011 [3];

(iii) the progressive decommissioning or mothballing of traditional thermal power plants due to economic viability concerns (e.g. reduced equivalent operating hours, increasing CO_2 price, uncertainties on fossil fuel prices, etc.), steered also by policy-driven commitments like coal decommissioning campaigns, voluntary country climate pledges and European emission targets [2].

Uncertainties on the generation side, together with the progressive network and market integration at a pan-European level, may increase the need for ancillary services and balancing reserves. Moreover, the security of the electricity supply may be jeopardized due to insufficient firm generation or transmission capacity. Security of supply concerns, including energy dependence on foreign resources [4], are gaining strong political and economic importance, as shown, for instance, by the emerging needs and employment of SR or other types of CRMs in Europe. In this context, it is crucial to monitor the adequacy of the system in future scenarios, i.e. its capability to always meet the demand for electricity every hour of the year. Several system adequacy processes and methodologies have been established under the umbrella of the ENTSO-E, in compliance with the European Electricity Regulations.

1.1 The concept of Adequacy Forecasting

The concept of "adequacy" for the electricity sector adopted and reported here is the one validated by the ENTSO-E [16]. Adequacy relies upon the need for a continuous balance on the grid between available generation and demand for electricity via the network infrastructure. When it comes to adequacy forecasting, both the supply and demand side estimates can be assessed either through a purely deterministic methodology or through the combination of a deterministic forecast, together with stochastic uncertainties. Such uncertainties arise from climatic variables and their influence on RES infeed and load profiles, as well as unpredictable forced outages affecting transmission assets and generating units. Figure 1.1 provides a condensed yet comprehensive overview of the concept of generation adequacy, showing the main inputs involved, with a general distinction between the ones usually gathered via a deterministic forecast and the ones implying a certain degree of stochasticity. Different methodologies

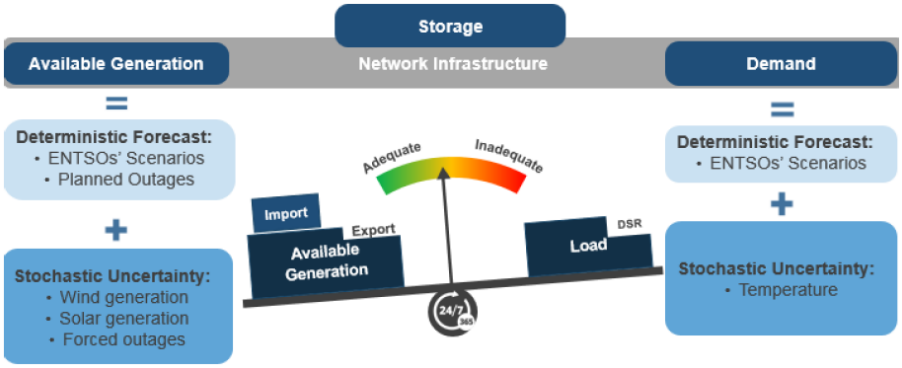

Figure 1.1: Adequacy Balance according to ENTSO-E [16].

have been developed, as well as a wide range of tools and software to accommodate the aforementioned complexities, depending on the specific purpose of each adequacy study and its time horizon. When stochastic variables are taken into consideration utilizing different techniques, e.g. Monte Carlo simulations or stochastic optimization, the results are usually expressed in terms of "expected" or "averaged" adequacy metrics. The common practice is to report at least the estimates for the EENS and the LOLE, as defined later in Section 3.2.4. Accordingly, a region of the system is deemed "adequate" when the expected indices lie below a certain threshold, defined as Reliability Standard (RS). In Europe, setting the RS is usually a prerogative of Member States, whereas a common methodology has been recently developed by ENTSO-E, followed by ACER's amendments and final approval [17].

1.2 Key Adequacy Processes in Europe

Within the regulatory framework of the CEP [9], Article 23 of the Regulation (EU) 2019/943 of the European Parliament and of the Council of 5 June 2019 on the internal market for electricity (often referred to as the new "Electricity Regulations") [18] and other directives, invest ENSTO-E with multiple mandates. These include

from 2021 a yearly European Resource Adequacy Assessment (ERAA) [8] to monitor generation adequacy in the European electricity sector for the mid to long-term horizon (up to ten years ahead). European Member States shall also monitor resource adequacy within their countries based on existing European processes (e.g. the ERAA), and complement them, if needed, leveraging a National Resource Adequacy Assessment (NRAA), as defined in the Article 24 of the Electricity Regulations [18].

Distinct assessments occur within ENTSO-E or other multilateral frameworks, which engage several European TSOs and other stakeholders. They address generation adequacy at a pan-European or macro-regional level and span over a wide range of time horizons, from one week ahead up to twenty years in the future. Figure 1.2 presents, in a nutshell, the processes listed below, which are described in more detail in a paper recently published [19].

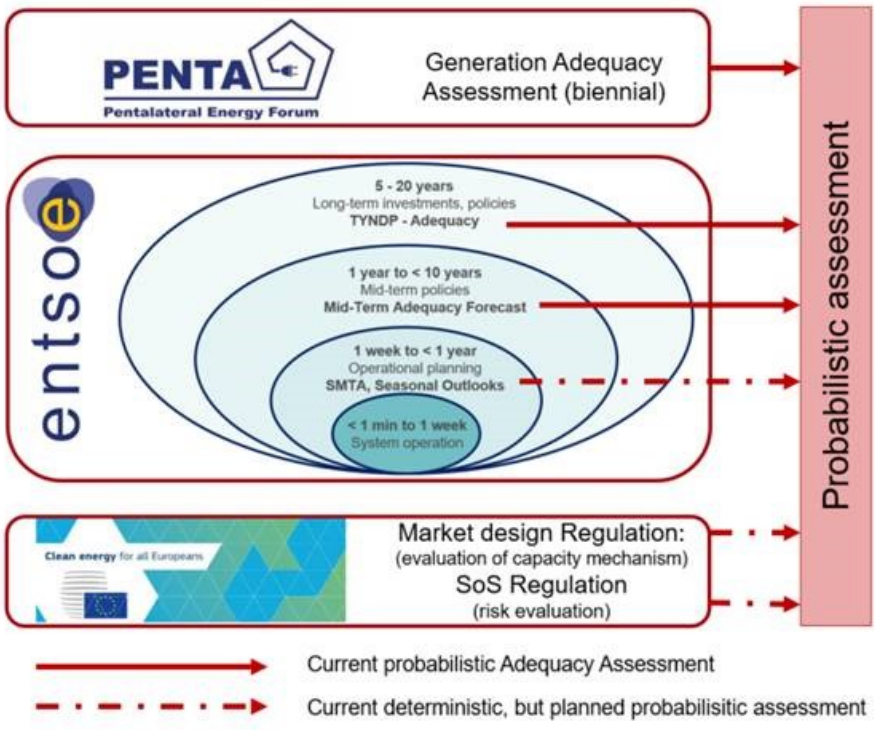

Figure 1.2: Overview of existing adequacy processes in Europe [19].

The key probabilistic adequacy processes are (i) the TYNDP [20], a bi-annual process assessing transmission adequacy for the European grid up to 20 years ahead; (ii) the MAF [5, 6, 7], a yearly process evaluating generation adequacy up to 10 years ahead (soon to be integrated and expanded within the new ERAA); (iii) the Pentalateral Energy Forum (PLEF) adequacy assessment [21, 22, 23], a bi-annual process which brings together Central-West European TSOs, National Regulatory Authorities (NRAs) and representatives from the Energy Ministries.

The key deterministic adequacy processes include (i) the Winter and Summer Outlook Reports (WOR & SOR) [24, 25], two seasonal outlooks carried out for the upcoming winter and summer months respectively; (ii) the Short-Term Adequacy Assessment (STA), a weekly process assessing adequacy for the following one. Staring in 2020, both the SOR and WOR will be performed through a probabilistic assessment, leveraging a methodology similar to the one of the MAF.

Aside from multilateral processes, NRAAs target country-specific scenarios and sensitivities. Examples are the French "Bilan prévisionnel" [26] and the "Adequacy and flexibility study for Belgium 2020-2030" [27].

Chapter 2

Motivation and Framework

My thesis developed inside the framework of the ENTSO-E's Mid-Term Adequacy Forecast, which is the reference report and methodology for mid to long-term generation adequacy assessments in Europe. More precisely, the target was set on hydropower modelling within the MAF 2019 edition [7]. The following section presents the drivers and the research question, as well as the research methodology and the thesis structure.

2.1 Hydropower Modelling in Adequacy Assessments

The key role played by hydro reservoirs and PSPs during peak load hours is well known by TSOs. Hydro storage often provides the additional capacity required to meet the peak electricity demand, acting as the balance's needle to ensure the electricity supply. This is especially true for Austrian Power Grid AG (APG), the Austrian TSO and Control Area (CA) manager, which deals every day with the peculiar energy mix of Austria. The Austrian fleet of ROR and storage hydropower plants counts more than 10 GW of installed capacity (equal to around 50% of the total net generation capacity in 2019) and supplies around two-thirds of the total electric energy generated in the country every year. It follows that choosing an adequate hydropower modelling methodology is crucial in generation adequacy forecasting, which investigates the security of the electricity supply through the system capability to always meet the demand in future scenarios. Even minor differences in the set of assumptions and constraints concerning hydroelectric power modelling may lead to significant differences in terms of adequacy metrics and power supply.

A sensitivity analysis on hydro reservoir constraints, specifically concerning the reservoir level trajectories, was published in the MAF 2018 detailed report [16]. It evaluated the following cases: (i) "Strict Constraints", i.e. hard constraints imposed on the weekly reservoir trajectories; (ii) "Relaxed Constraints 1", i.e. relaxing the weekly constraints, replaced by monthly constraints; (iii) "Relaxed Constraints 2", i.e. relaxing all reservoir trajectories and imposing only the reservoir level at the start and at the end of the year. Figure 2.1 reports the results of the sensitivity on the LOLE for Belgium (BE), France (FR) and Northern Ireland (NI), for one of the five modelling

tools (VP5) used to perform the MAF 2018 simulations. It is noticeable that a more relaxed set of constraints allowed the tool to allocate the hydro storage resources more cost-effectively, avoiding up to 50% of the LOLE hours and hence their high unsupplied energy costs. Nevertheless, granting the tool with as much freedom as in the case of the "Relaxed Constraints 2" settings may lead to unrealistic modelling of hydro storage generation, thus making the results too optimistic and not trustworthy.

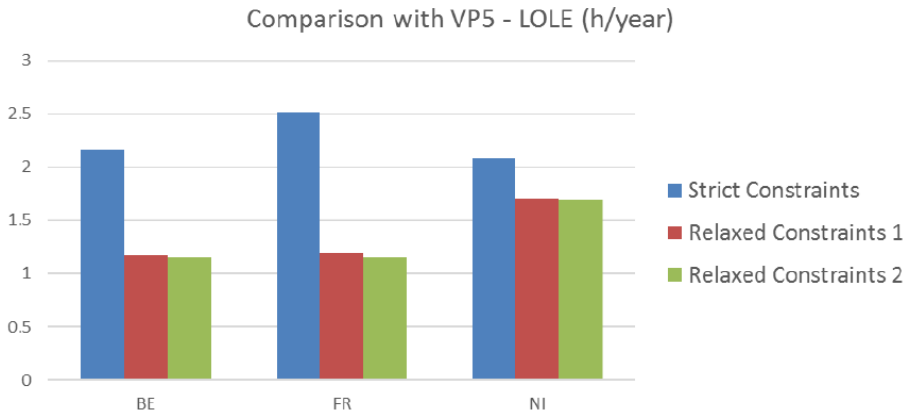

Figure 2.1: LOLE sensitivity on reservoir level trajectories [16].

2.2 Research Question

A substantial change in the hydropower modelling methodology was introduced in the MAF 2019 edition [10], for which a new hydro database was established in the PECD and used for the first time [11]. This new PECD Hydro database contained all the data for hydro energy inflows and the technical or historical climate constraints for hydropower generation. The major novelties, compared to the hydro database formerly used in the MAF 2018 edition, included a new methodology to infer historical time series for the natural inflows, for the first time provided for the 35 historical CYs consistently with the other PECD data. The previous edition only considered three possible hydrological scenarios, namely "dry", "normal" and "wet". New criteria for the categorization and aggregation of hydropower plants were also defined.

The introduction of this new hydro database was the main driver of my research. As an employee of APG and a member of the ENTSO-E MAF modelling team, I aimed to deepen the understanding of how the underlying assumptions and format of this new hydro database, thus of the new hydropower modelling methodology developed, affected the results of mid-term generation adequacy forecasts within the MAF 2019 framework. My analysis focused on the data and modelling for the target year 2025. The spotlight was naturally set on the peculiar case of Austria, the control region where APG operates.

My thesis specifically investigated the following research question:

what was the impact of the new PECD Hydro database on the Austrian hydropower dispatch in the Mid-Term Adequacy Forecasts?

The objective was not to set up a mere comparison between the old and new hydro datasets from a purely numerical perspective, but rather to dig into the explicit and implicit changes that this new hydro framework brought about in the hydropower modelling methodology and as a consequence reflected on the adequacy results. Trying to breakdown and address the research question clearly and comprehensively, I focused the assessment on three complementary and equally important aspects, which were mutually changed and affected by the adoption of the new database:

(i) The description of the new modelling methodology through which the new hydro data were processed and fed as input to the simulator, in comparison with the old hydro data structure and methodology used in the MAF 2018 edition.

(ii) The results of the Monte Carlo simulations and the evolution of the expected adequacy indices such as LOLE, EENS and LOLP.

(iii) The scrutiny of the power dispatch of the UCED solution, down to the hourly resolution, with a close focus on hydropower generation profiles and their impact on the likelihood and magnitude of load shedding events during periods of generation scarcity (i.e. when ENS occurs).

2.3 Research Methodology

I performed this analysis at the APG's premises, subsequently to the MAF 2019 process, adopting the same methodology and definitions reported in Chapter 3. To perform the simulations, I used A New Tool for Adequacy Reporting of Electric Systems (ANTARES) v6.1 [12], a large-scale multi-area Monte Carlo simulator, developed by RTE, the French TSO, and available open-source. The large magnitude of the full pan-European model, which included 50 market bidding zones and thousands of generating units, made it not suitable for my study. It would have been too complex to properly isolate and identify the impact of the sole new hydropower methodology since the effects would have been likely to be mitigated by the numerous cross-border interconnectors, as well as by thermal-dominated zones, where hydropower only counted as a minor share of the electricity mix.

Therefore, I identified and "carved out" ad hoc a suitable subset of the pan-European perimeter from the model. The research methodology followed six key steps:

1. The geographical boundaries were arbitrarily restricted to Austria (AT) and two neighboring bidding zones with high hydropower capacity, namely Switzerland (CH) and Italy North (ITN). Such a tri-lateral model was used as a "test bench" to run the Monte Carlo simulations.

2. The ANTARES v6.1 simulator was set up and calibrated for the target year 2025 using the same input data and methodology as for the MAF 2019 process. The main variables and parameters were the installed generation capacity per technology type, the fuels and CO2 prices, the thermal unit characteristics, Demand Side Response (DSR), the RES availability and demand profiles, the data for the Net Transfer Capacities (NTCs), planned outages (maintenance schedule) of thermal units, and the parameters for the stochastic simulation of forced outages.

3. The analysis used the MAF 2018 hydro modelling methodology as a reference for the comparison. The structure of the hydropower input data and the corresponding modelling methodologies for ANTARES v6.1 were described and compared in detail. To isolate the impact of the new PECD hydro database, the old hydro data from the MAF 2018 edition could not be used as such. Instead, the same data collected for the MAF 2019 edition were reaggregated to fit the old MAF 2018 template and to comply with the old hydropower plant classification. The data granularity as well as the historical time series for hydro energy inflows were also adapted to the old methodology through a clustering process. This allowed to exclude any difference in the results driven by the updated estimates of the installed capacities and hydro inflows, with respect to the 2018 expectations.

4. Two Monte Carlo simulations were performed based on two versions of the same tri-lateral model, which were identical except for the data and modelling of hydropower generation. The reference model was set up with the MAF 2018 hydro data and methodology, whereas the other one used the new PECD Hydro data and methodology developed for the MAF 2019.

5. The results from the two models were analyzed and compared with multiple approaches, ranging from averaged yearly results down to the hourly UCED profiles. The comparison of the results was conducted with the support of a visualization tool that I developed in the R environment [13].

6. Conclusive statements were made thanks to the insights provided by the analysis of the results and the detailed benchmark of the hydropower modelling methodologies. Reflections on the criticalities identified as well as on future work and developments on the topic were also placed.

2.4 Thesis Structure

It follows the structure of the thesis:

- Chapter 1 introduces the landscape of adequacy forecasting and its definition according to the ENTSO-E. It also summarizes the general framework and the key generation adequacy processes in Europe.

- Chapter 2 presents the drivers for my thesis and the research question. It includes the description of the six steps followed as the research methodology to setup the modelling tool and analyze the results.

- Chapter 3 summarizes the key elements of the ENTSO-E MAF 2019 framework. It includes a description of the main input data, as well as the modelling methodology to set up the Monte Carlo simulations. It also defines the adequacy metrics typically reported in mid-term adequacy studies, namely EENS, LOLE and LOLP.

- Chapter 4 reports the main features of ANTARES v6.1, the open-source modelling tool used to perform the required Monte Carlo simulations. It includes a description of the embedded Hydro Energy Manager which performs the preallocation of hydro storage energy resources. A synthetic mathematical formulation of the UCED optimization problem is also provided.

- Chapter 5 describes the structure and the key data available in the hydro database used in the MAF 2018 compared with the new PECD Hydro database introduced in the MAF 2019. The criteria used to categorize and aggregate the hydropower units are also reported. The heuristic followed to adapt the new hydro data to the old framework is reported, including summary tables with the key hydropower inputs for the three market nodes.

- Chapter 6 provides a detailed description of the "Hydro 2018" and "Hydro 2019" modelling methodologies for hydropower generation developed for ANTARES v6.1 and used in the MAF 2018 and MAF 2019 editions respectively. Each methodology includes the handling process of the hydro data to be fed as input to the modelling tool.

- Chapter 7 elaborates on the results from the tri-lateral models and their comparison. Both the adequacy metrics and hydropower generation are analyzed with different approaches in terms of time resolution and visualization supports.

- Chapter 8 closes the thesis pondering on the insights gathered on the research question, as well as the lessons learnt on hydropower modelling in ANTARES v6.1. Statements on envisaged future work and developments are also placed.

Chapter 3

The MAF 2019 Framework

The Mid-term Adequacy Forecast process occurs every year under the direction and coordination of ENTSO-E. It aims to provide policymakers and stakeholders with a state-of-the-art forecast of the generation adequacy status of the pan-European electricity network, targeting one or more years in the mid-term future horizon (from 1 up to 10 years ahead). The target years for the MAF 2019 edition were 2021 and 2025. The MAF 2019 edition was the framework for my thesis, from which it inherits the modelling assumptions, methodology and input data. This chapter provides a synthetic overview of these matters, while a detailed and complete description is available in the official MAF 2019 documentation published on ENTSO-E website [7, 10].

3.1 MAF 2019 Input Data

The cores of the MAF process are the PEMMDB and the PECD: a comprehensive set of data provided by the European TSOs, which are collected, validated and structured by ENTSO-E in different templates. These data are available for each of the 50 explicitly modelled bidding zones (i.e. market nodes) which constituted the geographical perimeter of the MAF 2019 study.

3.1.1 PEMMDB Data

The PEMMDB database collected detailed data concerning the different generation capacities available in each bidding zone, including:

- Data for the thermal generating units: net generation capacity, net conversion efficiency, commissioning and decommissioning date, capacity derating, must-run obligations, ramp-up and ramp-down constraints, minimum up and down time, startup costs, fixed and variable costs, CO_2 emission rates, planned outages, forced outage rates, etc.

- Data for RES deployed capacity: best estimates for the future year-by-year expansion of solar photovoltaic, solar thermal, wind onshore, wind offshore and miscellaneous.

– Availability of battery storage and DSR.

– Fixed exchanges with non-explicitly modelled market nodes (outside the ENTSO-E perimeter).

– Data for the demand forecasting: the evolution of industrial, household and transport consumption, the growth of electric vehicles, the evolution of installed heat pumps and others.

The MAF 2019 process used two versions of the PEMMDB database, referred to as PEMMDB 2.1 and PEMMDB 3.0. Their main difference was the level of aggregation of thermal units: data were aggregated per fuel technology type (e.g. Combined Cycle Gas Turbine, Lignite New, Light Oil, etc.) in the PEMMDB 2.1 database, while the PEMMDB 3.0 database reported unit-by-unit specific data, hence with higher granularity. The models I used for my thesis leveraged the PEMMDB 2.1 database. An aggregated summary of the database was published by ENTSO-E and it is available for download [28].

3.1.2 PECD Data

The PECD database, developed in cooperation with the Technical University of Denmark, collected the climate-dependent data necessary to model RES availability. Such data were delivered per each bidding zone and reported as time series for 35 historical Climate Years (CYs). The historical climate data considered in the MAF 2019 ranged from 1982 until 2016, including:

– Time series of capacity factors for solar photovoltaic and solar thermal generation at an hourly resolution.

– Time series of capacity factors for wind onshore and wind offshore generation at an hourly resolution.

– Historical temperature profiles used for demand forecasting.

– Introduced in the MAF 2019: historical time series of hydro energy natural inflows, available at different time resolutions, according to the new classification of hydropower plants.

– Introduced in the MAF 2019: historical time series of hydropower constraints (e.g. reservoir level trajectories, minimum and maximum power output, etc.), available at different time resolutions, according to the new classification of hydropower plants.

The wind and solar time series in terms of available power infeed were computed simply by multiplying the installed capacity of each target year (e.g. 2025) by the capacity factors available in the PECD. Instead, hydro inflows were provided already in terms of available power infeed according to the installed capacities of the target year considered. The detailed climate-dependent data for hydropower generation, i.e.

inflows and constraints, were collected and provided in specific templates of the PECD database, which are hereafter referred to as "PECD Hydro" or simply "hydro data". The PECD wind and solar data for the MAF 2019 were published and are available for download [29], while a detailed description of the PECD Hydro data is presented in Section 5.2.

3.1.3 Electricity Demand and Additional Inputs

The hourly time series for the demand forecasts were computed starting from historical load profiles and climate data. This task was performed leveraging the TRAPUNTA tool [30], a temperature regression and load projection model. In short, historical data were analyzed to retrieve load profiles, which considered also the sensitivity of the demand with respect to the ambient temperature (and other PECD climatic data). Moreover, the profiles were rescaled and reshaped according to the impact on the demand of the expected values for sectoral consumption, electric vehicles, heat pumps, etc. as collected in the PEMMDB database. The country-specific holiday calendars were also considered. The final deliverables were 35 climate-dependent forecasted yearly demand profiles, at an hourly resolution. Each historical Climate Year of the simulation was finally constituted by consistent time series of solar, wind, hydro and demand forecasts. Aggregated demand profiles used in the MAF 2019 were also published [28].

Additional input data necessary to perform the assessment were: estimates for the CO_2 and the fuel prices, time series for the maximum cross-border commercial exchanges, commonly referred to as NTCs, and forced outage rates on high voltage cross-border interconnectors.

3.2 Delivering Results

To deliver consistent and robust results, five modelling tools (i.e. ANTARES v6.1 [12], BID3 [31], GRARE [32], PLEXOS [33] and POWRSYM [34]) were used in parallel to perform the analysis, delivering the expected adequacy metrics through Monte Carlo simulations. Both the MAF 2019 averaged and tool-specific results were published [35].

3.2.1 Underlying Assumptions

The key set of assumptions within the MAF 2019 methodology were [10]:

1. Perfect market competition.
2. Elasticity of demand to price limited to the explicit DSR potential.
3. Day-ahead/Intraday market perspective.
4. Perfect foresight of RES, hydro inflows, forced outages and demand.

The pan-European system was therefore modelled as an interconnected network of bidding zones (market nodes), whose exchanges were ruled by the NTC commercial limits (accounting for the "N-1" and other operational security measures) collected in the input data. Since real-time and contingent balancing operations were out of scope, the chosen time step for the simulation was one hour (8760 per year), consistently with the day-ahead market approach. It follows that balancing reserves including Frequency Containment Reserves (FCRs), Automatic Frequency Restoration Reserves (aFRRs) and Manual Frequency Restoration Reserves (mFRRs) were excluded from the available generation capacity. Since they are designed for and dedicated to different needs of operational security, it is TSOs' common position to deem balancing reserves as not suitable to cope with structural generation adequacy, especially in mid to long-term adequacy forecasting. The exclusion of reserves was achieved in the simulations simply inflating the hourly demand by their contracted capacity, or by reducing the maximum hydropower generation by the "reserved volume". Instead, Replacement Reserves (RRs) were treated and modelled in the same way as any other capacity available on the market.

3.2.2 The Optimization Problem

The optimization problem can be generally identified and formulated as a large-scale Mixed-Integer Linear Programming (MILP) problem, also referred to, for this specific case, as "Optimal Unit Commitment and Economic Dispatch" (UCED). The tools aim to find the optimal power dispatch to fulfill the hourly electricity demand, considering the marginal costs of the available generation units within a system cost minimization problem. As usual in optimization problems, the least-cost solution needs to comply with several technical and market constraints, either "hard" (i.e. non-violable) or "soft" (i.e. potentially violable at the expense of high-cost penalties), rising from the generation and transmission assets. Nevertheless, in the MAF 2018 and 2019 methodologies the constraints on ramp-up, ramp-down, minimum up and down time of thermal units were relaxed. Therefore, the simplified optimization problem could be classified and solved accordingly as a pure Linear Programming (LP) assessment.

It is important to stress that the MAF aimed to perform a generation adequacy assessment, based on many possible combination of future contingencies, rather than to deliver the optimal market clearance. For this purpose, the system was set up with a very high Value of Lost Load (VoLL), which within the simulation can be simplistically considered as the marginal cost of Energy not Served (ENS). Since the VoLL was higher than all the marginal costs of generating units, it follows that the least-cost solution was implicitly equivalent to the least-ENS solution for the system. To reduce the magnitude and the complexity of the problem, the tools performed a weekly breakdown of the yearly period, so that the hourly optimal UCED solution was delivered week by week. Moreover, hydro storage generation required a preoptimization process to allocate resources and comply with the reservoir trajectories collected in the PECD Hydro data. This preoptimization was performed on a monthly basis, down

to the weekly or even to the daily one, following different methodologies or heuristics peculiar to each modelling tool. Other differences in the model structure and solver, as well as in the subproblem partitioning, stood within each of the five tools.

3.2.3 Monte Carlo Samples

The effectiveness and efficiency of Monte Carlo simulations to estimate the adequacy metrics can be identified in the large number of variables, potentially not fully independent, which need to be represented and assessed. Reporting from Doquet et al. [36]: assuming that a specific combination of a given winter cold spell event (W) with a simultaneous low generation availability configuration (G) would lead to X MW of ENS during Y hours; the expected behavior of a suitable simulator should be not only to compute with the desired accuracy the values of X and Y, but also to assess with similar accuracy the probabilities of occurrence, i.e. $P(W)$ and $P(G)$. In the case of correlated events, the complexity would further increase, given that $P(W\&G) \neq P(W) \times P(G)$. Moreover, it can be desirable from the simulator to also assess all the other possible instances of W_i and G_i and to compute accordingly the values of $P(W_i)$, $P(G_i)$, X_i and Y_i. It has been found that for this typology of problems, the analytical convolution of random events was highly complex and led to weak numerical accuracy. That is why Monte Carlo simulators have, in applications such as generation or transmission adequacy assessments, outperformed probabilistic approaches based on combinatory techniques.

In the MAF 2019, the simulated yearly scenarios were labelled as Monte-Carlo Years (MCYs). Every MCY was characterized on the one hand by certain climatic variables, embedded in the input time series of wind, solar, hydro and demand profiles, and constituting a full "Climate Year" (CY). On the other hand, a so-called "forced outage pattern" was added, representing the random occurrence of forced outages of thermal units and transmission lines. Figure 3.1 depicts the Monte Carlo sampling method adopted in the MAF 2019 simulations, where M was equal to the 35 historical CYs (i.e. 1982 – 2016), while N was the number of different forced outage patterns. N was defined independently per each tool to achieve convergence of the results in a reasonable computational time while granting a good representation of the forced outage rates.

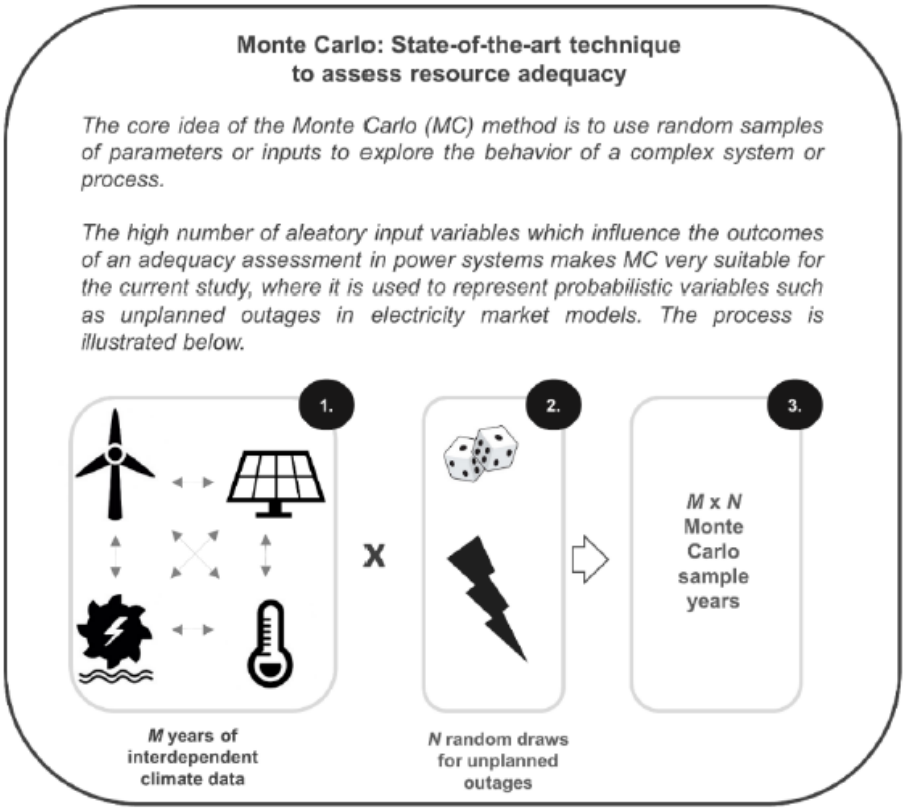

Figure 3.1: Monte Carlo approach to assess resource adequacy, in a nutshell [10].

3.2.4 Key Adequacy Metrics

Three main adequacy indices are usually reported to assess and evaluate the expected adequacy status of the system in the mid to long-term horizon, with a focus on the generation side. The following definitions are edited from [16] and [10]:

- *Expected Energy Not Served (EENS) [GWh/year]* is the averaged energy not supplied on a yearly basis due to system inadequacy, i.e. when the demand is exceeds the available internal generation plus the import capacity. The EENS is usually computed as the average of the ENS over a number of Monte Carlo years. Accordingly, it is a metric that quantifies the lack of security of supply and it is mathematically described as:

$$\mathrm{EENS} = \tfrac{1}{\mathrm{N}} \sum_{\mathrm{j} \in \mathrm{S}} \mathrm{ENS_j} \ ,$$

  where ENS_j is the energy not supplied by the system state j (j $\in$ all simulated system states S) associated with a loss of load event in one of the Monte Carlo years of the simulation. N is the total number of Monte Carlo years sampled.

- *Loss of Load Expectation (LOLE) [h/year]* is the average number of hours per year in which the available generation (plus imports) is not sufficient to cover the totality of the electricity demand in a region:

$$\mathrm{LOLE} = \frac{1}{\mathrm{N}} \sum_{\mathrm{j} \in \mathrm{S}} \mathrm{LLD_j} \ ,$$

where LLD_j is the Loss of Load Duration of the system state j (j $\in$ all simulated system states S) associated with a loss of load event in one of the Monte Carlo years of the simulation. N is the total number of Monte Carlo years sampled. It should be noted that LLD occurring during each Monte Carlo year is usually reported as an integer number of hours, due to the hourly resolution of the simulation methodology. It follows that LOLE is not a suitable index to indicate the severity and magnitude of the energy deficiency, but rather a counter.

- *Loss of Load Probability (LOLP) [%]* is the probability of occurrence of a load shedding event during a designated time frame. Different tools may have different methods to report LOLP. Nevertheless, a general definition of the LOLP resulting from a Monte Carlo simulation can be given as:

$$\mathrm{LOLP_t} = \frac{MCY(\mathrm{LLD_t}>0)}{\mathrm{N}} \ ,$$

where $MCY(LLD_t > 0)$ is the number of Monte Carlo years in which at least one load shedding event has occurred (i.e. $LLD_t > 0$) during the designated timeframe t. N is the total number of Monte Carlo years sampled.

3.2.5 Result Consolidation

The five tools covered the same geographical perimeter and were fed with the same input data. The only difference was that three tools were using the PEMMDB 2.1 data, with thermal units aggregated by fuel technology, while the remaining two were using the PEMMDB 3.0, with granular unit-by-unit data for thermal plants.

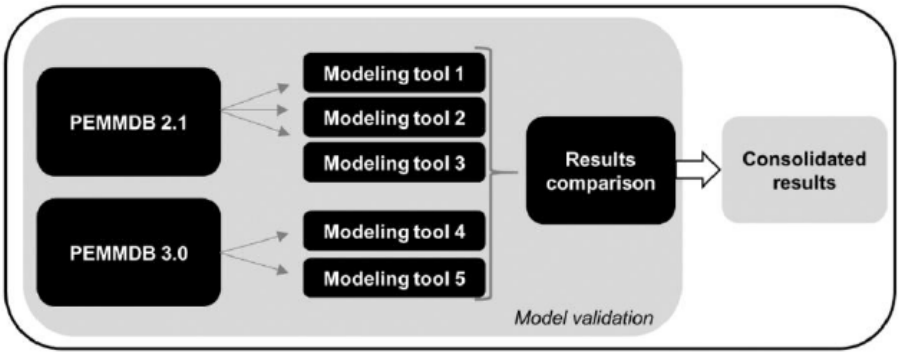

Figure 3.2: Iterative result consolidation process within the MAF 2019 [10].

Figure 3.2 shows the four-step iterative process adopted during the modelling activities to ensure that the results delivered by each tool were as aligned and consistent as possible among each other.

1. Execution of the simulation and delivery of the averaged yearly results.
2. Scrutiny of the results (all five tools) in the form of comparison charts.

3. Discussion and feedback within the MAF modelling team.

4. Definition of specific actions concerning the development of the models or the improvement of the input data quality.

The iterations started with the first model calibration and proceeded with increasing modelling and resolution complexity, until the delivery of the very last consolidated results. The final results published in the MAF 2019 executive report [7] were the average of tool-specific results, after removing outliers, if occurring for any of the bidding zones (e.g. one tool showing out of scale value of EENS compared to the other four). The detailed results for each tool were also published as an appendix to the MAF 2019 report [35].

Chapter 4

ANTARES Simulator

A New Tool for Adequacy Reporting of Electric Systems (ANTARES) is a multi-area large-scale Sequential Monte-Carlo Simulator (SMCS), whose first version was developed by the French TSO RTE between 2005 and 2008. It is specifically designed for multipurpose adequacy and market modelling of energy systems. ANTARES' first use in a multilateral operational study dates to 2007, as part of the technical toolbox adopted to fulfill the objectives set in the PLEF Memorandum of Understanding [37], although the first public Generation Adequacy Assessment report was released in 2015 [21]. After this first-hand experience, ANTARES has been used, up to the present day, in many diverse studies in the electric power sector, including ENTSO-E processes (e.g. [7] and [20]), as well as NRAAs [27, 26]. ANTARES v6.1 is the modelling tool I used to perform the simulations presented in my thesis.

The choice of a probabilistic (or hybrid deterministic-probabilistic) approach in mid to long-term adequacy studies was motivated in Chapter 3, among other reasons, due to the high variability of RES climatic variables, as well as the unpredictable occurrence of forced outages either affecting the generation facilities or grid assets. The ANTARES Monte Carlo simulator was designed as a (i) sequential and (ii) multi-area large-scale. These needs arise especially considering its application to multilateral adequacy studies [36]:

(i) Sequentiality arises from the very nature of adequacy problems, within which, for instance, the availability status of a certain generator is not independent of its status in adjacent hours. This time dependency affects indeed most of the variables involved, including demand time series, as well as hydro, wind and solar power availability. The simulator has therefore to assess the different time steps of the optimization through a chronological and sequential procedure, keeping an internal memory of the passing of time.

(ii) Climatic variables can be assumed, for "local-area" studies, as time-dependent but spatially univariate. Instead, for "large-area" studies, the same climatic variables should be treated as potentially correlated multivariates. ANTARES, as a multi-area SMCS, is designed to be capable of taking into account also the spatial correlation between the meteorological variables of the geographic regions in the

model. This applies to all the macroclimatic variables, i.e. wind profiles, solar radiation and hydrological data.

4.1 ANTARES Simulation Session

The ANTARES software comes with a practical Graphical User Interface (GUI) which allows the user to control, set and update most of the input data and the parameters used for the simulation. A typical ANTARES simulation session counts several sequential steps, whereas differences apply according to the nature of the study to perform. The main steps, as reported by the ANTARES v6.1 documentation [38], are listed below and displayed in Figure 4.1:

1. GUI session dedicated to insert, update, or control the input data. These include the ready-made time series, the settings for the internal probabilistic time series generator, the settings for the internal hydro manager, parameters concerning the thermal fleet, etc. The grid network with nodes and links constituting the spine bone of the model can also be designed.

2. GUI session to set the sampling preferences, i.e. the overall number of Monte Carlo years to be generated and assessed, as well as the sampling approach. Specifically, the scenario builder can be set to follow almost any user-defined approach, spanning from a completely deterministic approach (i.e. time series $\hat{x}$ for hydro, time series $\hat{y}$ for solar, time series $\hat{z}$ for wind, etc.) to a completely random approach (i.e. random sampling of time series x_i, y_i, z_i among the ones available per each generation type).

3. Core optimization session assessing the Monte Carlo years sampled. The optimization leverages a Hydro Energy Manager and a power schedule & unit commitment optimizer.

4. Final session dedicated to export and analyze the results delivered by the optimization.

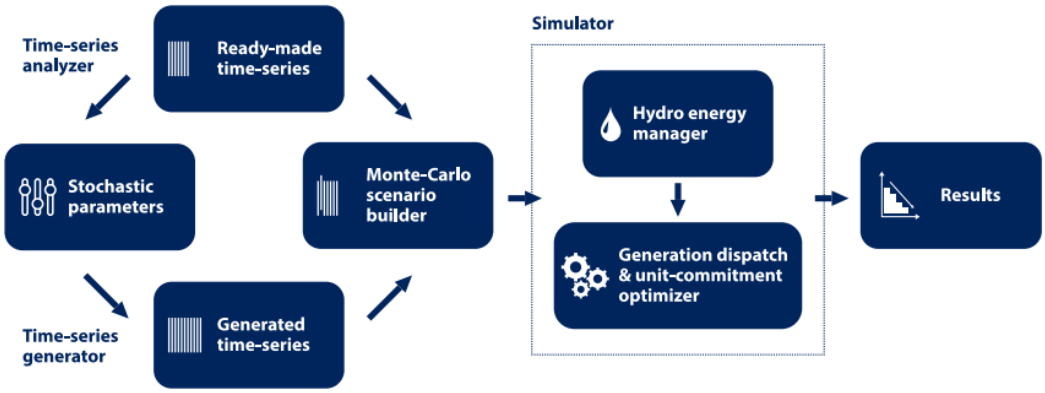

Figure 4.1: Functional view of ANTARES v6.1 simulation sessions [38].

The present chapter will investigate in further detail only the Monte Carlo scenario builder, the Hydro Energy Manager and the power schedule & unit commitment optimizer, which are considered of higher interest given the framework of my work.

4.2 Monte Carlo Scenario Builder

Each element of the sample within an ANTARES simulation is a set of hourly availability time series, covering all the problem dimensions per each modelled area (native demand, available wind and solar power, hydroelectric energy and availability of thermal power plants). Every set of time series covers a time span of one year (8760 hours) and constitutes a so-called Monte Carlo year (MCY). The MCY definition and assembly depend on the methodology of the assessment and may follow a hybrid deterministic-probabilistic approach (as in the case of the MAF), leveraging either external data and tools or internal functions to prepare the required time series. The size of the sample, i.e. the total number of MCYs, is also simulation-dependent and it must count enough sample years to grant the statistical convergence of the results, whereas it is usually the outcome of a trade-off between the computational time and the accuracy of the solution. The Monte Carlo year sampling in compliance with the MAF 2019 methodology is described in Section 3.2.3, while a short comment on the requirements for statistical convergence of the results from the model I developed is given in Section 7.1.

4.3 Hydro Energy Manager

Modelling a consistent and accurate hydropower generation dispatch requires to face several challenges. On the one hand, the generation of run-of-river plants can be simulated with enough accuracy based on the estimated hydro inflows, therefore similarly to how wind and solar generation are modelled. The real-life operation of storages and PSPs is on the other hand multifaceted. This is due to the main drivers of hydro storage reservoir management, which are not only the natural inflows and seasonal climatic patterns but most importantly the economic considerations and bidding strategies of hydropower plant owners. Storage generation is highly price-driven and may vary significantly even from a day-by-day perspective, making it more complex to model and forecast.

To better accommodate this twofold climate and price-driven nature of hydro storage dispatch, the ANTARES v6.1 Hydro Energy Manager performs a first preallocation of the total annual hydroelectric energy availability. It is based on (i) the expected inflows, (ii) the reservoir capacity, and (iii) the net residual load of the bidding zone served by the very reservoir. The net residual load is computed starting from the market node native demand, from which wind, solar, other RES and must-run thermal generation is directly deducted.

4.3.1 Breakdown Parameters

The preallocation of hydroelectric energy into monthly and daily energy lots follows a load-proportional heuristic based on 5 parameters, which should be estimated upon average historical data (at least 10 years suggested) per each market node:

- Inter-monthly generation breakdown: $\alpha = \frac{log(GEN_{M,RES})}{log(LOAD_M)}$;
- Inter-monthly correlation;
- Inter-daily generation breakdown: $\beta = \frac{log(GEN_{D,RES})}{log(LOAD_D)}$;
- Intra-daily modulation: $\gamma = \frac{Daily\ max\ power}{Daily\ mean\ power}$.

where $GEN_{M,RES}$ and $GEN_{D,RES}$ are the monthly and daily measured historical hydro storage generation. $LOAD_M$ and $LOAD_D$ are the monthly and daily net residual loads respectively.

ANTARES v6.1 has an internal reservoir management functionality that can be optionally activated for each market node and let the software fully optimize the reservoir usage according to the total yearly hydro storage energy availability, the reservoir capacity, and the minimum, average and maximum reservoir level trajectories of each month.

4.3.2 Monthly Hydro Energy Preallocation

In more detail, the monthly hydro energy breakdown is performed as follows [38]:

1. If the reservoir management functionality is set to *off*, the user shall give as input the total monthly reservoir energy availability, including inflows and reservoir internal stored energy usage, which are treated as fixed energy lots to be generated within each month and no further redistribution between different months occurs. The Hydro Energy Manager performs only the daily hydro energy preallocation as described in Section 4.3.3.

2. If the reservoir management functionality is set to *on*:

   (a) The user shall input only the monthly natural energy inflows into the reservoir, which are summed to obtain the total annual hydro reservoir energy availability. The software proceeds setting the optimal energy targets for the months, which are assumed to be not linearly related to the monthly net residual load, but rather proportional to the net load of the month at

the power of the inter-monthly breakdown (α):

$$ENE_{Y,RES}[MWh] = \sum_{year} INF_{M,RES} = \sum_{year} \widehat{ENE}_{M,RES},$$
$$\frac{\widehat{ENE}_{M,RES}}{\widehat{ENE}_{M+1,RES}} = \left(\frac{LOAD_M}{LOAD_{M+1}}\right)^{\alpha};$$

where, per each specific market node, $\widehat{ENE}_{M,RES}$ [MWh] are the computed monthly energy targets for the storage generation. $INF_{M,RES}$ are the user inputs for the monthly inflows. $LOAD_M$ is the net residual load of the month and α is the inter-monthly breakdown parameter.

(b) The software computes the actual monthly reservoir energy lots by minimizing the absolute deviation from the optimal energy targets computed in (a), solving a linear optimization problem with the following formulation.

$$min \left| ENE_{M,RES} - \widehat{ENE}_{M,RES} \right|, \text{ subject to:}$$

energy balance (year): $\sum_{year} INF_{M,RES} = \sum_{year} \widehat{ENE}_{M,RES} = \sum_{year} ENE_{M,RES}$;

energy balance (month): $INF_{M,RES} - ENE_{M,RES} = L_{M+1,RES} - L_{M,RES}$;

reservoir level soft constraint: $L^{min}_{M,RES} \leq L_{M,RES} \leq L^{max}_{M,RES}$;

reservoir level hard constraint: $0 < L_{M,RES} < CAPA_{RES}$;

where $ENE_{M,RES}$ are the actual computed monthly energy lots. $L_{M,RES}$ are the monthly reservoir levels, whereas the superscripts min and max denote the lower and upper bound reservoir level trajectories given as input by the user. $CAPA_{RES}$ is the reservoir capacity.

From the formulation of the annual and monthly hydro energy balance, it is possible to evince that all and only the annual energy inflows into the reservoir constitute the total annual available energy. This implies the following conservative assumption:

$$\sum_{year} (L_{M+1,RES} - L_{M,RES}) \approxeq 0 \, .$$

The reservoir level soft constraint can be violated at a high-cost penalty. The reservoir level hard constraint must always be respected by the solver, as it represents a strict physical or technical limitation.

4.3.3 Daily Hydro Energy Preallocation

The daily hydro energy preallocation is always performed by ANTARES v6.1, regardless of the *on/off* status of the reservoir management functionality. A similar procedure as the one described for the monthly preallocation occurs also for the daily hydro energy

breakdown [38].

(a) The sum of the daily energy targets has to be consistent with the actual monthly targets $ENE_{M,RES}$ computed by the monthly hydro energy preallocation, or directly with the user monthly input if the reservoir management functionality is set to *off*:

$$ENE_{M,RES}[MWh] = \sum_{month} \widehat{ENE}_{D,RES},$$
$$\frac{\widehat{ENE}_{D,RES}}{\widehat{ENE}_{D+1,RES}} = \left(\frac{LOAD_D}{LOAD_{D+1}}\right)^{\beta};$$

where, per each market node, $\widehat{ENE}_{D,RES}$ [MWh] are the computed daily energy targets for hydro storage generation. $LOAD_D$ is the net residual load of the day and β is the inter-daily breakdown parameter.

(b) Again, the tool computes the actual daily reservoir energy lots by minimizing the absolute deviation from the optimal energy targets computed in (a), solving the LP problem:

$$min \left| ENE_{D,RES} - \widehat{ENE}_{D,RES} \right|, \text{ subject to:}$$

monthly energy constraint: $\sum_{month} ENE_{D,RES} \leq \sum_{month} \widehat{ENE}_{D,RES} = ENE_{M,RES}$;

maximum power constraint: $0 \leq ENE_{D,RES} \leq P_{max,D} \times 24$;

where $ENE_{D,RES}$ are the actual computed daily energy targets. $P_{max,D} \times 24$ indicates the technical limit to the maximum daily generation.

When $\sum_{month} ENE_{D,RES} < \sum_{month} \widehat{ENE}_{D,RES}$, it follows that the sum of the actual daily lots is lower than the actual preallocated energy for the month. Additional system costs may occur due to the necessary spillage of the excess energy if the cost of spilled energy (a user-defined parameter) is set to a value greater than zero.

The intra-daily modulation parameter (γ) also affects the detailed dispatch optimization within each day, since it poses an upper limit to the maximum power (if dispatched at least for 1 h during the day):

$$1 \leq \frac{P_{max,D}}{P_{mean,D}} \leq \gamma \leq 24, \tag{4.1}$$

where $P_{max,D}$ is the maximum dispatched power during the day and $P_{mean,D}$ is the average daily power generated from the same reservoir.

The daily energy budgets resulting from the preallocation are delivered to the power schedule & unit commitment optimizer as an input to the UCED optimization. The

power schedule & unit commitment optimizer takes care of the price-dependent factors driving hydro storage and PSP generation, thus completing the hydro optimization.

4.4 Power Schedule & Unit Commitment Optimizer

ANTARES v6.1 features two main optimization modes, namely the "Adequacy" and the "Economy" modes, which are designed to address fast adequacy assessment or accurate UCED optimization respectively. The GUI allows the user to define the desired level of complexity of the simulation, according to the requirements. Table 4.1 shows the standard configuration modes [39]:

Optimization mode	Adequacy	Simplified Economy	Economy-Fast	Economy-Accurate
Power Availability	✓	✓	✓	✓
Power Bid	✓	✓	✓	✓
Overall Reserve	✓	✗	✓	✓
Spinning Reserve	✗	✗	✓	✓
Min stable power	✗	➜	✓	✓
Start-up cost	✗	➜	➜	✓
Min up/down time	✗	➜	✓	✓
No Load Heat cost	✗	➜	➜	✓

✓: Done	➜: Done ex-post	✗: Skipped

Table 4.1: System complexity in different ANTARES optimization modes [39].

4.4.1 Economy Mode

The Economy mode targets system cost minimization problems, typically to deliver a least-cost UCED with an hourly resolution and throughout the year. It is the mode used for the MAF simulations, as well as to deliver the results presented in my thesis. Concerning the standard "Economy-Accurate" mode in Table 4.1, reserves were not considered according to the assumptions in Section 3.2.1, while no-load heat costs were not relevant for the assessment. Moreover, economic optimization is performed under the hypothesis of perfect market behavior, which allows formulating the problem with MILP. The solver minimizes the overall costs of the system dispatch while complying with the following main directives:

- Wind, solar and other RES are considered as cost-free resources and therefore are promptly dispatched and deducted from the native demand profile.
- Hydropower energy availability, with run-of-river given as hourly zero-cost time series (therefore dispatched similarly to solar and wind power), while hydro storage availability is given as input to the solver through the daily preallocated energy targets as described in Section 4.3.3.

– Maximum and minimum power output for each unit of the thermal fleet, as a result of the different constraints to be respected (e.g. minimum stable power, must-run, ramping rates, planned maintenance, forced outages, and so on).

– Maximum capacities of the cross-border interconnectors (NTCs) and their respective binding constraints, including the energy balance as Kirchhoff's first law. Country-to-country impedances and Kirchhoff's second law are considered only when physical flows are simulated in Flow-Based marked coupling modelling.

– Additional binding constraints set by the user (e.g. to model flexibility and storage like DSR, batteries, power to gas, peculiarities of hydropower generation and others).

The need for MILP is mainly due to the minimum generation and minimum *on/off* time constraints of thermal clusters, according to the minimum stable power and ramping up/down rate parameters. They determine the minimum hours of dispatch duration and lead to the existence of integer variables to describe the *on/off* status of thermal units. To avoid the use of integer programming algorithms, which negatively affect the optimization time, ANTARES adopts a three-step heuristic approach, here reported from [36]:

1. The first optimization of each week is performed upon time steps of n hours, during which the load and generation curves can be levelled off and the maximum power output of power plants is computed according to the ramping rate constraints. It follows that n shall be chosen by the tool to best accommodate the ramping needs of power plants in the input.

2. The weekly dispatch costs are minimized again, this time with a one-hour time step, considering the maximum output from the power plants computed in step 1. Minimum output requirements are still not fully met (except for must-run plants, which are considered as directly dispatched regardless of their cost). The main purpose of step 2. is to identify all power plants that are called on duty.

3. A third and final minimization of the overall system costs is performed, again with a one-hour time step, considering the units identified in step 2. and imposing the maximum power output identified in step 1., together with the minimum generation constraints.

4.5 Synthetic Formulation of the Elementary Problem

The general UCED problem comprehends the minimization not only of variable and fixed generation costs, but also of transmission expenses and "external" costs such as the Value of Lost Load (VoLL) for energy not supplied and, vice versa, the value of wasted energy for the power spilled (if non-dispatchable power penalties are set). The objective function f is synthesised below. All the notations should report a superscript k, spanning the weeks of each Monte Carlo year, which was omitted for a

neater formulation. A complete and detailed description of the formal mathematical formulation for the elementary economic optimization, including Kirchhoff's laws and other constraints, is available in the ANTARES documentation [40].

$$f = Min\left(\Omega_{Dispatch}\right) = Min\left(Overall\ system\ dispatch\ costs\right),$$

$$\Omega_{Dispatch} = \Omega_{Transsmission} + \Omega_{Reservoir} + \Omega_{Thermal} + \Omega_{Spillage} + \Omega_{Unsupplied}\ ,$$

$$\Omega_{Transmission} = Transmission\ costs = \sum_{l \in L} \left(\gamma_l^+ \times F_l^+ + \gamma_l^- \times F_l^-\right)\ ,$$

$$\Omega_{Reservoir} = Reservoir\ flexibility\ costs = \sum_{n \in N} \sum_{\lambda \in \Lambda_n} \varepsilon_\lambda \times H_\lambda\ ,$$

$$\Omega_{Thermal} = Thermal\ generation\ costs = \sum_{n \in N} \sum_{\theta \in \Theta_n} \left(\chi_\theta \times P_\theta + \sigma_\theta^+ \times M_\theta^+ + \sigma_\theta^- \times M_\theta^- + \tau_\theta \times M_\theta\right)\ ,$$

$$\Omega_{Spillage} = Spilled\ energy\ costs = \sum_{n \in N} \delta_n^- \times G_n^-\ ,$$

$$\Omega_{Unsupplied} = Unsupplied\ energy\ costs = \sum_{n \in N} \delta_n^+ \times G_n^+\ .$$

The following notations hold:

General

$k \in K$ — optimization weeks of all Monte Carlo years (omitted for simplicity);

$t \in T$ — singular time steps of any optimization week k ($|T| = 168$);

$G\left(N, L\right)$ — undirected graph (network) of the power grid;

$n \in N$ — ordered set of vertices of G (nodes of the grid network);

$l \in L$ — edges of G (interconnectors of the grid network).

Transmission grid

$F_l^+\ ,\ \ F_l^- \in \mathbb{R}_+^T$ — power flow through l in the positive and negative direction;

$\gamma_l^+\ ,\ \ \gamma_l^- \in\ \mathbb{R}^T$ — transmission costs through l (proportional to F_l^+ and $\ F_l^-$, with $\gamma_l^+ +\ \gamma_l^- \geq 0$).

Reservoirs and storage

$\lambda \in \Lambda_n$ — reservoirs connected to node n (hydro storage, PSPs, batteries etc.);

$H_\lambda \in \mathbb{R}_+^T$ — nominal power output from reservoir λ;

$\varepsilon_\lambda \in \mathbb{R}^T$ water value (or shadow price) of power outputs from reservoir λ.

Thermal units

$\theta \in \Theta_n$ thermal clusters (sets of identical units) installed in n;

$P_\theta \in \mathbb{R}_+^T$ nominal power output from cluster θ;

$\chi_\theta \in \mathbb{R}^T$ cost of running units in θ (proportional to the cluster power output);

$\sigma_\theta^+ \ , \ \sigma_\theta^- \in \mathbb{R}^T$ startup and shutdown costs of a single unit in cluster θ;

$\tau_\theta \in \mathbb{R}^T$ fixed cost of a single running unit in θ (no load heat cost);

$M_\theta \in \mathbb{N}^T$ number of running units in cluster θ;

$M_\theta^+ \ , \ M_\theta^- \in \mathbb{N}^T$ units of cluster θ changing from state *off* to state *on* and vice versa.

Spilled and unsupplied energy

$\delta_n^+ \in \mathbb{R}_+^T$ unsupplied energy cost in node n (value of lost load);

$\delta_n^- \in \mathbb{R}_+^T$ spilled energy cost in node n (value of wasted energy);

$G_n^+ \ , \ G_n^- \in \mathbb{R}_+^T$ unsupplied and spilled energy in node n.

Chapter 5

The PECD Hydro Data

Acknowledged the primary role of hydropower dispatch in generation adequacy studies, it is important to analyze the input data, pointing out the key novelties. The main differences between the two versions, i.e. the old hydro database used for the MAF 2018 edition and the new PECD Hydro used for the MAF 2019 edition, are on the one hand the new criteria for hydropower plant categorization and aggregation. On the other hand, a new and common methodology to infer historical time series for hydro energy inflows was introduced, making them available for 35 historical years (1982 – 2016), consistently with the wind, solar and demand data. The MAF 2018 edition only used three reference hydrological conditions and related inflows, namely "dry", "normal" and "wet".

Since the PECD Hydro database used for the MAF 2019 was not published by ENTSO-E, the following chapter lists the key hydro data used to develop the hydropower modelling methodologies, while the actual numerical values and time series are presented only in a graphical or tabular aggregated manner. Nevertheless, the updated PECD Hydro database will be fully released together with the MAF 2020 report, hence a future reference will be available on the ENTSO-E adequacy web page [41]. This chapter also contains a description of the heuristics adopted to reaggregate the MAF 2019 hydro data, available in the new format, into the old classification and granularity. This procedure granted a level playing field for the simulations and the comparison of the results.

5.1 The Hydro Data for the MAF 2018

The Hydro 2018 database (used in the MAF 2018 edition) contained data for installed capacity, hydro energy inflows, maximum generation, reservoir levels and other constraints peculiar to each market node. Each TSO was responsible for delivering such data per three different hydrological conditions, representing the dry, normal and wet scenarios with the increasing availability of total yearly hydro energy inflows. The data of the hydropower plants were consolidated into five main categories: (i) run-of-river (ROR), (ii) swell ROR & Daily storage, (iii) Daily PSP reservoir,

(iv) Weekly PSP reservoir, and (v) Annual PSP reservoir. The capital letters are used hereafter to identify the hydro storage categories and avoid confusion with the temporal resolution of the data, e.g. stating that *weekly* hydro energy inflows were available for the *Daily* PSP reservoir. While the definition of the run-of-river category is straightforward, the ROR & Daily storage category contained ROR power plants with pondage capabilities, e.g. the ability to store a minor share of the inflows acting on the level of the low-head dam ahead of the turbines. It also included minor hydro storages (with no pumping capacity) whose ratio between the reservoir size [MWh] and the installed turbine capacity [MW] was lower than 24 hours. The criteria to aggregate PSP and large-dam reservoirs were based on the ratio between the reservoir size [MWh] and the installed pump (or turbine if not a PSP plant) capacity [MW]. As the naming suggests, power plants with a ratio lower than 24 hours belonged to the PSP Daily reservoir category. Power plants with a ratio between 25 and 168 hours were classified as PSP Weekly reservoirs. Finally, storage plants with a ratio greater than 168 hours were labelled as PSP Annual reservoirs.

The data for each of these categories were provided in the database in an aggregated way. For example, the turbine capacity of the PSP Daily reservoir in a market node was the sum of the turbine capacities of all the storage power plants within the very market node which complied with the corresponding classification criteria. Since the data for the wind and solar capacity factors were provided already in the form of the aforementioned 35 historical time series, while the data for hydro were collected only for the three "dry", "normal" and "wet" conditions, the TSOs marked each of the historical years from 1982 to 2016 as a dry, normal or wet year. The Climate Years for the MAF 2018 edition were thus defined coupling the wind, solar and demand time series for each historical year with the corresponding hydro conditions as indicated by the TSOs.

Table 5.1 shows the key data of the Hydro 2018 database per each hydropower category. The installed capacities reported included both turbine and pump, where applicable. The maximum and minimum power referred to specific data restraining hydro generation on top of the installed capacity. The contingent availability of the data varied depending on the input data actually provided by the TSOs for the market nodes within their control areas. It follows that the data in the table shall not be assumed as fully available for all the market nodes, but rather an indication of the template and structure of the database itself. Moreover, not all the data provided were used in the simulations. Section 6.1 describes the process of how and which hydro data were treated according to the ANTARES v6.1 hydropower modelling methodology for the MAF 2018.

MW / GWh	Run-of-River	Swell ROR & Daily st.	Daily PSP res.	Weekly PSP res.	Annual PSP res.
Hydro inflows	W	W	W	W	W
Max. power output	-	-	-	-	W
Min. power output	-	W	W	W	W
Max. pumping power	-	-	-	-	W
Max. pumped energy	-	-	-	-	W
Min. pumped energy	-	-	-	-	W
Reservoir level	-	-	-	-	W
Reservoir size	-	✓	✓	✓	✓
Installed capacity	✓	✓	✓	✓	✓

D: Daily	W: Weekly	- : N/A

Table 5.1: Key data available in the Hydro 2018 database.

5.2 The Hydro Data for the MAF 2019

The new PECD Hydro (also referred to as the "Hydro 2019 database") replaced the previous one with a new set of hydro energy inflows, introducing the 35 historical time series, as well as new criteria for the hydropower plant classification. Detailed historical data about hydro energy inflows were not available for most if not all the market nodes; thus, the time series were the outcome of a harmonized and centralized analysis commissioned by ENTSO-E. In particular, historical "total unregulated inflows" [m^3/day] for rivers and basins were procured from the Swedish Meteorological and Hydrological Institute, which delivered such data covering the geographical perimeter with catchments at the highest granularity available and for the required historical timespan from 1982 till 2017. Besides, statistical data for the hourly generation (and pumping) of unit-by-unit hydroelectric power plants were collected for the same geographical perimeter, spanning eight years from 2010 to 2017. A transfer function was built, correlating plant by plant generation with the corresponding unregulated natural inflows, and trained on the eight years of measured data for hydropower generation. Subsequently, the transfer function was used to infer the hydro energy inflows [GWh] for the historical years since 1982. The inferred energy inflows were then reaggregated according to the geographical perimeters of European bidding zones and provided for the 35 historical years at a daily resolution for run-of-river power plants and a weekly resolution for hydro storage power plants. Since the statistical measured data for hydropower generation used to train the model were not available for all hydropower plants within the perimeter, the inferred inflows were linearly rescaled to account for such "missing capacity". A more detailed description of the analysis is available in the documentation published by ENTSO-E [11].

The power plants were aggregated into four new categories: (i) run-of-river & pondage, (ii) reservoir (hereafter referred to as "traditional reservoir" to avoid confusion), (iii) open-loop PSP reservoir, and (iv) closed-loop PSP reservoir. The new run-of-river & pondage label was practically the result of merging the previous

run-of-river category with the swell ROR & Daily storage, using similar criteria for the classification. Instead, the major hydro storage plants without pumping capabilities were merged into the traditional reservoir category. PSPs were differentiated between basins with natural inflows, i.e. the open-loop PSP reservoir, and PSPs without natural inflows, i.e. the closed-loop PSP reservoir.

Table 5.2 shows the key data of the new PECD Hydro database per each hydropower category. As for the Hydro 2018 database, the installed capacities included both turbine and pump, where applicable. Again, the maximum and minimum power referred to specific data restraining hydro generation on top of the installed capacity. The contingent availability of the data varied depending on the input data actually provided by the TSOs for the market nodes within their control areas. It follows that the data in the table shall not be assumed as fully available for all the market nodes, but rather an indication of the template and structure of the database itself. Moreover, not all the data provided were used in the simulations. Section 6.2 describes the process of how and which hydro data were treated according to the ANTARES v6.1 hydropower modelling methodology for the MAF 2019.

MW / GWh	ROR & Pondage	Trad. Reservoir	Open-Loop PSP	Closed-Loop PSP
Hydro inflows	D	W	W	-
Max. power output	D	W	W	W
Min. power output	D	W	W	W
Max. generated energy	-	W	W	W
Min. generated energy	-	W	W	W
Max. pumping power	-	-	W	W
Min. pumping power	-	-	W	W
Max. pumped energy	-	-	W	W
Min. pumped energy	-	-	W	W
Reservoir level	-	W	W	W
Max. reservoir level	-	W	W	W
Min. reservoir level	-	W	W	W
Reservoir size	✓	✓	✓	✓
Installed capacity	✓	✓	✓	✓

D: Daily	W: Weekly	- : N/A

Table 5.2: Key data available in the Hydro 2019 database.

5.3 Hydro Data Preparation

The new PECD Hydro data used for the MAF 2019 did not differ solely in the terms described above, but they also reflected the updated TSOs' best estimates concerning

the installed capacities and all the other data for each target year. It follows that the hydro data already available in the old format for the target year 2025, which were collected during the MAF 2018 process, could not be used as input to set up the reference model for the result comparison. Not only the underlying assumptions changed, but also the best estimates for the Net Generation Capacity (NGC) and the related inflows. Moreover, different methodologies were used by different TSOs when collecting and defining the data for the dry, normal and wet scenarios. Instead, a common and consistent set of criteria, to choose and relate those three scenarios to the new inferred historical hydro data, needed to be defined and applied to the three market nodes in the model. For this purpose, I used only the new 2019 PECD Hydro data as input for the simulations. Nevertheless, since the comparison of the results used the old MAF 2018 hydro modelling methodology as a reference, I reaggregated the new hydro data to comply with the old criteria and template.

5.3.1 Aggregation of Hydropower Plants

I split and assigned the Hydro 2019 data to the old Hydro 2018 categories. I relied on available information from TSOs and compared the data provided in the old format with the new ones.

- Austria: detailed data for single hydropower plants were available in APG's internal database. The hydro storage units of Austria were precisely regrouped according to the old classification criteria. By definition, the new run-of-river & pondage category was the result of merging the old (non-dispatchable) run-of-river and the swell ROR & Daily storage categories. Therefore, it was simply split again to retrieve the previous format.

- Switzerland: in the old version of the database, CH only had installed capacities for run-of-river, Annual PSP reservoir and Weekly PSP reservoir, with the latter reporting no natural inflows. In the new database, CH reported capacities only for run-of-river & pondage (with no pondage capabilities), traditional reservoir and closed-loop PSP. Thus, it was straightforward to match the run-of-river data and to simply allocate the closed-loop PSP data to the Weekly PSP reservoir. The traditional reservoir data and inflows were allocated to the old Annual reservoir category.

- Italy North: in the old version of the database, ITN only had installed capacities for run-of-river, Annual PSP reservoir and Daily PSP reservoir, with the latter reporting pumping capabilities and no natural inflows. Instead, in the new database, ITN reported capacities for run-of-river & pondage (with no pondage capabilities), traditional reservoir and open-loop PSP. Thus, the run-of-river data were again directly matched, while the traditional reservoir and open-loop PSP ones were merged into the Annual PSP reservoir. The installed capacities and reservoir size for the Daily PSP reservoir were kept constant as provided by the TSO and hence deducted from the Annual PSP reservoir.

The installed capacities and reservoir sizes allocated to the new and the old categories are reported in Table 5.3. Additionally, Table 5.4 summarizes the statistical measures of the hydro historical data in terms of yearly total energy inflows per each category.

		AT			CH			ITN		
	MW / GWh	Turbine	Pump	Size	Turbine	Pump	Size	Turbine	Pump	Size
Hydro 2019	Run-of-river & pondage	6130	-	17	4113	-	-	4762	-	-
	Traditional reservoir	2430	-	762	8152	-	8155	7634	-	3707
	Open-loop PSP	3888	2860	1727	-	-	-	2500	1706	194
	Closed-loop PSP	300	300	2	3989	3937	670	2505	2502	17
Hydro 2018	Run-of-river	4782	-	-	4113	-	-	4762	-	-
	Swell ROR & Daily storage	1348	-	17	-	-	-	-	-	-
	Daily PSP reservoir	1181	611	31	-	-	-	2505	2502	17
	Weekly PSP reservoir	274	19	99	3989	3596	670	-	-	-
	Annual PSP reservoir	5163	2529	2360	8152	341	8155	10134	1706	3901
	Total Hydro 2019	12748	3160	2508	16254	3937	8825	17401	4208	3918
	Total Hydro 2018	12748	3159	2507	16254	3937	8825	17401	4208	3918

Table 5.3: Hydropower installed capacities according to the Hydro 2019 and 2018 categories.

		AT			CH			ITN		
	GWh	Mean	St. Dev.	Range	Mean	St. Dev.	Range	Mean	St. Dev.	Range
Hydro 2019	Run-of-river & pondage	31709	2030	7844	16885	1062	4053	16254	1890	10385
	Traditional reservoir	1873	154	751	19435	1698	7120	15217	1922	10134
	Open-loop PSP	5708	485	2295	-	-	-	2395	313	1559
	Closed-loop PSP	-	-	-	-	-	-	-	-	-
Hydro 2018	Run-of-river	24785	1087	3767	16932	623	2140	16324	2035	9771
	Swell ROR & Daily storage	6987	307	1062	-	-	-	-	-	-
	Daily PSP reservoir	94	11	38	-	-	-	-	-	-
	Weekly PSP reservoir	298	34	122	-	-	-	-	-	-
	Annual PSP reservoir	7085	805	2886	19795	1947	7061	17650	2552	11629
	Total Hydro 2019	39290	2670	10890	36320	2761	11174	33866	4126	22079
	Total Hydro 2018	39249	2243	7875	36728	2570	9201	33974	4586	21399

Table 5.4: Statistical measures of the 35 CYs for Hydro 2018 and Hydro 2019.

5.3.2 Clustering of Historical Inflows

For each market zone, I conducted the clustering of the 35 inferred historical hydro energy inflows based primarily on the sum of the yearly inflows into hydro storages (traditional reservoir and open-loop PSP), taken as a key quantity due to its high impact on the hydro dispatch from a generation adequacy perspective. I assigned the reference "dry" and "wet" conditions to the historical years with the minimum and maximum yearly hydro storage inflows respectively, which may therefore differ

for each market node. Instead, I chose the "normal" reference climate year to be as close as possible to the averaged yearly hydro storage inflows, that being verified for the three market nodes. The most suitable historical year for this purpose was 2016. Figure 5.1 shows the total weekly hydro storage inflows (traditional reservoir plus open-loop PSP) from 1982 to 2016, depicting in yellow, green and blue the "dry", "normal" and "wet" years respectively.

The smoother and less disperse profiles for AT and CH are due to a harmonization process conducted by APG and Swissgrid (the TSO of Switzerland), based on internal historical measures from hydro storage power plants, which allowed them to polish and homogenize their data to be collected in the PECD Hydro database. In particular, only the actual measured inflows from 2010 to 2016 were deemed as representative of the topical hydropower system for adequacy assessments. Accordingly, those time series were best-fitted to the past years based on their correlation with the ones inferred from 1982 to 2009. This task was performed independently for both the traditional reservoir and open-loop PSP inflows. The same procedure was adopted also for the run-of-river & pondage inflows of CH, as shown in Figure 5.2, while the intrinsic variability of the inferred historical years is clearly noticeable in the spiked profiles of AT and ITN. Acknowledged the differences above, I did not manipulate further the PECD Hydro input data, to ensure consistency with the data used in the MAF 2019 assessment.

Choosing a common historical year as the reference "normal" conditions was of key importance to set up a consistent comparison between the results of the two models. In fact, the "normal" Climate Year 2016 was the only one characterized exactly by the same wind, solar, demand and hydro conditions for the three bidding zones in both models. Therefore, I used the CY 2016 for the detailed UCED comparison presented in Section 7.3.

Once identified the three reference years, I marked each historical year as "dry", "normal", or "wet" based on the minimum absolute deviation of its total yearly storage inflows with respect to the reference ones. Moreover, the statistical correlation between the inflow time series was also considered as an additional parameter to drive the clustering decision. Finally, the clustering based on the hydro storage inflows was benchmarked against the outcome of a similar process based on the inflows to the run-of-river plants. Only a severe mismatch between the two approaches was considered in the final clustering decision, given the higher volatility of ROR inflows and its non-dispatchable nature. Table 5.5 reports the outcomes of the clustering process, including the yearly inflows for each market node. The averaged yearly inflows to each Hydro 2018 category, in compliance with the clustering outcomes, is reported in Table 5.4

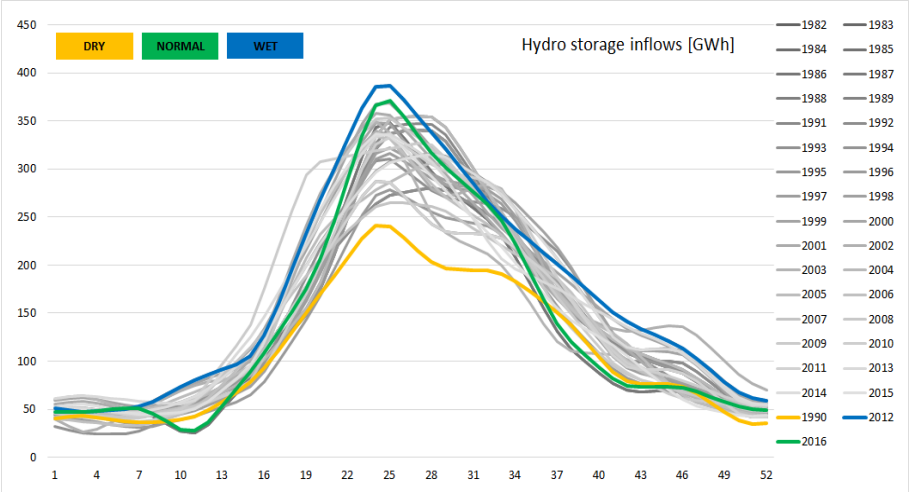

(a) AT

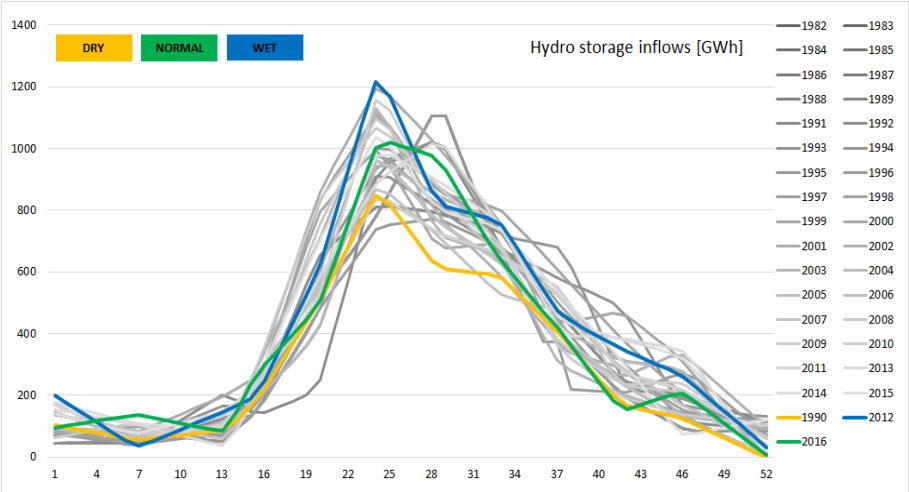

(b) CH

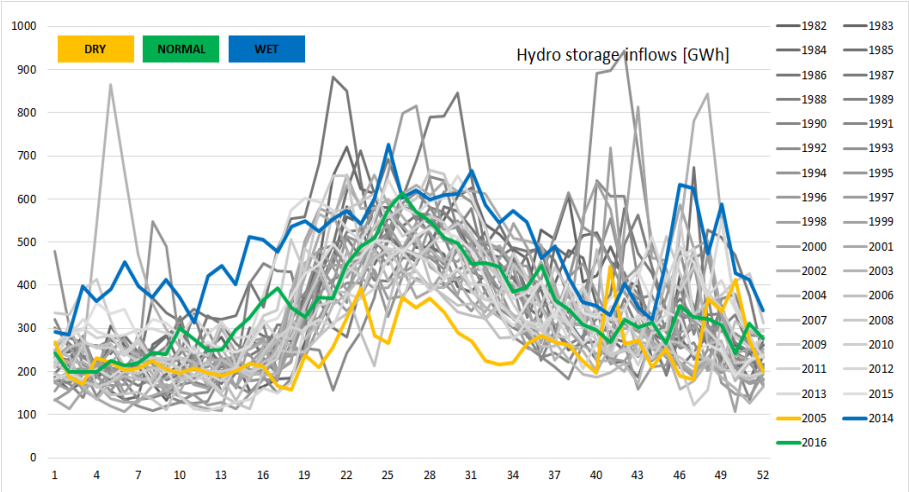

(c) ITN

Figure 5.1: Total hydro storage energy natural inflows for AT, CH and ITN.

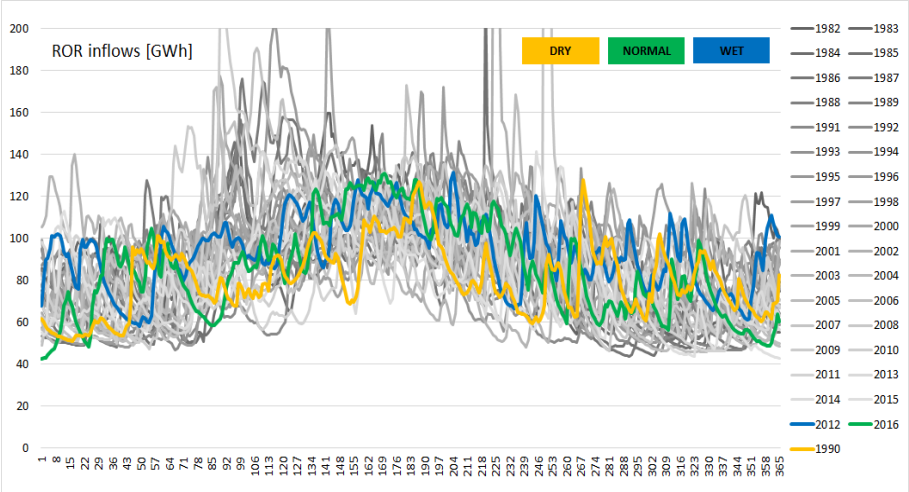

(a) AT

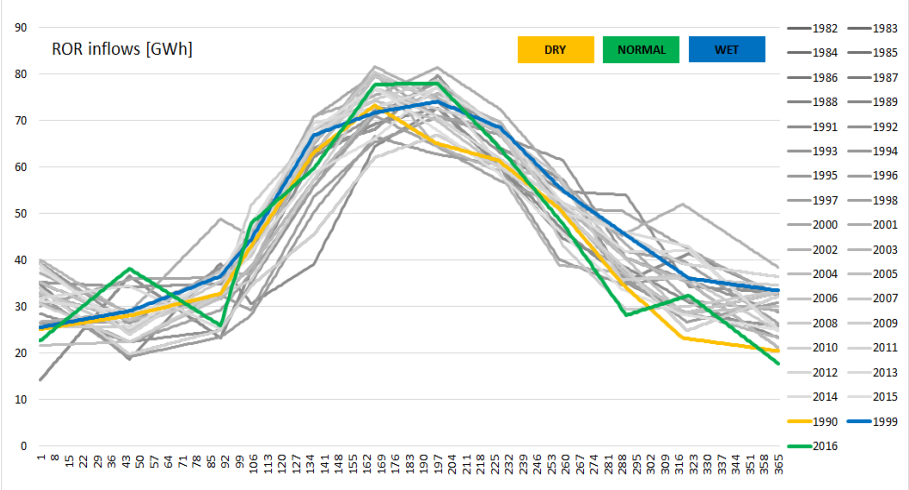

(b) CH

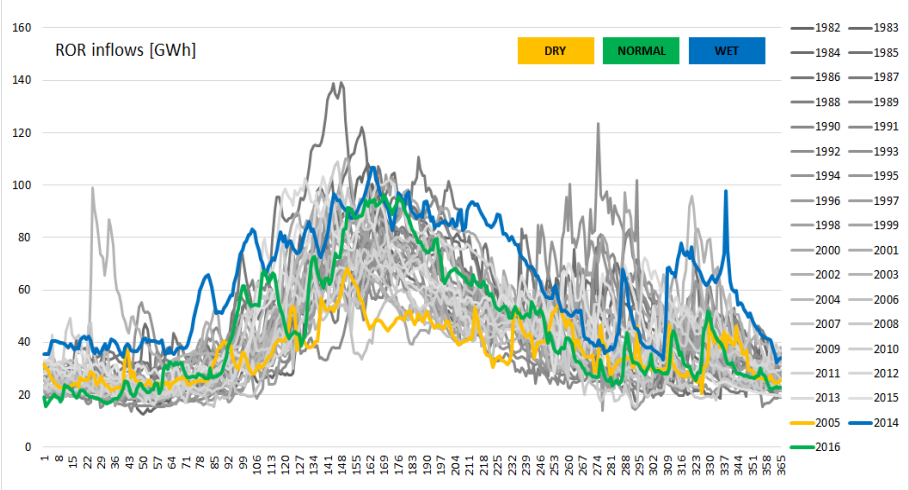

(c) ITN

Figure 5.2: Total run-of-river & pondage energy natural inflows for AT, CH and ITN.

	AT			CH			ITN		
GWh	Normal	Dry	Wet	Normal	Dry	Wet	Normal	Dry	Wet
Run-of-river	24523	22960	26727	16774	15915	18055	16443	13480	23251
Swell ROR & Daily st.	6913	6472	7534	-	-	-	-	-	-
Daily PSP reservoir	92	74	112	-	-	-	-	-	-
Weekly PSP reservoir	293	234	355	-	-	-	-	-	-
Annual PSP reservoir	6946	5550	8436	19520	15903	22964	18111	13188	24817

CY	AT	CH	ITN	CY	AT	CH	ITN	CY	AT	CH	ITN
1982	N	N	N	1994	N	W	N	2006	N	D	D
1983	N	N	N	1995	N	N	N	2007	N	N	D
1984	N	N	N	1996	D	D	D	2008	N	N	N
1985	N	N	N	1997	N	N	N	2009	N	N	N
1986	N	N	N	1998	N	N	N	2010	N	N	N
1987	N	N	N	1999	W	W	N	2011	D	N	N
1988	W	W	N	2000	W	N	N	2012	W	W	D
1989	D	N	N	2001	N	W	N	2013	W	W	W
1990	D	D	N	2002	W	N	N	2014	W	W	W
1991	N	N	N	2003	N	N	N	2015	N	N	N
1992	N	N	N	2004	N	N	D	2016	N	N	N
1993	N	N	N	2005	N	D	D				

Table 5.5: Normal, dry and wet yearly hydro inflows and clustering of the 35 CYs.

Chapter 6

Hydropower Modelling

The following chapter addresses the first aspect touched by the research question: the hydropower modelling methodology. I describe how the key hydro data were manipulated and fed into the ANTARES v6.1 models, pointing out the differences and the novelties introduced in the new methodology developed in the MAF 2019, employing the new PECD Hydro data. In particular, the reference model was set up with the hydropower modelling methodology used in the MAF 2018 edition, hereafter referred to as the "Hydro 2018" methodology and model, while I built the second one following the new hydro modelling methodology developed for the MAF 2019 edition, hence referred to as the "Hydro 2019" methodology and model. The approaches described in this chapter are the product of a joint effort of the team responsible for delivering the ANTARES results for the ENTSO-E MAF 2018 and 2019 studies. The team involved professionals from different TSOs, including myself joining in April 2019. Being developed specifically for ANTARES v6.1, they complied with the requirements as well as the assumptions, but also limitations, peculiar to this specific version of the software. Therefore, they may not be valid for different modelling tools or outside of the context described here. Moreover, they are the contingent outcome of a continuously developing process with a learning-by-doing attitude; thus, I am reporting them with no prejudice towards alternative methods or assumptions.

The description makes use of the following notation:

$$Q_{x,CAT}\ [Unit]\ ,$$

where Q stands for a general numeric quantity available in the hydro data. The subscript x indicates its available time resolution (M for monthly, W for weekly, D for daily, or h for hourly). CAT indicates the corresponding hydro category (e.g. ROR for run-of-river etc.). $Unit$ is the unit of measure (e.g. MWh). The approach and the formulas used to transform the hydro energy inflows or other quantities are reported for each hydropower plant category. The trivial conversion factors (e.g. the conversion factors from GWh to MWh, from power to energy, from weekly to monthly time series, etc.) are intentionally omitted for the sake of a neater formulation.

6.1 The Hydro 2018 Modelling Methodology

It follows a description of the ANTARES v6.1 modelling methodology used to handle hydropower generation in the MAF 2018 framework. Since I was not part of the modelling team back in 2018 and no official detailed documentation was available, I am reporting the approach which I deducted through a reverse investigation of the final structure and data available in the ANTARES v6.1 model for the MAF 2018, thanks also to the interaction with colleagues directly involved in its development.

The process described below was repeated for each of the three datasets characterizing "dry", "normal" and "wet" conditions. Figure 6.1 reports a schematic representation of all the different elements characterizing the Hydro 2018 methodology in the ANTARES v6.1 GUI style for a generic market node.

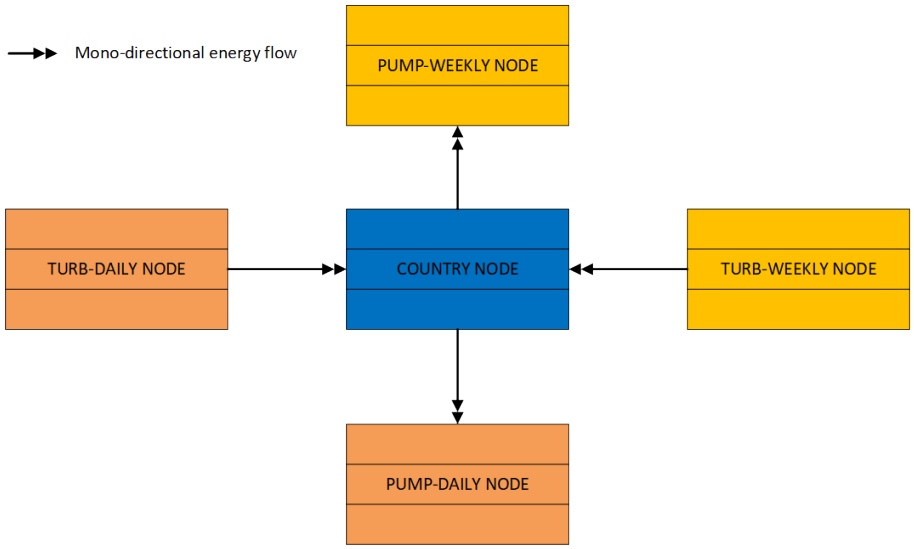

Figure 6.1: Schematic representation of Hydro 2018 elements in the ANTARES v6.1 GUI.

6.1.1 Run-of-River

Run-of-river generation was modelled directly within the market node, entering an hourly availability time series computed as follows:

$$ENE_{h,ROR}\,[MWh] = \frac{INF_{W,ROR}}{168} \quad ,$$

where $ENE_{h,ROR}\,[MWh]$ is the hourly ROR energy availability and $INF_{W,ROR}$ are the weekly hydro energy inflows available in the input data.

The maximum power output for ROR generation was equal to its hourly availability (set to be always lower or equal to the total installed turbine capacity), since no additional constraints were available in the Hydro 2018 database.

As imposed by ANTARES v6.1, the minimum power generation from the different hydro storage categories were accounted as an addition to the ROR hourly generation availability:

$$ENE_{h,ROR}\,[MWh] = \frac{INF_{W,ROR}}{168} + \sum_{Storage} P_{min,W,RES} \ ,$$

where $\sum P_{min,W,RES}$ is the sum of all the minimum power constraints (if any) from the Daily, Weekly and Annual PSP reservoirs, including minimum generation from the swell ROR & Daily storage. Being the time resolution of the ROR time series within the model equal to 1 hour, the values for the minimum power were directly summed to the hourly available energy, multiplied by an implicit time factor of 1 hour.

6.1.2 Reservoir Generation from Natural Inflows

In ANTARES v6.1 a rigid split between reservoirs with natural inflows only and PSP was mandatory. In fact, PSP generation could be modelled only via "daily" or "weekly" optimization cycles with no natural hydro energy inflows, as explained later. As a consequence, different assumptions and modelling strategies were adopted to process the natural inflows on the one hand and to reflect pumping capabilities on the other hand. Natural hydro energy inflows to the Annual, Weekly and Daily reservoirs were aggregated and processed as hydro storage generation within the market node. Furthermore, the inflows to the swell ROR & Daily storage, when provided, were merged with the other reservoir inflows. The calculation of total inflows took into account also the Annual PSP reservoir levels at the beginning of each week, since ANTARES v6.1 was designed to allow for reservoir level optimization only utilizing monthly minimum and maximum reservoir level trajectories (see Section 4.3.2). The implementation of such minimum and maximum trajectories together with the activation of the ANTARES reservoir energy manager implied a different processing of inflows, which is described in Section 6.3. Thus, the following procedure to compute the energy availability and the maximum power output applied to most of the marked nodes characterized by deterministic weekly reservoir levels:

$$ENE_{M,RES}\,[MWh] = \textstyle\sum_{month} \left(INF_{W,RES} - \Delta L_{W,A\_RES} - E_{min,W,RES}\right) ,$$

with $INF_{W,RES} = INF_{W,A\_RES} + INF_{W,W\_RES} + INF_{W,D\_RES} + INF_{,W,Swell\ ROR}$,

$\Delta L_{W,A\_RES} = L_{W+1,A\_RES} - L_{W,A\_RES}$,

$E_{min,W,RES} = \left(P_{min,W,A\_RES} + P_{min,W,W\_RES} + P_{min,W,D\_RES} + P_{min,W,Swell\ ROR}\right)$,

where $ENE_{M,RES}$ $[MWh]$ are the total monthly hydro storage energy available. $INF_{W,RES}$ are the total weekly hydro energy from natural inflows. $\Delta L_{W,A\_RES}$ is the delta of the Annual PSP reservoir levels at the beginning of two consecutive weeks. $E_{min,W,RES}$ is the total weekly minimum energy generation (the factor 168 h is omitted), which has been already accounted for in the ROR time series.

Due to the aggregation of all the hydro storage inflows, a heuristic was defined to compute the weekly equivalent maximum power output from such an aggregated reservoir within the market node:

$$P_{\max\_EQ,W,RES}\ [MW] = P_{max,W,A\_RES} - P_{min,W,A\_RES} +$$

$$+ \left[P_{max,W,Swell\ ROR} - P_{min,W,Swell\ ROR}\right]_{if\ \exists\ Swell\ ROR} +$$

$$+ \left[\left(INF_{W,D\_RES} - P_{min,W,D\_RES} \times 168\right)/70\right]_{if\ (\exists\ Daily\ RES\ \wedge\ PUMP\_D > 0)} +$$

$$+ \left[P_{max,W,D\_RES} - P_{min,W,D\_RES}\right]_{if\ (\exists\ Daily\ RES\ \wedge\ PUMP\_D = 0)} +$$

$$+ \left[\left(INF_{W,W\_RES} - P_{min,W,W\_RES} \times 168\right)/70\right]_{if\ (\exists\ Weekly\ RES\ \wedge\ PUMP\_W > 0)} +$$

$$+ \left[P_{max,W,W\_RES} - P_{min,W,W\_RES}\right]_{if\ (\exists\ Weekly\ RES\ \wedge\ PUMP\_W = 0)} +$$

$$- \left[P_{\max\_pump,W,A\_RES}\right]_{if(>100MW\ \wedge\ COUNTRY \neq ES,ITN,ITCS)} ,$$

where the equivalent maximum power $P_{\max\_EQ,W,RES}$ is equal to the Annual PSP reservoir maximum power minus the minimum power, plus several correction terms taking into account the contribution of swell ROR & Daily storage generation, Daily reservoir generation, and Weekly reservoir generation, whether existing for the considered market node. The factor 1/70 [1/h] originates from the average equivalent hours of operation, assumed for peak PSPs to be 70 hours per week.

6.1.3 Reservoir PSP Generation

Daily and Weekly reservoir PSP generation was explicitly modelled through two virtual external nodes. Virtual nodes are here defined as nodes that are not part of the electricity network and hence shall not be confused with market nodes but are rather added for the sole purpose of the modelling methodology. One virtual node had ideally unlimited generation availability, the Turb-Daily (or Turb-Weekly) node, while the other one had ideally unlimited demand availability, the Pump-Daily (or Pump-Weekly) node. Both virtual nodes were directly linked to the respective market node. The values for maximum pump and turbine power were extracted from the database as follows and imposed as the maximum energy flows on the links between the market node and the virtual Turb-Daily (Turb-Weekly) and Pump-Daily (Pump-Weekly) nodes respectively. This holds per each week of the simulation, being the maximum power data available on a weekly basis:

- $P_{max,W,TURB\_D} = C_{TURB\_D} - INF_{W,D\_RES}/70$,
- $P_{max,PUMP\_D} = C_{PUMP\_D}$;

- $P_{max,W,TURB\_W} = C_{PUMP\_A} + C_{TURB\_W} - INF_{W,W\_RES}/70$,
- $P_{max,PUMP\_W} = C_{PUMP\_A} + C_{PUMP\_W}$;

where $C_{TURB\_D\,(W)}$ and $C_{PUMP\_D\,(W)}$ are the PSP Daily (Weekly) reservoir turbine and pump capacity [MW] respectively. C_{PUMP_A} is the Annual reservoir maximum pumping power, if provided in the data, or the Annual reservoir installed pump capacity instead. In both cases, the PSP Annual reservoir share was assumed to be generated through a perfectly reversible PSP plant (i.e. $C_{TURB\_A} = C_{PUMP\_A}$) and it was aggregated to the PSP Weekly reservoir generation, as a simplifying assumption while building the model. This was done to comply with ANTARES v6.1 requirements, according to which the PSP cycle optimization cannot exceed the weekly timeframe. Since PSP generation could not directly account for natural inflows, which were aggregated to one single reservoir as described above, the maximum power was reduced by the weekly inflows multiplied by the factor 1/70 [1/h]. As mentioned already, the factor originated from the average equivalent hours of operation assumed to be equal to 70 hours for peak PSPs.

The values for $P_{max,W,TURB\_D\,(W)}$ and $P_{max,PUMP\_D\,(W)}$ inserted in the model were only the ones computed for the "normal" hydrological conditions. This simplification was imposed by the software, which could handle only one time series as the hourly maximum energy flow on each link.

The PSP cycle efficiency was assumed to be equal to 75%, consistently with MAF 2018 indications. It was imposed as a linear binding constraint between the cumulated energy flow on the links between the market node and the virtual Turb-Daily (Turb-Weekly) and Pump-Daily (Pump-Weekly) nodes, on a daily (or weekly) basis:

$$\sum_{D\,(W)} \left(ENE_{TURB\_D(W)} \Rightarrow M\text{-}NODE\right) = 0.75 \times \sum_{D\,(W)} \left|ENE_{PUMP\_D(W)} \Rightarrow M\text{-}NODE\right| \ ,$$

where $ENE_{PUMP\_D(W)} \Rightarrow M\text{-}NODE$ [MWh] is the energy flown from the Pump-Daily (Pump-Weekly) node to the market node (conventionally negative) during the daily (weekly) optimization.

6.1.4 Swell ROR & Daily Storage

Swell ROR & Daily storage data available in the Hydro 2018 database were embedded in the definition of the hydro storage energy availability and equivalent maximum power for the reservoir generation from natural inflows, as described in Section 6.1.2. It follows that in the ANTARES v6.1 model, the whole category did not constitute a peculiar type of hydro generation, whereas its inflows were added to the reservoir generation within the market node and its installed capacity and reservoir size were accordingly implemented. This constituted a major simplifying modelling assumption, whose impact is further discussed in Section 8.1.

6.2 The Hydro 2019 Modelling Methodology

The hydro modelling methodology to handle the new PECD Hydro data in ANTARES v6.1 was developed during the MAF 2019 starting from the experience made and the lessons learnt from the previous year. Therefore, it shows many similarities but key improvements and new solutions to address the modelling of the new hydropower generation types, together with their new data and higher granularity. The process described below was implemented via an R-script that delivered 35 ready-made hydro time series, consistent with each of the historical hydro data. Figure 6.2 depicts the schematic elements of the Hydro 2019 methodology, as in the ANTARES v6.1 GUI, including all the different typologies of hydropower generation.

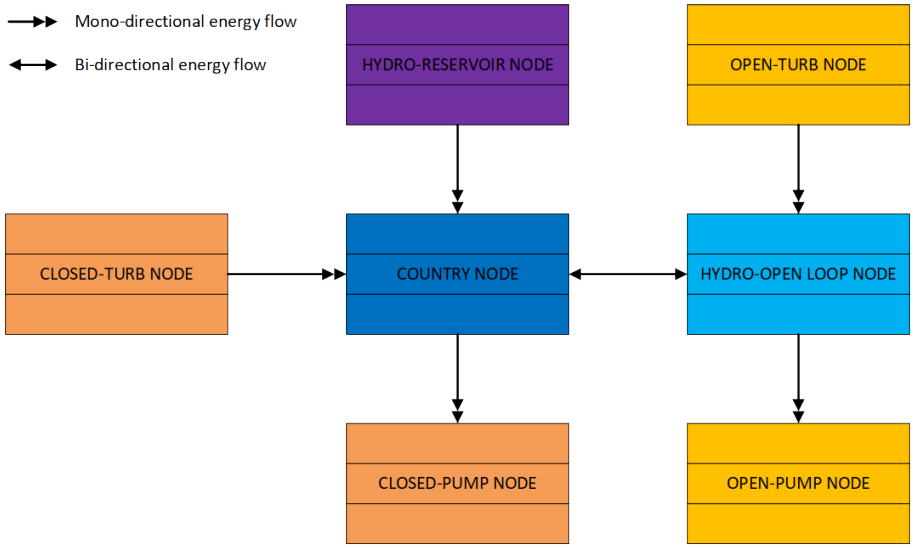

Figure 6.2: Schematic representation of Hydro 2019 elements in the ANTARES v6.1 GUI.

6.2.1 Run-of-River & Pondage

Run-of-river & pondage generation was modelled within the market node, similarly to ROR generation for the Hydro 2018 methodology, with an hourly availability time series computed as follows:

$$ENE_{h,ROR}\,[MWh] = \frac{INF_{D,ROR}}{24} \quad ,$$

where $ENE_{h,ROR}\,[MWh]$ is the hourly energy availability and $INF_{D,ROR}$ are the daily hydro energy inflows taken from the database.

ROR & pondage daily minimum and maximum power constraints, despite potentially available in the new PECD Hydro format as shown in Table 5.2, were generally not provided during the first data collection from TSOs, and thus neglected in the simulations. This choice caused in ANTARES v6.1 the loss of the peculiar short-term flexibility given by ROR pondage generation. Nevertheless, a sensible amount of

such hydro capacity was available only in AT (and a few other nodes in the MAF perimeter), while CH and ITN did not report pondage capabilities.

Minimum generation profiles from hydro storages were also added to the hourly ROR generation, in compliance with ANTARES v6.1 requirements (except for a few exceptional market nodes, as explained in Sections 6.2.3 and 6.2.6):

$$ENE_{h,ROR}\,[MWh] = \frac{INF_{D,ROR}}{24} + P_{min,W,RES} + P_{min,W,OL} \ ,$$

where $P_{min,W,RES}$ and $P_{min,W,OL}$ are the minimum generation from traditional reservoir and open-loop PSP respectively. Being the time resolution of the simulation equal to 1 hour, the minimum power was directly added to the hourly energy, multiplied by an implicit time factor of 1 hour.

6.2.2 Traditional Reservoir

Traditional reservoir generation for the majority of the market nodes was also modelled within the very market node. Despite the weekly availability of hydro energy inflows, ANTARES v6.1 required the storage energy in its input to have a monthly resolution. Similarly to the Hydro 2018 methodology, inflows to hydro storages accounted for the fixed reservoir level trajectories at the beginning of each week (if provided). A different approach was followed for the market nodes whose minimum and maximum reservoir level trajectories were available. It implied the activation of the ANTARES reservoir energy manager and it is later described in Section 6.3. Nevertheless, none of the three bidding zones selected for my thesis used the reservoir energy manager functionality, therefore the following formulation holds for the traditional reservoir generation of the Hydro 2019 tri-lateral model:

$$ENE_{M,RES}\,[MWh] = \textstyle\sum_{month} (INF_{W,RES} - \Delta L_{W,RES} - E_{min,W,RES}) \ ,$$

with $\Delta L_{W,RES} = L_{W+1,RES} - L_{W,RES}$,

$E_{min,W,RES} = P_{min,W,RES} \times 168$,

where $ENE_{M,RES}\ [MWh]$ is the monthly hydro energy availability. $INF_{W,RES}$ are the weekly available energy inflows. $\Delta L_{W,RES}$ is the delta between the reservoir levels at the beginning of two consecutive weeks. $E_{min,W,RES}$ is the weekly minimum energy generation, which was already merged into the ROR time series. $INF_{W,RES}$, $L_{W,RES}$ and $P_{min,W,RES}$ were all directly taken from the PECD Hydro database.

In strong opposition to the old methodology, the equivalent maximum power set in the model was directly computed as:

$$P_{\mathrm{max\_}EQ,W,RES}\ [MW] = \ P_{max,W,RES} - P_{min,W,RES} \ ,$$

where the equivalent maximum power $P_{\mathrm{max\_}EQ,W,RES}$ was equal to the actual maximum power minus the minimum power, which has been already added to ROR

generation.

Some differences applied to the market nodes characterized by maximum and/or minimum power constraints changing for all or some of the historical year (hence referred to as "climate-dependent"). Since ANTARES v6.1 could handle only one hourly time series for the maximum power of a reservoir, these countries were set up with an additional external "Hydro-Reservoir" virtual node containing the 35 hydro energy time series. To bound the respective maximum and/or minimum power flowing from the external virtual node to the market node, a virtual zero-cost thermal unit was created ad hoc, whose available generation corresponded to the 35 climate-dependent $P_{max,W,RES}$ and/or $P_{min,W,RES}$. An hourly binding constraint was finally placed in the model imposing the virtual thermal unit generation as a hard upper and/or lower bound on the hourly flow (hence generation) from the external Hydro-Reservoir node to the market node. Such alternative solutions, adopting virtual nodes and thermal units to bypass certain limitations of the modelling tool, are sometimes complex if not cumbersome. Thus, they may appear unclear to a reader without experience with ANTARES modelling. Nevertheless, they have been used as a common practice in these and many other ANTARES-based models, addressing also different purposes rather than hydropower modelling.

6.2.3 Reservoir Exceptions for Maximum and Minimum Power

None of the market nodes modelled in my thesis was characterized by different historical time series for the minimum or maximum power of the traditional reservoir. Nevertheless, I am reporting here the full details for the sake of transparency and completeness of the Hydro 2019 methodology description.

- If only $P_{min,W,RES}$ was climate-dependent and modelled through a virtual thermal unit:
  - $E_{min,W,RES}$ was no more accounted as additional ROR generation.
  - Thus, $ENE_{M,RES}\ [MWh] = \sum_{month} (INF_{W,RES} - \Delta L_{W,RES})$.
  - Thus, $P_{\max\_EQ,W,RES}\ [MW] = P_{max,W,RES}$.
  - $P_{\max\_EQ,W,RES}$ was imposed as the hourly maximum flow on the mono-directional link between the external Hydro-Reservoir node and the market node.
  - $P_{min,W,RES}$ was imposed with an hourly hard constraint, setting the generation of the corresponding virtual thermal unit as a lower bound to the actual flow on the mono-directional link between the external Hydro-Reservoir node and the market node.
- If only $P_{max,W,RES}$ was climate-dependent and modelled through a virtual thermal unit:
  - $E_{min,W,OL}$ was still accounted as additional ROR generation.

  - Thus, $ENE_{M,RES}\ [MWh] = \sum_{month} (INF_{W,RES} - \Delta L_{W,RES} - E_{min,W,RES})$.
  - Thus, $P_{\max\_EQ,W,RES}\ [MW] = P_{max,W,RES} - P_{min,W,RES}$.
  - $P_{\max\_EQ,W,RES}$ was imposed with an hourly hard constraint, setting the generation of the corresponding virtual thermal unit as an upper bound to the actual flow on the mono-directional link between the external Hydro-Reservoir node and the market node.

- If both $P_{max,W,RES}$ and $P_{min,W,RES}$ were climate-dependent and modelled through a virtual thermal unit:
  - $E_{min,W,RES}$ was no more accounted as additional ROR generation.
  - Thus, $ENE_{M,RES}\ [MWh] = \sum_{month} (INF_{W,RES} - \Delta L_{W,RES})$.
  - Thus, $P_{\max\_EQ,W,RES}\ [MW] = P_{max,W,RES}$.
  - $P_{\max\_EQ,W,RES}$ was imposed with an hourly hard constraint, setting the generation of the corresponding virtual thermal unit as an upper bound to the actual flow on the mono-directional link between the external Hydro-Reservoir node and the market node.
  - $P_{min,W,RES}$ was imposed with an hourly hard constraint, setting the generation of the corresponding virtual thermal unit as a lower bound to the actual flow on the mono-directional link between the external Hydro-Reservoir node and the market node.

6.2.4 Closed-Loop PSP Reservoir

The closed-loop PSP reservoir generation was modelled through two virtual external nodes, similarly to the Daily and Weekly PSP reservoir generation in the Hydro 2018 methodology. One node had ideally unlimited generation availability, the "Closed-Turb" node, while the other had ideally unlimited load, the "Closed-Pump" node. Both nodes were directly connected to the market node. The values for the maximum turbine and pump power were extracted from the PECD Hydro database as follows and imposed as the hourly maximum energy flows on the links between the market node, and the virtual Closed-Turb and Closed-Pump nodes respectively:

- $P_{max,TURB,CL}$ = Total installed Closed Loop turbine capacity [MW] ,
- $P_{max,PUMP,CL}$ = Total installed Closed Loop pump capacity [MW] .

The PSP cycle efficiency was assumed to be equal to 75%, unchanged from the MAF 2018 modelling assumptions, and it was imposed as a linear binding constraint between the cumulated energy flows on the links between the market node and the virtual Closed-Turb and Closed-Pump nodes, over an optimization cycle T_{CL}:

$$\sum_{T_{CL}} (ENE_{TURB\_CL} \Rightarrow M\text{-}NODE) = 0.75 \times \sum_{T_{CL}} |ENE_{PUMP\_CL} \Rightarrow M\text{-}NODE| \ ,$$

where $ENE_{PUMP\_CL} \Rightarrow M\text{-}NODE$ [MWh] is the energy flow from the market node to the Closed-Pump node (negative according to the model convention). In ANTARES

v6.1, the binding constraint could be imposed only over a daily or weekly cycle T_{CL}.

The optimization cycle was set as daily or weekly, based on the value of the time constant τ_{CL}, to ensure that the cumulated pumped or generated energy was as consistent as possible with the closed-loop PSP reservoir size:

$$\tau_{CL}\ [h] = min\left(\frac{SIZE_{CL}}{P_{max,TURB,CL}}, \frac{SIZE_{CL}}{P_{max,PUMP,CL}}\right); \left\{ \begin{array}{l} \tau_{CL} > 12 \rightarrow T_{CL} = Week \\ \tau_{CL} \leq 12 \rightarrow T_{CL} = Day \end{array} \right\} .$$

6.2.5 Open-Loop PSP Reservoir

The open-loop PSP reservoir generation was modelled through an additional virtual external "Hydro-Open-Loop" node, directly linked to the market node, which was set up to function as a combination of a traditional reservoir and a closed-loop PSP. In particular, the generation from the natural hydro energy inflows was modelled exactly in the same way as for the traditional reservoir generation, this time within the Hydro-Open-Loop node instead of the market node. Accordingly, its monthly hydro energy time series were computed as follows:

$$ENE_{M,OL}\ [MWh] = \sum_{month} \left(INF_{W,OL} - \Delta L_{W,OL} - E_{min,W,OL}\right) ,$$

with $\Delta L_{W,OL} = L_{W+1,OL} - L_{W,OL}$,

$E_{min,W,OL} = P_{min,W,OL} \times 168$,

where $ENE_{M,OL}\ [MWh]$ is the monthly energy availability. $INF_{W,OL}$ are the weekly hydro energy inflows. $\Delta L_{W,OL}$ is the delta between the reservoir levels at the beginning of two consecutive weeks. $E_{min,W,OL}$ is the weekly minimum energy generation, which has been already accounted in the ROR time series. $INF_{W,OL}$, $L_{W,OL}$ and $P_{min,W,OL}$ were directly taken from the PECD Hydro data.

The equivalent open-loop maximum power to set up the model was in general computed as:

$$P_{\text{max\_}EQ,W,OL}\ [MW] = \ P_{max,W,OL} - P_{min,W,OL} ,$$

where the equivalent maximum power $P_{\text{max\_}EQ,W,OL}$ was equal to its maximum power minus its minimum power.

$P_{\text{max\_}EQ,W,OL}$ was imposed as the hourly maximum power flow on the link between the market node and the virtual Hydro-Open-Loop node.

The PSP contribution to the total open-loop generation was modelled as a perfectly reversible closed-loop PSP reservoir. Hence, through two virtual external nodes, one with ideally unlimited generation availability, the "Open-Turb" node, and one with ideally unlimited demand availability, the "Open-Pump" node. Both nodes were directly linked to the Hydro-Open-Loop node. The values for the maximum pump and

turbine power were extracted from the PECD Hydro database as follows and imposed as the maximum hourly energy flows on the links between the Hydro-Open-Loop node, and the virtual Open-Turb and Open-Pump nodes respectively:

- $P_{max,PUMP,OL} = P_{max,TURB,OL}$ = Total installed open-loop pump capacity [MW].

The PSP cycle efficiency was again assumed to be equal to 75% and imposed as a linear binding constraint between the cumulated energy flows on the links between the Hydro-Open-Loop node, and the virtual Open-Turb and Open-Pump nodes, over an optimization cycle T_{OL}:

$$\sum_{T_{OL}} (ENE_{TURB\_OL} \Rightarrow OL\text{-}NODE) = 0.75 \times \sum_{T_{OL}} |ENE_{PUMP\_OL} \Rightarrow OL\text{-}NODE| \,,$$

where $ENE_{PUMP\_OL} \Rightarrow OL\text{-}NODE$ [MWh] is the energy flow from the Hydro-Open-Loop node to the Open-Pump node (negative according to the convention of the tool).

Similarly to the closed-loop PSP, the binding constraint could be imposed only over a daily or weekly optimization cycle T_{OL}, based on the value of the time constant τ_{OL}, to ensure that the cumulated pumped or turbined energy was as consistent as possible with the open-loop reservoir size:

$$\tau_{OL} \ [h] = \frac{SIZE_{OL}}{P_{max,TURB=PUMP,OL}}; \left\{ \begin{array}{l} \tau_{OL} > 12 \rightarrow T_{OL} = Week \\ \tau_{OL} \leq 12 \rightarrow T_{OL} = Day \end{array} \right\} .$$

6.2.6 Open-Loop Exceptions for Maximum and Minimum Power

The same exceptions applied as for the traditional reservoir, although not affecting the market nodes in the tri-lateral Hydro 2019 model:

- If only $P_{min,W,OL}$ was climate-dependent and modelled through a virtual thermal unit:
  - $E_{min,W,OL}$ was no more accounted as additional ROR generation.
  - Thus, $ENE_{M,OL}\ [MWh] = \sum_{month} (INF_{W,OL} - \Delta L_{W,OL})$.
  - Thus, $P_{\max\_EQ,W,OL}\ [MW] = P_{max,W,OL}$.
  - $P_{\max\_EQ,W,OL}$ was imposed as the hourly maximum flow on the link between the external Hydro-Open-Loop node and the market node (positive direction).
  - $P_{min,W,OL}$ was imposed with an hourly hard constraint, setting the generation of the corresponding virtual thermal unit as a lower bound to the actual flow on the link between the external Hydro-Open-Loop node and the market node (positive direction).
- If only $P_{max,W,OL}$ was climate-dependent and modelled through a virtual thermal unit:

- $E_{min,W,OL}$ was still accounted as additional ROR generation.
- Thus, $ENE_{M,OL}\ [MWh] = \sum_{month} (INF_{W,OL} - \Delta L_{W,OL} - E_{min,W,OL})$.
- Thus, $P_{\max\_EQ,W,OL}\ [MW] = P_{max,W,OL} - P_{min,W,OL}$.
- $P_{\max\_EQ,W,OL}$ was imposed with an hourly hard constraint, setting the generation of the corresponding virtual thermal unit as an upper bound to the actual flow on the link between the external Hydro-Open-Loop node and the market node (positive direction).

- If both $P_{max,W,OL}$ and $P_{min,W,OL}$ were climate-dependent and modelled through a virtual thermal unit:
  - $E_{min,W,OL}$ was no more accounted as additional ROR generation.
  - Thus, $ENE_{M,OL}\ [MWh] = \sum_{month} (INF_{W,OL} - \Delta L_{W,OL})$.
  - Thus, $P_{\max\_EQ,W,OL}\ [MW] = P_{max,W,OL}$.
  - $P_{\max\_EQ,W,OL}$ was imposed with an hourly hard constraint, setting the generation of the corresponding virtual thermal unit as an upper bound to the actual flow on the link between the external Hydro-Open-Loop node and the market node (positive direction).
  - $P_{min,W,OL}$ was imposed with an hourly hard constraint, setting the generation of the corresponding virtual thermal unit as a lower bound to the actual flow on the link between the external Hydro-Open-Loop node and the market node (positive direction).

6.3 Hydro Energy Reservoir Management

The ANTARES Hydro Energy Manager could be optionally activated for the Annual reservoir of the Hydro 2018 or the traditional reservoir and/or the open-loop generation (from natural hydro energy inflows only). ANTARES v6.1 requires monthly minimum and maximum reservoir level trajectories for the proper functioning of the reservoir manager, which enables the preoptimization of hydro storage resources over the whole year of the simulation. It leverages a heuristic which distributes the total yearly hydro energy inflows proportionally to the net residual load of each month, week and day. When the option was activated for a certain node, the reservoir levels were set by the tool during the optimization within its minimum and maximum trajectories. Thus, the monthly availability time series were computed as follows:

$$ENE_{M,RES}\ [MWh] = \sum_{month} (INF_{W,RES} - E_{min,W,RES})\ ,$$
$$ENE_{M,OL}\ [MWh] = \sum_{month} (INF_{W,OL} - E_{min,W,OL})\ .$$

The definition and implementation of $E_{min,W}$ and $P_{\max\_EQ,W}$ followed the same rules previously described, also in the case of climate-dependent $P_{max,W}$ and/or $P_{min,W}$.

If the option was deactivated, the hydro energy preallocation was performed by the tool only internally to each month of the simulation, hence taking the monthly cumulated inflows as a fixed dispatch quantity. The standard values for the minimum and maximum reservoir level trajectories would have been 0% and 100% for most of the market nodes since consistent trajectories were provided only for very few market nodes. Therefore, a decision was taken to set to *off* the reservoir management option for the nodes not providing explicit trajectories. This approach brought about several implications, either positive or negative, which I identified in my analysis and are discussed in detail in Section 8.1. A detailed description of the ANTARES Hydro Energy Manager and its functioning is available in Section 4.3.

6.4 Preliminary Findings

The evolution of the hydro modelling methodologies peculiar to the use of the ANTARES v6.1 simulator is described accurately in this chapter to set a reference point and critical analysis for its future use and development either within or outside the ENTSO-E framework. On the other hand, I attempted to include all the details required to make it convenient and usable also for a reader with little or no experience with ANTARES.

Moreover, confronting the two hydropower modelling methodologies was crucial to get a preliminary feeling on how the results of the simulations were likely to be impacted, identifying the potential advantages and criticalities of one approach against the other. However, some of the modelling choices and assumptions identified were imposed by the specific design and requirements of the modelling tool, rather than by the sole data availability and structure peculiar to the different hydro databases. Nevertheless, this was not perceived as a threat to the validity of the analysis, as the setting of my work was intentionally placed within the ANTARES environment, being the main tool used in APG for mid-term generation adequacy studies at the time of my assessment.

Figure 6.3 shows in the ANTARES v6.1 GUI the resulting tri-lateral model configurations after applying the hydropower modelling methodologies described in this chapter.

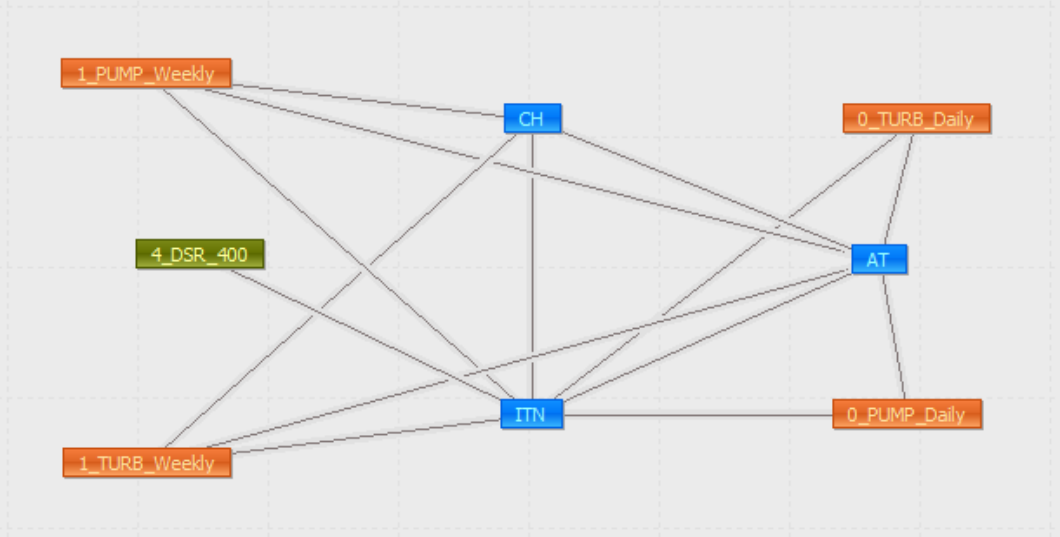

(a) Hydro 2018 tri-lateral model.

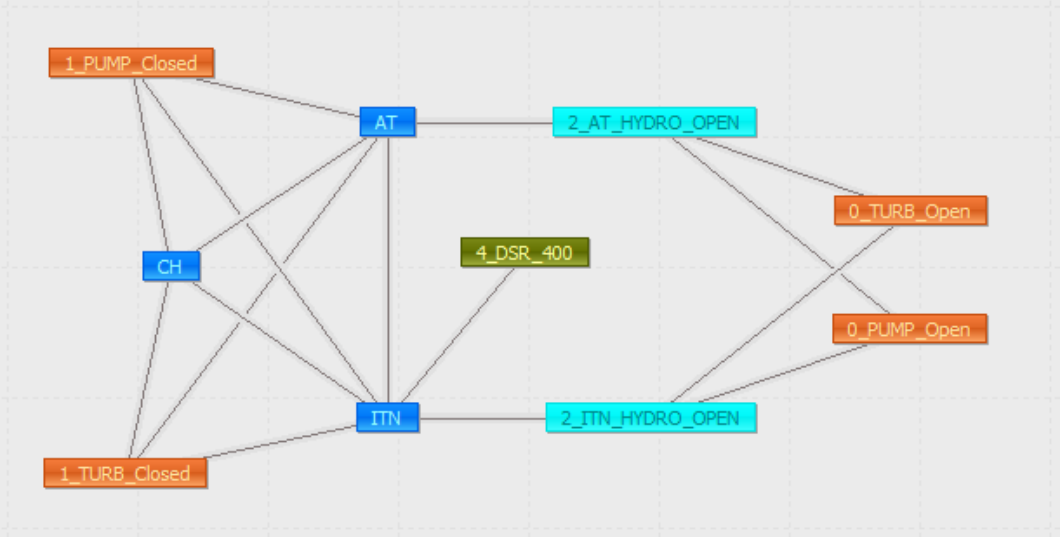

(b) Hydro 2019 tri-lateral model.

Figure 6.3: The tri-lateral models in the ANTARES v6.1 GUI.

Chapter 7

Simulation and Results

The following chapter contains a detailed comparison of the results obtained from the ANTARES v6.1 Monte Carlo simulations. Its main purpose is to provide insight into the research question from the perspective of the adequacy metrics and the UCED, in all respects, from the averaged yearly results down to the hourly energy dispatch. As stated previously, the models I used for the simulations were the two tri-lateral models including Austria, Switzerland and Italy North. Following the reasoning described in the research methodology (Section 2.3), the two models were built identically and in compliance with the ENTSO-E MAF 2019 data and methodology described in Chapter 3. In particular, the thermoelectric power generation, the availability time series for wind and solar dispatch, the domestic demand, the NTCs, the forced outage patterns and all the other variables were exactly the same in both models. This approach granted a fair and level basis before adding the hydropower layer: one model was set up with the Hydro 2018 data and modelling methodology described in Section 6.1, while the other one was set up with the new Hydro 2019 data and modelling methodology presented in Section 6.2. A schematic representation of the tri-lateral models in the ANTARES v6.1 GUI is given in Figure 6.3. The Net Generation Capacities (NGCs) expected for the target year 2025, aggregated by fuel type as published by ENTSO-E [28], are collected in Table 7.1 together with demand and NTC data. The detailed hydropower capacities are reported in Table 5.3.

The starting point of the comparison is a summary of the averaged yearly generation by fuel type and the expected adequacy indices, to provide a high-level picture of the overall system results. It follows a brief description of the visualization tool that I developed in the R environment [13]. This interactive graphical instrument proved to be a useful support to browse the results and provide insightful charts. The analysis proceeds with a scrutiny of the UCED hourly profiles for a sample of days selected ad hoc to compare the hydropower dispatch capabilities during scarcity periods. Finally, the intensity and the probability distribution of ENS events are investigated trying to identify the changes arising from the differences in the two hydropower modelling methodologies.

NGC [MW]	AT	CH	ITN
Nuclear	0	2200	0
Lignite	0	0	0
Hard Coal	0	0	1090
Gas	3416	0	15789
Oil	168	0	0
Hydro-ROR	6130	4113	4762
Hydro-turbine (Reservoir)	2430	8152	7634
Hydro-turbine (PSP)	4188	3989	5005
Wind Onshore	5500	180	226
Solar PV	5002	4000	11326
Others renewable	609	907	2384
Others non-renewable	955	830	3076
Total FCR and FRR	544	869	1500
Demand Data			
Avg. total demand [TWh]	76.59	61.93	182.98
St. Dev. [MWh]	461.20	464.65	1569.21
Range [MWh]	2001.38	2006.39	8565.54
Max Peak [TW]	13.21	11.24	36.40
NTC (exp.) [MW]			
AT	-	1200	380
CH	1200	-	3750
ITN	200	1700	-

Table 7.1: NGCs, demand and NTCs for the target year 2025. MAF 2019 data [28].

7.1 Convergence

In the MAF 2019 study, convergence was monitored through a dimensionless coefficient of variation α, defined on the adequacy metric EENS for the total system [10]:

$$\alpha = \frac{\sqrt{Var(EENS_{tot})}}{EENS_{tot}} ,$$

where $EENS_{tot}$ is the average of the total system ENS, while $Var(EENS_{tot})$ is its variance over all the $M \times N$ Monte Carlo years of the simulation.

The convergence error of EENS was expected to be negatively correlated to the total number of Monte Carlo years $M \times N$. Since M was fixed and equal to the number of climate years, i.e. 35, the number of forced outage patterns N was defined to be sufficiently high to guarantee that α reached a low and stable value. No specific common threshold for α was set, whereas each of the five modelling tools in the MAF 2019 defined its own N number for an optimal trade-off between the accuracy of the results and computational time.

The Monte Carlo simulations for my thesis counted N equal to 30 forced outage patterns repeated per each of the 35 climate years, hence reaching a total sample size of 1050 simulated years. The sampled years were identical for both models, except of course for the hydro energy time series, which followed the "dry, normal, wet" pattern defined in Table 5.5 for the Hydro 2018 model. Figure 7.1 shows the evolution of the coefficient α for the 1050 Monte Carlo years.

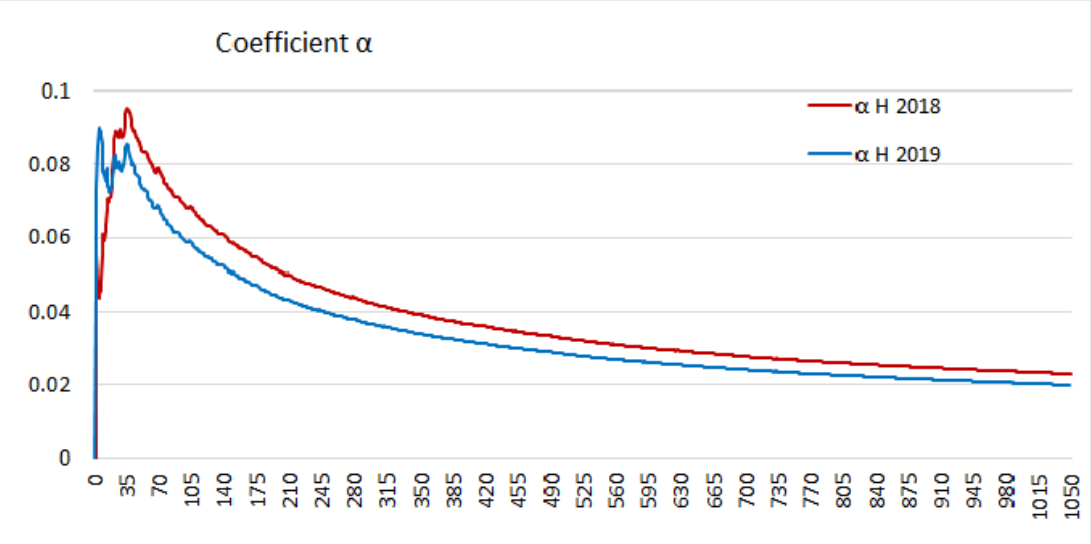

Figure 7.1: Evolution of the coefficient of variation α for the tri-lateral models.

7.2 Yearly Averaged Results

As a common practice in several mid-term adequacy reports, the adequacy forecasts are here expressed in terms of expected adequacy metrics, namely LOLE and EENS (Section 3.2.4). Table 7.2 contains also the averaged output per generation type, reporting the deltas and their percentage change, taking as a basis the results obtained from the Hydro 2018 model. Acknowledged the purely academic nature of my simulations, whose only purpose was to describe, compare and evaluate the evolution of the hydropower modelling methodologies developed for ANTARES v6.1, it clearly follows that only the appreciable differences between the results from the two models are relevant for my analysis. Moreover, setting up the models with the arbitrary tri-lateral configuration allowed on the one hand to reduce the complexity and better isolate the effects of the single contributors from the hydropower modelling perspective. On the other hand, such an islanded configuration determined a highly stressed and not secure status of the system, making the results far from being representative of the system behavior under real conditions within the interconnected pan-European network. In other words, the results obtained were suitable to assess the hydropower dispatch and its impact on the generation adequacy indices but did not give any realistic estimate of the future adequacy status of the system. The above statements shall be intended as a disclaimer to avoid any potential misinterpretation of the results.

Looking at the averaged results per generation type, it was possible to notice that the values for the thermal generation as well as wind and solar production were substantially unchanged. This proved the successful setup of the models with an equal availability of such resources. Significant differences could be identified, as expected, in the hydropower generation. Since the categories of hydropower plants were different in the two models, the generation was reported in the table divided into run-of-river, PSP and hydro storage. The first value to consider was the total hydro generation, showing only a minimal variation. This was a positive feedback on the methodology adopted for the hydro data reaggregation and the clustering of the historical years. In fact, the average hydro energy availability over the whole sample years was fairly equivalent. Austria showed the main differences, with **an increase of run-of-river generation of around 27%** at the expense of the **total hydro storage generation, which decreased by 49%** (excluding PSP). This should not come as a surprise, since in the Hydro 2019 methodology the inflows to the swell ROR & Daily storage were merged into the new run-of-river & pondage category, which was modelled as hourly non-storable ROR generation (Section 6.2.1). This internal shift of natural inflows was confirmed by the almost equal but opposite delta of the two categories in terms of actual energy generated, around 7000 GWh, which was consistent with the average yearly inflows to the swell ROR & Daily storage reported in Table 5.4. This reduction of hydro storage availability partially explained the increased employment of PSP generation, + 78%, as an attempt of the system to compensate for such deficiency. A further reason determining the higher PSP generation in Austria was found in the definition of its maximum power, which was reduced by 1/70 of the weekly natural

	Delta [GWh]			Delta [%]		
Averaged results	AT	CH	ITN	AT	CH	ITN
Nuclear	0.0	-9.2	0.0	0.00%	-0.06%	0.00%
Hard Coal	0.0	0.0	-56.2	0.00%	0.00%	-1.31%
Gas	-97.5	0.0	503.4	-0.51%	0.00%	0.49%
Oil	-47.6	0.0	0.0	-9.31%	0.00%	0.00%
Run-of-river	**6812.7**	**67.5**	**143.0**	**27.60%**	**0.40%**	**0.88%**
Tot PSP Turbine	568.0	81.2	13.6	77.66%	33.19%	0.80%
Tot PSP Pump	757.3	108.3	18.1	77.66%	33.19%	0.80%
Tot hydro generation	**455.5**	**24.3**	**-32.2**	**1.14%**	**0.07%**	**-0.09%**
Tot hydro storage exc. PSP	-6925.2	-124.5	-188.7	-47.99%	-0.63%	-1.07%
Tot hydro storage	**-6357.2**	**-43.2**	**-175.2**	**-41.93%**	**-0.22%**	**-0.91%**
Wind	0.0	0.0	0.0	0.00%	0.00%	0.00%
Solar	0.0	0.0	0.0	0.00%	0.00%	0.00%
Other RES	0.0	0.0	0.0	0.00%	0.00%	0.00%
Other non-RES	0.0	0.0	0.0	0.00%	0.00%	0.00%
DSR	0.0	0.0	-122.8	0.00%	0.00%	-4.64%
Net balance (exp. > 0)	-172.2	-253.9	426.0	-2.08%	-7.43%	3.65%
EENS	**280.9**	**-160.7**	**152.0**	**43.14%**	**-12.58%**	**3.15%**
LOLE [hour]	**166.1**	**-52.5**	**24.1**	**34.86%**	**-4.98%**	**2.16%**

Table 7.2: Absolute and relative differences (w.r.t. Hydro 2018) in the averaged yearly results.

inflows in the Hydro 2018 methodology (Section 6.1.3), while directly taken equal to the installed capacity in the Hydro 2019 approach. Nevertheless, also for CH, a 33% increase of PSP usage was noticeable, despite being closed-loop generation, hence not affected by the natural inflows. A possible explanation was that the Hydro 2019 model dispatched PSP differently reacting to the new maximum power of the traditional reservoir category, with respect to the complex heuristic used to define the maximum power of the aggregated hydro reservoir in the Hydro 2018 model (Section 6.1.2). On the other hand, the higher continuous availability of non-dispatchable ROR generation in Austria potentially fostered higher pumping operations also in the neighboring zones during low-demand hours. These remarks on hydropower generation were likely to be the main source of change for the EENS and LOLE in the system. It is interesting to point out that despite the total hydro energy generated increased in Austria by around 500 GWh, the adequacy status of the system seemed highly deteriorated, with a 43% increase of EENS and 35% more LOLE. This clearly confirms that **generation adequacy is a matter of contingent availability of resources and their maximal dispatch during hours of peak demand or critical system status, rather than their average availability**. CH and ITN showed a lower impact on the adequacy metrics, consistently with the lower impact on their averaged hydropower generation.

This was due to the lower diversity and complexity of the hydropower resources in CH and ITN, for which the new methodology mainly caused an internal shift from the Annual PSP reservoir to the traditional reservoir or open-loop PSP categories, as shown in Table 5.3. In fact, the yearly average delta in terms of total hydro storage generation was less than 1% for both market nodes. Interesting to notice that ITN actually achieved slightly lower EENS and LOLE values, thanks to the higher employability of its PSP capacity.

7.3 Hourly UCED Results

The comparison of the averaged yearly results allowed me to formulate general remarks and get a high-level perspective on the adequacy indices and hydropower dispatch. The hourly UCED results were also investigated to better identify the impact of the new modelling methodology on the hydropower generation in ANTARES v6.1. The UCED analysis provided also a benchmark for the insights reported in the previous section.

Averaging the results, a common practice in Monte Carlo adequacy simulations, allows on the one hand to get an estimate of the mean expected generation, demand, and system security. On the other hand, consistency is lost in terms of internal energy balance, Kirchhoff's laws and technical operation of power plants. Let us assume that the simultaneous occurrence of low RES availability and forced outages of generating units and transmission lines cause ENS to occur, in a specific hour $\hat{h}$, for 10% of the years in the sample. The averaged hourly results would show for $\hat{h}$ a non-zero value of ENS, while the average total generation would still be greater than the total average native demand, being that true for the remaining 90% of the occurrences. A similar reasoning holds, for instance, for PSP generation, for which simultaneous pump and turbine operations can emerge from the averaged hourly dispatch, due to the different contingent resource availability peculiar to each Monte Carlo year of the simulation. It follows that the hourly results are sensible only if analyzed internally to a single Monte Carlo year of the sample.

I chose to target one of the years characterized by the historical climate conditions of 2016 (CY 2016). As described in Section 5.3.2, 2016 was chosen as the reference climate year for "normal" hydrologic conditions for all three market nodes. Thus, the climate year 2016 was characterized by the same availability of solar, wind and hydro resources, as well as demand profile, for the whole system in both the Hydro 2018 and Hydro 2019 models. This choice was of key importance to ensure that the differences in the UCED results were driven by the sole changes in the hydropower modelling methodology, being all the other variables perfectly aligned between the two models.

For the sake of completeness, Table 7.3 reports also they yearly aggregated results for the CY 2016. Similar trends can be identified to the ones shown by the averaged yearly results, since the "normal" hydrological conditions were chosen to be as close as

possible to the average availability of hydro storage resources.

	Delta [GWh]			Delta [%]		
Averaged results	AT	CH	ITN	AT	CH	ITN
Nuclear	0.0	-2.2	0.0	0.00%	-0.01%	0.00%
Hard Coal	0.0	0.0	12.1	0.00%	0.00%	0.28%
Gas	-55.4	0.0	113.0	-0.28%	0.00%	0.11%
Oil	-7.7	0.0	0.0	-1.30%	0.00%	0.00%
Run-of-river	**6882.4**	**-4.2**	**-4.4**	**28.17%**	**-0.02%**	**-0.03%**
Tot PSP Turbine	624.7	12.1	79.1	93.68%	6.18%	4.33%
Tot PSP Pump	833.0	16.1	105.4	93.68%	6.18%	4.33%
Tot hydro generation	**721.5**	**7.2**	**74.6**	**1.84%**	**0.02%**	**0.21%**
Tot hydro storage exc. PSP	-6785.7	-0.7	0.0	-47.75%	0.00%	0.00%
Tot hydro storage	**-6160.9**	**11.3**	**79.1**	**-41.41%**	**0.06%**	**0.40%**
Wind	0.0	0.0	0.0	0.00%	0.00%	0.00%
Solar	0.0	0.0	0.0	0.00%	0.00%	0.00%
Other RES	0.0	0.0	0.0	0.00%	0.00%	0.00%
Other non-RES	0.0	0.0	0.0	0.00%	0.00%	0.00%
DSR	0.0	0.0	41.7	0.00%	0.00%	1.37%
Net country balance	13.5	-134.2	120.7	0.17%	-5.37%	1.16%
EENS	**175.2**	**-128.7**	**34.8**	**17.12%**	**-8.72%**	**0.67%**
LOLE [hour]	**82.7**	**-99.8**	**13.3**	**11.83%**	**-7.86%**	**1.05%**

Table 7.3: Absolute and relative differences (w.r.t. Hydro 2018) in the yearly results for CY 2016.

To examine and compare the detailed dispatch effectively and conveniently, I developed a visualization tool, coded in the R programming language [13], which enabled a detailed and interactive scrutiny of the hourly results. The code leveraged the R package "antaresViz" [42] and other open-source libraries. The main advantage provided by the visualization tool was its capability to plot all the results from all the Monte Carlo years of the simulation, with several options to dynamically change the variables displayed, the level of aggregation, the time resolution, the market node, and so on. The different views available included variegate features like customizable stacked charts, heat maps, bar charts and others.

Figure 7.2 shows some examples of custom stacked area charts reporting the hourly energy mix and the detailed hydropower dispatch in the tri-lateral system. Although the analysis was dynamically performed over the whole year, the timeframe in the figure is restricted to one significant week, i.e. the Calendar Week (CW) 45, for a neater visualization.

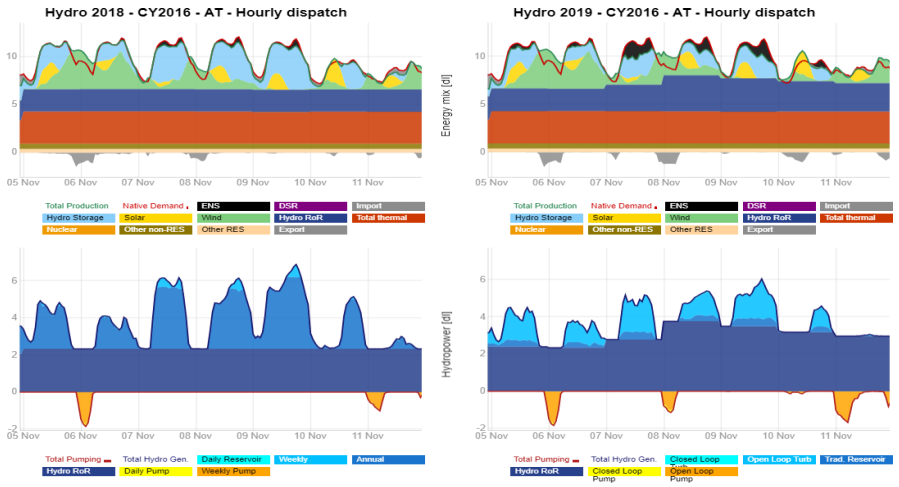

(a) AT

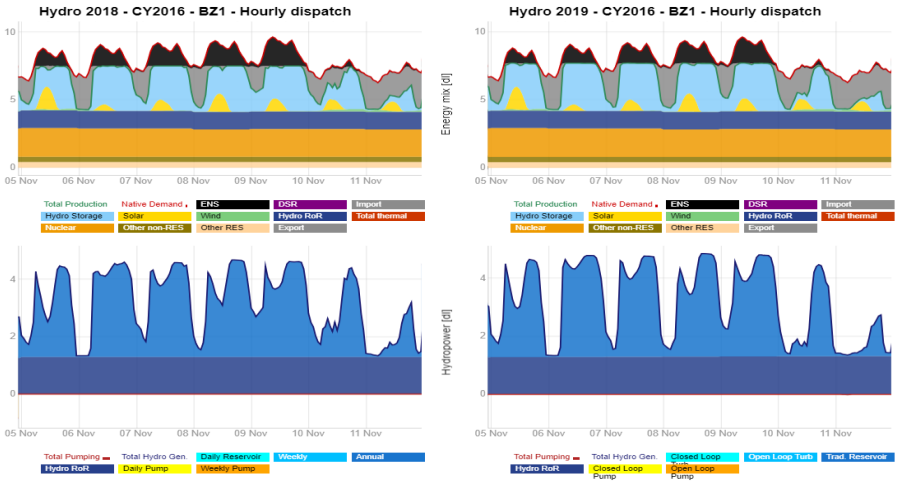

(b) CH

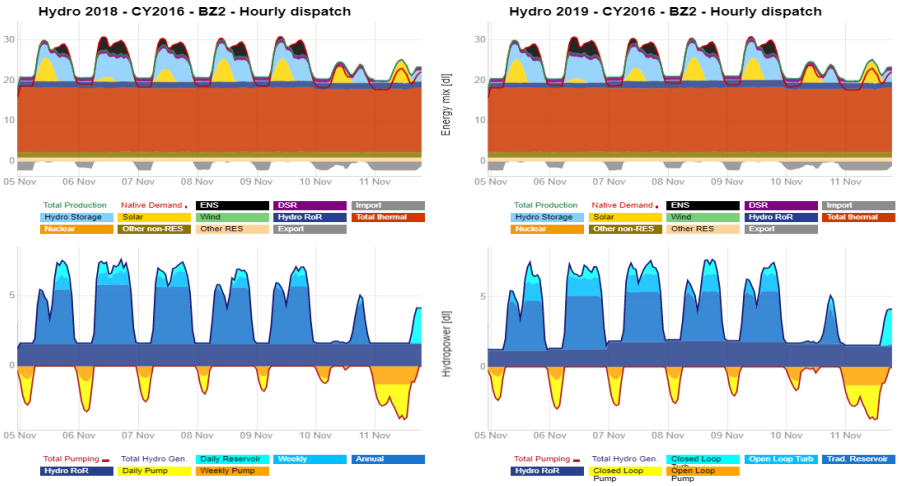

(c) ITN

Figure 7.2: Hourly UCED results for the tri-lateral system, CY 2016, CW 45.

The stacked charts report the power dispatch on the grid on a comparative dimensionless scale to better highlight the differences between the two methodologies. The upper half of each chart depicts the hourly "balance", including all the generation types. The red line shows the internal demand (including pumping consumption), while the green line is the total internal generation. The energy balance is of course always respected: if the internal generation exceeds the internal demand, the delta is exported (the gray negative band). Instead, if the internal demand exceeds the internal availability, the delta is either covered by imports (the gray positive band, e.g. visible for CH) or is accounted for as ENS (the black band). The lower half of each chart shows, instead, the detailed hydropower dispatch, including pumping consumption (the negative orange and yellow bands). Both views are reported for the Hydro 2018 model, on the left side, and for Hydro 2019 model, on the right side.

Looking at the Austrian figures, it was clear that the duration and the magnitude of the load shedding events during peaks of demand were far more severe in the results from the Hydro 2019 model. It was also evident that these discrepancies were due to the different dispatch capabilities of hydropower resources. In particular, as identified in the yearly averaged results, the ROR generation (dark blue band) was inflated by the inflows from the swell ROR & daily storage, which however needed to be continuously dispatched at a fixed hourly rate by ANTARES v6.1 and hence did not contribute to fulfill adequacy during peak hours. The total hydro storage generation in the Hydro 2018 model was considerably higher, since these inflows were treated as available to the Annual reservoir. Moreover, there was a sensible difference in the peak hydropower generation, which raised multiple times above 6 in the Hydro 2018 dispatch, while it was always conspicuously below the threshold of 6 in the Hydro 2019 results. The reason was still identified in the allocation of the inflows. In fact, despite the installed capacities in both models would allow the system to reach similar values of maximum power, fewer inflows meant that the ANTARES Hydro Energy Manager had less energy to preallocate and hence lower lots to be distributed during the week. The solver then preferred a smoother dispatch of hydro resources rather than isolated peaks, consistently with a more realistic profile. The smoothing of the daily profiles was also driven by the intra-daily generation coefficient γ, set on 2 for all the nodes, which posed a daily upper bound on the peak over the average storage generation, as described in Section 4.3.1. It was also possible to notice the increase of night pumping operations, employing the extra energy available thanks to the higher continuous dispatch of ROR inflows.

The focus was naturally set on the figures of the Austrian market node, which was also the one showing the most significant changes in the hourly dispatch due to the introduction of the new methodology. Nevertheless, the analysis of CH and ITN confirmed that the internal shift from the Annual PSP reservoir to the traditional reservoir and open-loop PSP generation did not have any substantial impact on the UCED results, in the absence of pondage and Daily storage inflows. It is interesting to report also that CH showed a negative remaining capacity (i.e. total generation lower

than the internal demand) during the whole CW45, hence posing itself in a so-called "negative net position" trying to import as much as possible from the neighboring nodes. This explained the absence of pumping operations in its UCED profile. This artificially prolonged state of inadequacy in CH highlighted the "peak-shaving" strategy of the solver, which distributed ENS almost evenly during consecutive days of scarcity.

7.4 Loss of Load Probability Distribution

The averaged yearly results in Table 7.2 did not provide any information about the distribution and magnitude of load shedding events, as well as their likelihood. These aspects, rising from the probabilistic nature of Monte Carlo simulations, are equally interesting and complementary to the analysis of the generation profiles. The hourly expected LOLP proved to be an insightful indicator for this purpose, allowing me to grasp not only the probability of the ENS occurrences but also their temporal distribution during the target year. The R visualization tool was insightful also for this task: Figure 7.3 contains heat maps of the expected distribution of the hourly LOLP in the tri-lateral system out of the 1050 Monte Carlo years of the sample. The maps report both the Hydro 2018 results, in red, and the Hydro 2019 results, in blue.

The heat maps group the hourly LOLP values per month on the y-axis and per weekday on the x-axis. As expected, the most critical hours for the system can be identified in the peak hours during winter weekdays. The pictures show critical values of LOLP during the whole winter months as a natural consequence of the artificially stressed and inadequate tri-lateral configuration of the models. Thus, also the LOLP values are meaningful only within the comparative framework of my thesis. The EENS for the Hydro 2019 results is more homogeneously distributed during winter, with lower values but longer "tails" in spring and autumn. The main reason for these differences originated from the different distribution and variability of the hydro energy inflows available in Figure 5.1, whereas their intrinsic measures of dispersion were reported in Table 5.4. In fact, the Hydro 2019 model included all the 35 inferred historical time series of inflows, whose intrinsic variability was reflected also in the EENS distribution. Instead, the Hydro 2018 model inherited the simplified "dry", "normal" and "wet" clustering, with only three different profiles for hydro energy availability assigned to all the Monte Carlo years. It follows that resource scarcity tended to recur more often in the same hours of the year, hence causing very high and concentrated LOLP values up to 100%. The analysis is complemented by Figure 7.4 which compares the EENS hourly peaks. The same reasoning apply as for the heat maps, whereas it is possible to notice that more distributed EENS peaks lead also to a decrease of the maximum values reached by the spikes, as a natural effect of EENS, which is an averaged metric.

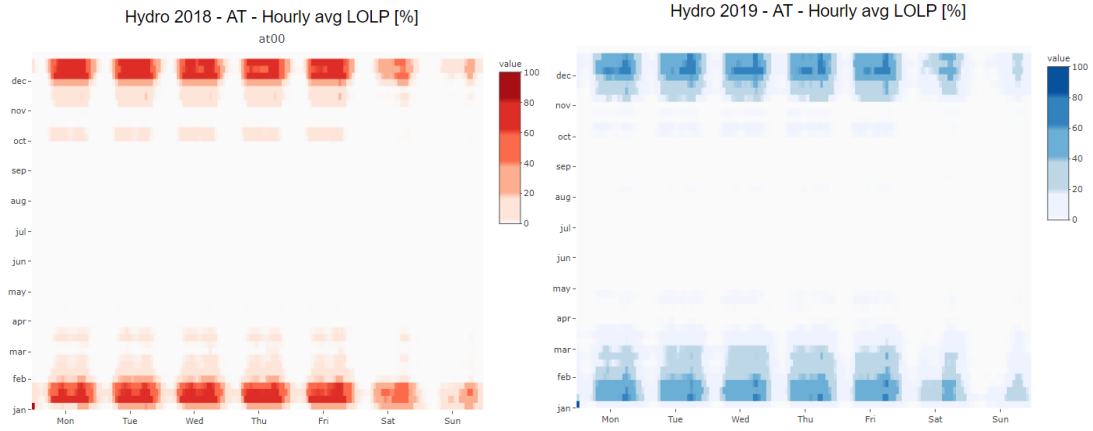

(a) AT

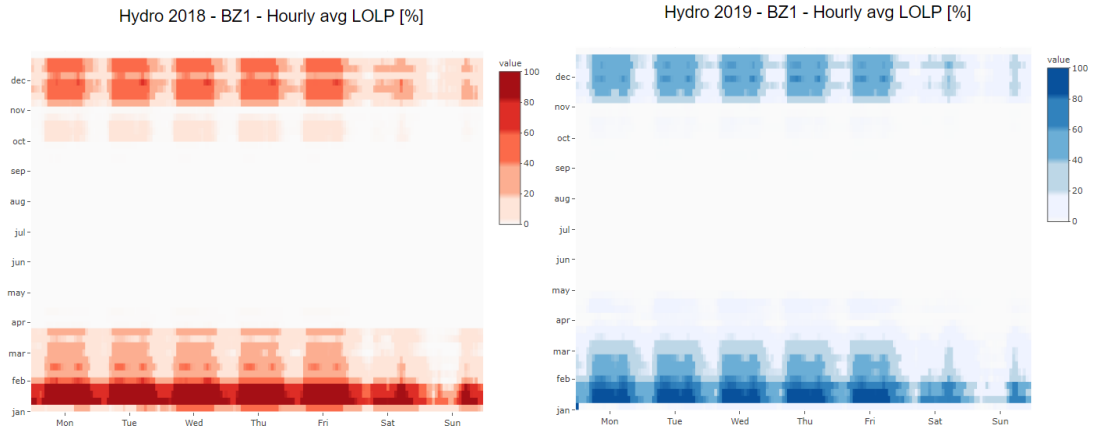

(b) CH

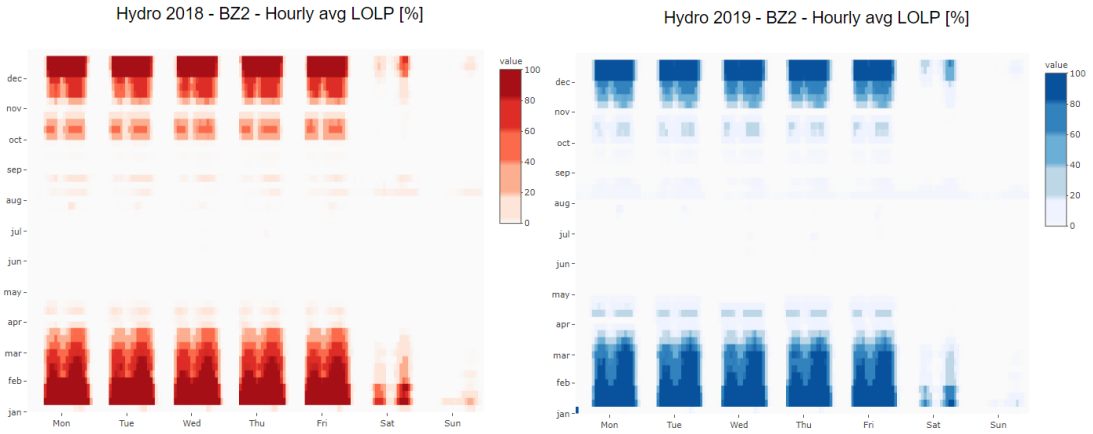

(c) ITN

Figure 7.3: Hourly LOLP distribution per month and day of the week.

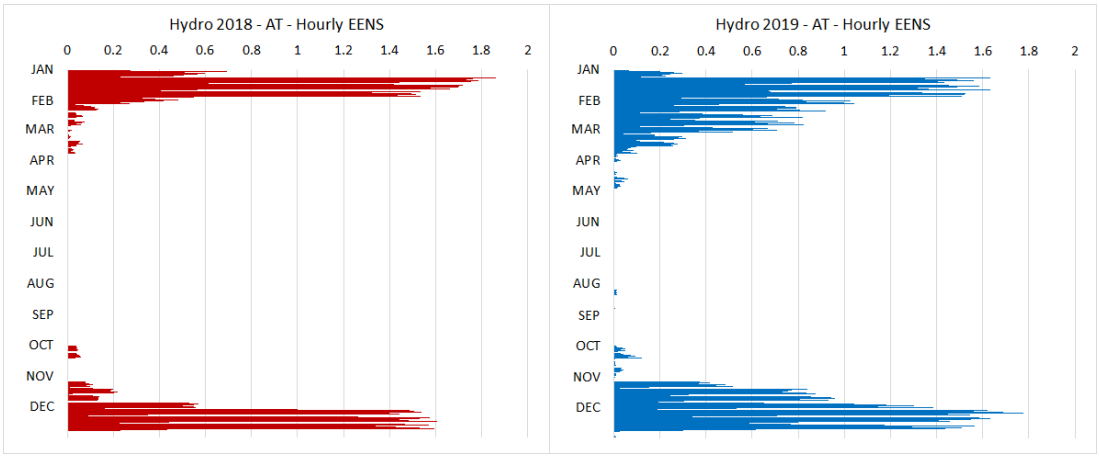

(a) AT

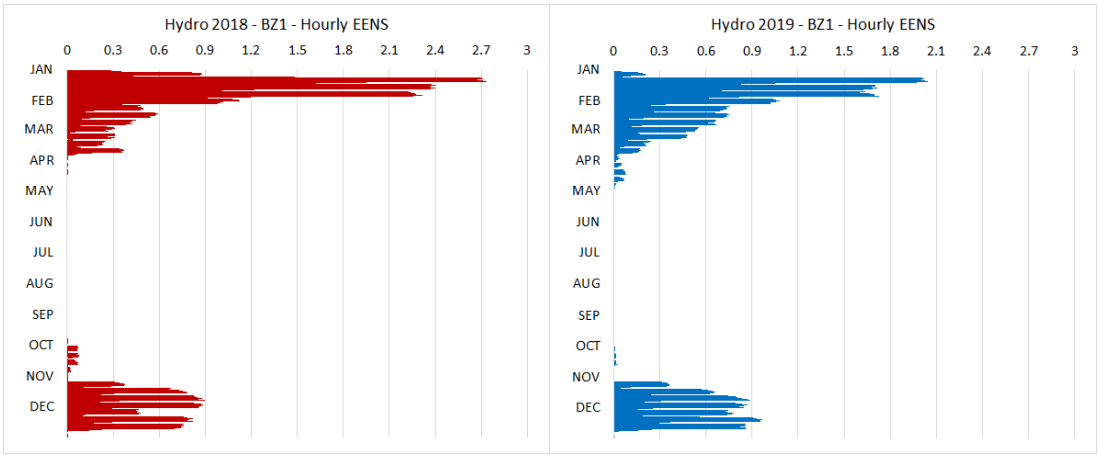

(b) CH

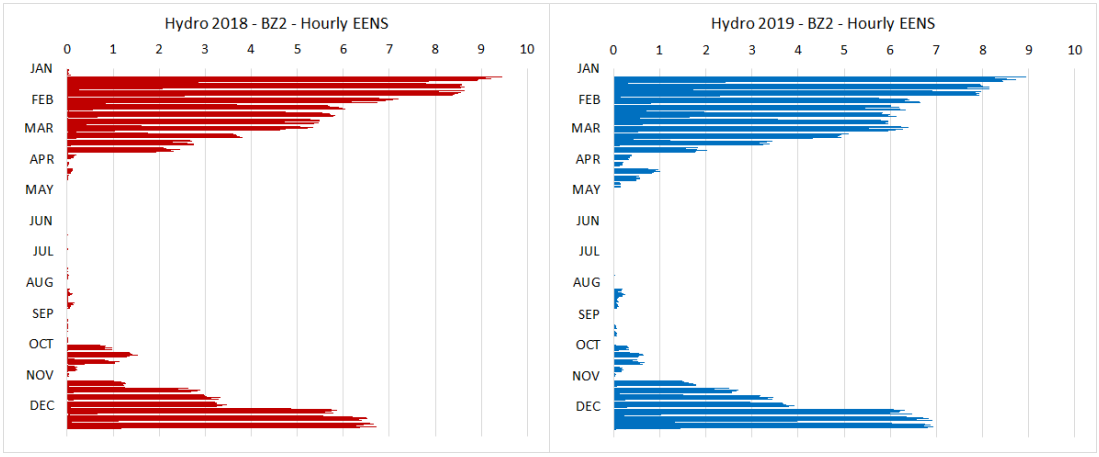

(c) ITN

Figure 7.4: Hourly EENS distribution on a comparative scale.

Chapter 8

Conclusions and Future Work

Approaching the analysis from the three complementary perspectives presented in Section 2.2, namely (i) the hydropower modelling methodology, (ii) the average adequacy results, and (iii) the hourly UCED, proved to be an effective method to achieve a comprehensive answer to the research question:

what was the impact of the new PECD Hydro database on the Austrian hydropower dispatch in the Mid-Term Adequacy Forecasts?

The results of the tri-lateral models for the target year 2025 indicated a severe deterioration of the expected adequacy metrics for the Austrian market node, with 43% increased EENS and 35% increased LOLE hours (Table 7.2). The key drivers seemed to be the new criteria for the aggregation of hydropower plants, especially merging the previous run-of-river and swell ROR & Daily storage category into the new run-of-river & pondage category. As shown in Figure 7.2, this led to a shift of hydro energy inflows from dispatchable hydro storage generation to non-dispatchable run-of-river sources, hence causing in the UCED less availability of hydro storage energy, as well as a lower maximum power output during peak hours. Notwithstanding, the comparison of the hydropower modelling methodologies in Chapter 6 highlighted that several modelling choices and assumptions were imposed by the specific design, requirements and limitations of the ANTARES v6.1 modelling tool, rather than by the actual availability and structure of the hydro databases. It follows that the analysis of the results could not provide a clear distinction between the changes driven solely by the new PECD Hydro database and the ones related to the proper setup and functioning of the ANTARES v6.1 simulator. Thus, it is important to stress that the findings here reported should be considered as tool-specific and may differ if the same research methodology would be applied to a different modelling tool. Nevertheless, an effect clearly attributable to the new hydro database was found in the distribution of the hourly LOLP and EENS peaks. As discussed in Section 7.4, the 35 historical inferred time series for hydro energy inflows brought higher variability in the availability of hydropower resources, which was reflected in the distribution of load shedding events in all the three market nodes.

Pondering on the research methodology described in Section 2.3, the choice of a tri-lateral system framework proved to be a flexible test bench for the simulations, thanks to the lower computational and time complexity. The two additional market nodes provided a simplified cross-border configuration as well as an insightful benchmark for the results. In fact, the impact of hydropower modelling on the adequacy metrics was clearly amplified by the peculiar energy mix of Austria, which counted for a numerous and diverse fleet of hydropower units, including river pondage capacity, while it did not affect so severely the neighboring zones. The tri-lateral islanded configuration was naturally an arbitrary setup which posed the system in an almost continuous state of scarcity. On the one hand it positively magnified the differences in the UCED and adequacy results under stressed conditions. On the other hand, it implicitly affected the UCED optimization of the very hydropower dispatch, which would differ in the full pan-European network configuration, thanks to the higher availability of imports. Nevertheless, several disclaimers have been placed in my thesis to avoid any potential misinterpretation of the results. Acknowledged also the tool-specificity of the hydropower modelling methodologies, a second modelling tool among the ones used for the ENTSO-E MAF simulations, not available at APG at the time of my assessment, would provide an interesting benchmark of the results obtained with ANTARES v6.1.

8.1 Reflections on Hydropower Modelling

The key points I believe it is worth reflecting on as the lessons learnt about hydropower modelling in ANTARES v6.1 are (i) the generation from natural inflows to hydro storages in the Hydro 2018 methodology, (ii) the run-of-river & pondage generation in the Hydro 2019 methodology, and (iii) some general remarks on PSP modelling.

(i) **Aggregating all natural hydro energy inflows to the various storage categories into one main reservoir**, as described in Section 6.1.2, had the modelling advantage of having all hydro storage generation inside each market node, hence avoiding the need for virtual external nodes and other additional complexities in the model. However, it **likely overestimated the flexibility of hydro storage generation**. In fact, the preallocation of hydro energy targets performed by ANTARES v6.1 freely distributed the cumulated monthly inflows to each day of the month with a direct correlation to the daily residual load, as described in Section 4.3.3. As a consequence, also the inflows to Daily PSP reservoirs or even to swell ROR & Daily storages could be dispatched by the tool over a longer timeframe than what would be prescribed by the real operation and technical constraints of these types of power plants. The choice of setting to *off* the hydro energy reservoir manager, as the standard option for all the market nodes not providing explicit minimum and maximum reservoir trajectories, had in general the positive side effect of preventing the preallocation to span over the whole year, rather than only internally to each month. It also avoided the additional extra flexibility potentially arising from the default 0% and 100% as the minimum and maximum reservoir levels, fixed for the whole year, in case of

lack of specific data provided for the market nodes. The impact was of course highly dependent on the hydropower resources peculiar to each market node and was surely relevant for Austria, due to the conspicuous amount of ROR pondage installed capacity, 1348 MW, and its hydro energy inflows, around 7000 GWh on average per year (see Tables 5.3 and 5.4).

(ii) As opposite to the previous remark, **the new run-of-river & pondage category defined in the Hydro 2019 data and methodology likely underestimated the dispatch flexibility granted by pondage capacity**. Neglecting the daily minimum and maximum power profiles for this type of generation (data originally not available for most if not all the market nodes) basically caused these hydro energy inflows to be treated as "pure" run-of-river generation, thus non-dispatchable but continuously processed according to the hourly availability profiles in ANTARES v6.1. The opposite modelling approach would be to set all the inflows as available to a hydro storage with reservoir size and total installed turbine capacity as reported in the PECD Hydro database. The issue with this second approach is that the tool would be allowed to freely modulate the generation from zero up to the total turbine installed capacity, which included also ROR plants with no pondage capabilities. As a consequence, this would lead to overestimating the maximum power modulation during peak hours. In fact, the extra maximum power achievable on top of the non-dispatchable generation from pure ROR plants should always be equal to the sole pondage capacity, when available, rather than the total installed capacity. Moreover, it is known that ROR plants, also the ones with pondage capabilities, usually cannot drastically reduce their generation to zero and store inflows (as potentially feasible for high dams). It follows that in the absence of proper minimum and maximum generation profiles, the first option was in my opinion the more conservative and likely the more suitable to generation adequacy studies. Nonetheless, the need for a more accurate modelling of ROR & pondage generation in Austria was identified.

(iii) **PSP modelling in ANTARES v6.1 employing two virtual nodes and a daily or weekly binding constraint**, in both methodologies (as described in Sections 6.1.3, 6.2.5, and 6.2.4), proved to provide a good estimate of pumping and peak operations. Nevertheless, it **lacked of a proper internal memory of the reservoir level**. In fact, PSP generation was optimized within independent daily or weekly cycles, during which all the pumped energy was constrained to be equal to the one generated (accounting for the efficiency losses). It follows that there was no explicit limit to the consecutive energy processed, provided that the daily or weekly balance was respected, **as well as there was no track of the reservoir level at the beginning and at the end of consecutive cycles**. Especially in the case of hydro storage plants characterized by a low ratio between the pump (or turbine) capacity and the storage size, this may lead to violations of the reservoir level constraints, e.g. excessive consecutive pumping, exceeding the storage size available, or excessive consecutive generation, exceeding the energy stored in the reservoir.

8.2 Future Work

Concerning the limitations and simplifications imposed by the modelling tool, some improvements are expected with the ANTARES v7.x releases. The new functionalities include the possibility to add pumping capabilities directly to hydro storage reservoirs, enabling a more robust and accurate modelling of the reservoir level trajectories. ANTARES v7.1 replaced version 6.1 and was used as one of the tools for the MAF 2020 study, soon to be published on the ENTSO-E adequacy webpage [41]. A detailed investigation and testing of its new functionalities and how they may affect the hydropower modelling methodology and the adequacy results is envisaged and planned based on the new models developed for the MAF 2020.

I openly presented and discussed the findings and the lessons learnt from my thesis to the ENTSO-E MAF modelling team. Acknowledged the crucial role of run-of-river pondage modelling in Austria and a few other market nodes, APG provided new consistent data for the minimum and maximum daily power profiles for the run-of-river & pondage category and exhorted other TSOs to do the same as an update to the PECD Hydro data. In fact, according to the description of the minimum and maximum ROR power constraints in the PECD Hydro database [11]: "[they] can be used for example to model RoR & Pondage output, to prevent Market Models from storing all the water during some hours (generation = 0 MW) to generate at maximum for prolonged periods later. If some true RoR (no reservoir at all) are present in the mix, there will always be some production."

Our request was welcomed by the ENTSO-E MAF working group and all the teams responsible for each modelling tool committed to enhancing the hydropower modelling methodology. The same challenge was also recognized and endorsed by the TYNDP working group for their transmission adequacy assessments. A common agreement was finally reached to enhance the modelling of ROR & pondage generation. I started working on the development of such methodology in ANTARES v7.1 to enable a more consistent split between pure ROR and pondage generation, improving its modulation and dispatch in the UCED profiles. Figure 8.1 shows the averaged ROR & pondage generation for Austria in the tri-lateral configuration, comparing the old Hydro 2019 continuous dispatch with the new Hydro 2020 test methodology on a dimensionless comparative scale.

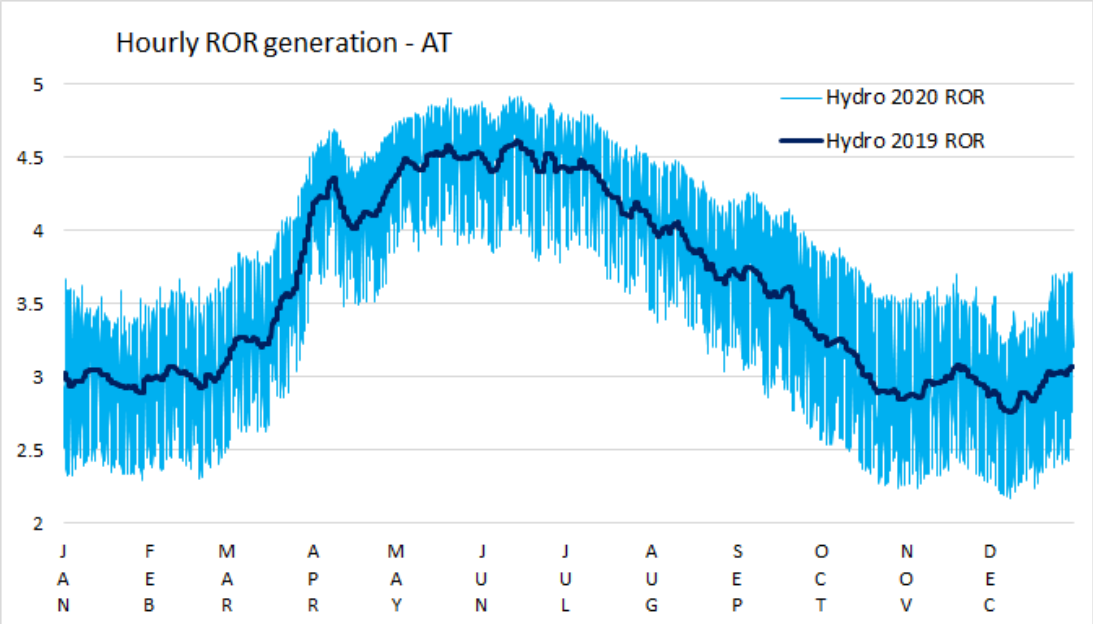

Figure 8.1: Hydro 2020 and 2019 averaged hourly ROR & pondage generation in Austria.

The chart shows that the new methotology allows the solver to modulate the ROR & pondage dispatch within a band around the old Hydro 2019 profile (i.e. the averaged availability of inflows), as defined by the new minimum and maximum constraints. The pondage generation is therefore optimized according to the contingent availability of resources and the demand profile.

Future works promoting further developments of the methodology in the field of hydropower modelling for adequacy studies, as well as benchmarks between different modelling tools, are warmly encouraged, especially alongside the pathway towards the new ERAA.

Bibliography

[1] D. Sarkar and Y. Odyuo, "An ab initio issues on renewable energy system integration to grid," *International Journal of Sustainable Energy Planning and Management*, vol. 23, 2019.

[2] C. Gerbaulet, C. von Hirschhausen, C. Kemfert, C. Lorenz, and P. Y. Oei, "European electricity sector decarbonization under different levels of foresight," *Renewable Energy*, vol. 141, 2019.

[3] NEA, "Impacts of the Fukushima Daiichi Accident on Nuclear Development Policies," *Nuclear Energy Agency*, 2017.

[4] J. P. Dorian, H. T. Franssen, and D. R. Simbeck, "Global challenges in energy," *Energy Policy*, vol. 34, no. 15, 2006.

[5] ENTSO-E, "Mid-term Adequacy Forecast 2017 - Executive Report," 2017. [Online]. Available: https://www.entsoe.eu/Documents/SDCdocuments/MAF/MAF_2017_report_for_consultation.pdf

[6] ——, "Mid-term Adequacy Forecast 2018 - Executive Report," Tech. Rep., 2018. [Online]. Available: https://www.entsoe.eu/Documents/SDCdocuments/MAF/MAF_2018_Executive_Report.pdf

[7] ——, "Mid-Term Adequacy Forecast 2019 - Executive Summary," Tech. Rep., 2019. [Online]. Available: https://www.entsoe.eu/outlooks/midterm/wp-content/uploads/2019/12/entsoe_MAF_2019.pdf

[8] ACER and ENTSO-E, "Methodology for the European Resource Adequacy Assessment ," 2020. [Online]. Available: http://www.acer.europa.eu/Official_documents/Acts_of_the_Agency/IndividualdecisionsAnnexes/ACERDecisionNo24-2020_Annexes/ACERDecision24-2020onERAA-AnnexI.pdf

[9] The European Commission, "Clean Energy for All Europeans." [Online]. Available: https://ec.europa.eu/energy/topics/energy-strategy/clean-energy-all-europeans_en

[10] ENTSO-E, "Mid-term Adequacy Forecast 2019 - Appendix 2: Methodology," 2019. [Online]. Available: https://www.entsoe.eu/Documents/SDCdocuments/MAF/2019/MAF2019Appendix2-Methodology.pdf

[11] ——, "Hydropower Modelling - New database complementing PECD v1.0," 2019. [Online]. Available: https://eepublicdownloads.blob.core.windows.net/public-cdn-container/clean-documents/sdc-documents/MAF/2019/Hydropower_Modelling_New_database_and_methodology.pdf

[12] RTE, "ANTARES Simulator." [Online]. Available: https://antares-simulator.org/

[13] R Core Team, *R: A Language and Environment for Statistical Computing*, R Foundation for Statistical Computing, Vienna, Austria, 2019. [Online]. Available: https://www.R-project.org/

[14] IPCC, *Fifth Assessment Report (AR5). Synthesis Report (SYR).*, 2014.

[15] ENTSO-E, "ENTSO-E Report of the January 2017 Cold Spell," 2017. [Online]. Available: https://eepublicdownloads.azureedge.net/clean-documents/news/170530_Managing_Critical_Grid_Situations-Success_and_Challenges.pdf

[16] ——, "Mid-term Adequacy Forecast 2018 - Appendix 1: Methodology and Detailed Results," 2018. [Online]. Available: https://www.entsoe.eu/Documents/SDCdocuments/MAF/MAF_2018_Methodology_and_Detailed_Results.pdf

[17] ACER and ENTSO-E, "Methodology for calculating the value of lost load, the cost of new entry and the reliability standard ," 2020. [Online]. Available: http://www.acer.europa.eu/Official_documents/Acts_of_the_Agency/IndividualdecisionsAnnexes/ACERDecisionNo23-2020_Annexes/ACERDecision23-2020onVOLLCONERS-AnnexI.pdf

[18] The European Parliament and Council, "Regulation (EU) 2019/943 of the European Parliament and of the Council of 5 June 2019 on the internal market for electricity," *Official Journal of the European Union*, 2019. [Online]. Available: https://eur-lex.europa.eu/legal-content/EN/TXT/?uri=uriserv:OJ.L_.2019.158.01.0054.01.ENG

[19] M. Petz, G. Achleitner, and R. Schurhuber, "Advanced modelling of generation adequacy in Europe," in *2019 54th International Universities Power Engineering Conference, UPEC 2019 - Proceedings*, 2019.

[20] ENTSO-E, "Network Development Plan 2018," 2018. [Online]. Available: https://eepublicdownloads.blob.core.windows.net/public-cdn-container/clean-documents/tyndp-documents/TYNDP2018/consultation/MainReport/TYNDP2018_ExecutiveReport.pdf

[21] PLEF SG2, "Generation Adequacy Assessment 2015," 2015. [Online]. Available: https://www.benelux.int/files/4914/2554/1545/Penta_generation_adequacy_assessment_REPORT.pdf

[22] ——, "Generation Adequacy Assessment 2018," 2018. [Online]. Available: https://www.benelux.int/files/1615/1749/6861/2018-01-31_-_2nd_PLEF_GAA_report.pdf

[23] ——, "Generation Adequacy Assessment 2020," 2020. [Online]. Available: https://www.benelux.int/files/4515/8998/1576/PENTAreport_FINAL.pdf

[24] ENTSO-E, "Winter Outlook Report 2019," 2019. [Online]. Available: https://eepublicdownloads.azureedge.net/clean-documents/sdc-documents/seasonal/WinterOutlook2019-2020_Report(forpublication).pdf

[25] ——, "Summer Outlook Report 2020," 2020. [Online]. Available: https://eepublicdownloads.blob.core.windows.net/public-cdn-container/clean-documents/sdc-documents/seasonal/SOR2020/Summer-Outlook-2020_Report.pdf

[26] RTE, "Bilan prévisionnel de l'équilibre offre-demande d'électricité en France," 2019. [Online]. Available: https://assets.rte-france.com/prod/public/2020-06/bp2019_synthegse_12_1_0.pdf

[27] ELIA, "Adequacy and flexibility study for Belgium 2020 - 2030," 2019. [Online]. Available: https://www.elia.be/-/media/project/elia/elia-site/company/publication/studies-and-reports/studies/13082019adequacy-and-flexibility-study_en.pdf

[28] ENTSO-E, "Mid-term Adequacy Forecast 2019 - Input Data PEMMDB Public," 2019. [Online]. Available: https://www.entsoe.eu/Documents/SDCdocuments/MAF/2019/MAF-2019-Dataset.zip

[29] ——, "Mid-term Adequacy Forecast 2019 - Input Data PECD Public," 2019. [Online]. Available: https://www.entsoe.eu/downloads/maf-data/PECD.zip

[30] ——, "Demand Forecasting Methodology - TRAPUNTA V1.1," 2019. [Online]. Available: https://eepublicdownloads.blob.core.windows.net/public-cdn-container/clean-documents/sdc-documents/MAF/2019/Demandforecastingmethodology.pdf

[31] AFRY, "BID3 Simulator." [Online]. Available: https://afry.com/en/service/bid3-afrys-power-market-modelling-suite

[32] CESI, "GRARE Simulator." [Online]. Available: https://www.cesi.it/views/system-adequacy-and-market-modelling/

[33] Energy Exemplar, "PLEXOS Simulator." [Online]. Available: https://energyexemplar.com/solutions/plexos/

[34] OSA, "PowrSym Simulator." [Online]. Available: http://www.powrsym.com/index.htm

[35] ENTSO-E, "Mid-term Adequacy Forecast 2019 - Appendix 1: Detailed Results, Sensitivities and Input Data," Tech. Rep., 2019. [Online]. Available: https://www.entsoe.eu/Documents/SDCdocuments/MAF/2019/MAF2019Appendix1-DetailedResults%2CSensitivitiesandInputData.pdf

[36] M. Doquet, R. Gonzalez, S. Lepy, E. Momot, and F. Verrier, "A new tool for adequacy reporting of electric systems: ANTARES," in *42nd International Conference on Large High Voltage Electric Systems 2008, CIGRE 2008*, 2008.

[37] PLEF, "PLEF Memorandum of Understanding," 2007. [Online]. Available: https://www.benelux.int/files/3214/2554/2929/Memorandum_of_understanding_Pentalateral_2007_-_EN.pdf

[38] RTE, "ANTARES: General Reference Guide v6.0.0," 2018. [Online]. Available: https://usermanual.wiki/Document/antaresgeneralreferenceguide.460111675/view

[39] ——, "ANTARES: Presentation," 2013. [Online]. Available: https://antares.rte-france.com/wp-content/uploads/2016/09/160913-Antares_public_long.pdf

[40] ——, "ANTARES: Optimization Problems Formulation," 2017. [Online]. Available: https://antares-simulator.org/media/files/page/UC4V8-170522-Antares-Optimization-Problems-Formulation.pdf

[41] ENTSO-E, "ENTSO-E Mid-Term Adequacy web page." [Online]. Available: https://www.entsoe.eu/outlooks/midterm/

[42] J.-E. ZAWAM, F. Guillem, B. Thieurmel, and T. Robert, *antaresViz: Antares Visualizations*, 2018, r package version 0.15.0.900. [Online]. Available: https://github.com/rte-antares-rpackage/antaresViz

List of Figures

1 Hourly UCED results for Austria, climate year 2016, CW45. XIII

1.1 Adequacy Balance according to ENTSO-E [16]. 2
1.2 Overview of existing adequacy processes in Europe [19]. 3

2.1 LOLE sensitivity on reservoir level trajectories [16]. 6

3.1 Monte Carlo approach to assess resource adequacy, in a nutshell [10]. . . 16
3.2 Iterative result consolidation process within the MAF 2019 [10]. 17

4.1 Functional view of ANTARES v6.1 simulation sessions [38]. 20

5.1 Total hydro storage energy natural inflows for AT, CH and ITN. 36
5.2 Total run-of-river & pondage energy natural inflows for AT, CH and ITN. 37

6.1 Schematic representation of Hydro 2018 elements in the ANTARES v6.1 GUI. 40
6.2 Schematic representation of Hydro 2019 elements in the ANTARES v6.1 GUI. 44
6.3 The tri-lateral models in the ANTARES v6.1 GUI. 52

7.1 Evolution of the coefficient of variation α for the tri-lateral models. . . . 55
7.2 Hourly UCED results for the tri-lateral system, CY 2016, CW 45. . . . 60
7.3 Hourly LOLP distribution per month and day of the week. 63
7.4 Hourly EENS distribution on a comparative scale. 64

8.1 Hydro 2020 and 2019 averaged hourly ROR & pondage generation in Austria. 69

List of Tables

1 Absolute and relative differences (w.r.t. Hydro 2018) in the yearly averaged results. XII

4.1 System complexity in different ANTARES optimization modes [39]. . . . 25

5.1 Key data available in the Hydro 2018 database. 31
5.2 Key data available in the Hydro 2019 database. 32
5.3 Hydropower installed capacities according to the Hydro 2019 and 2018 categories. 34
5.4 Statistical measures of the 35 CYs for Hydro 2018 and Hydro 2019. . . . 34
5.5 Normal, dry and wet yearly hydro inflows and clustering of the 35 CYs. 38

7.1 NGCs, demand and NTCs for the target year 2025. MAF 2019 data [28]. 54
7.2 Absolute and relative differences (w.r.t. Hydro 2018) in the averaged yearly results. 57
7.3 Absolute and relative differences (w.r.t. Hydro 2018) in the yearly results for CY 2016. 59